

ALTERNATIVE MATERIAL SELECTION & TOPOLOGY OPTIMIZATION FOR COMPONENTS OF STONERIDGE'S SMARTBAR ACTUATOR

Team 17

MECHENG 450 - Design and Manufacturing III - F23

Instructor: Randy Schwemmin

Sponsor: Harish Chowdhary Athipatla, Product Engineering Manager, Stoneridge

Lillian S. Adams, Marisa G. Bladecki, Andres Garcia, Avani Yerva

December 12, 2023

TABLE OF CONTENTS

EXECUTIVE SUMMARY	4
ABSTRACT	5
BACKGROUND	5
PROBLEM DEFINITION DEVELOPMENT	8
STAKEHOLDER ANALYSIS	8
Primary Stakeholders	9
Secondary Stakeholders	9
Tertiary Stakeholders	9
Intellectual Property Agreement	10
BENCHMARKING	10
Information Sources	10
Coupling and Decoupling System Benchmarking	10
Material Benchmarking	13
REQUIREMENTS AND SPECIFICATIONS	16
Specification Assessment Plans and Challenges	18
ENGINEERING DESIGN STANDARDS	18
DESIGN PROCESS	19
Design Process Structure	19
DESIGN CONTEXT	21
MATERIAL SELECTION	22
Concept Generation	22
Concept Selection Process	24
PROJECT SCOPE EXPANSION	25
Concept Generation	25
Topology Optimization	26
Concept Selection Process	27
Updated Requirements and Specifications	28
REPLACING HALL EFFECT SENSOR	29
Concept Generation	29
Concept Selection Process	30
Topology Optimization Alpha Solution	31
ENGINEERING ANALYSIS	32
Material Selection Alpha Solution	32
Material Selection Using Granta EduPack Material Filtering Tool	32
First Principles Force Analysis for FEA	33
Ansys Simulation Workbench Setup	41
Convergence Testing	42
Static Structural Analysis	42
Finding Baseline Yield Strength Values	47

Thermal Analysis - CTE	48
Thermal Analysis - Stress	50
Vibrational Analysis	50
Shock Analysis	52
Topology Optimization	52
Cost Analysis	52
Comparison of Capable Materials	54
FINAL TOPOLOGY OPTIMIZATIONS	56
Planet Carrier and Magnet Holder Optimizations	56
Final Topology Optimized Geometry Material Selection	59
Exclusion of Ring Gear	60
VERIFICATION AND VALIDATION PLAN	60
DISCUSSION	63
Problem Definition	63
Reflection	63
Design Critique	64
Threat Analysis	65
REFLECTION	67
Greater Context and Impacts	67
Inclusion and Equity	68
Ethics	68
RECOMMENDATIONS	69
CONCLUSION	69
ACKNOWLEDGEMENTS	70
APPENDIX A	71
Individual Concept Generation	71
APPENDIX B	73
Sensor Selection Pugh Chart Concepts	73
APPENDIX C	75
Benchmarked Materials	75
APPENDIX D	76
Random Vibration Data Provided by Stoneridge	76
Shock Data Provided by Stoneridge	76
APPENDIX E	77
Material Selection Pugh Charts	77
APPENDIX F	86
First Principle Analysis - Matlab Code	86
APPENDIX G	87
Convergence Testing for Mesh Size	87
APPENDIX H	88
First Principles - Thermal Analysis - Finding CTE Values	88

First Principles - Thermal Analysis - CTE Validation	90
First Principles - Thermal Analysis for Stress	91
APPENDIX I	94
Ring Gear Force Angle Derivation	94
APPENDIX J	95
Cost Analysis Spreadsheets	95
APPENDIX K	97
FMEAs for the Three Components and Two Manufacturing Methods	97
REFERENCES	100
TEAM MEMBER BIOS	107

EXECUTIVE SUMMARY

The SmartBar Actuator project, the scope of this report, focuses on reducing the cost and weight of the device, which is owned by Stoneridge, Inc. A SmartBar actuator is a component located on a sway bar, which is a stabilizing part that is commonly used to ensure that a vehicle remains level. This SmartBar actuator is a device that allows the sway bar, now deemed a “SmartBar,” to separate into two freely rotating halves so that offroading vehicles have the freedom to elect to engage or disengage this stabilizer bar, that on rough terrain could cause the opposite effect to its original purpose. The project involves changing materials for the magnet holder, planet carrier, and ring gear, as well as optimizing the assembly design. The stakeholder requirements include ensuring a minimum lifetime, withstanding specified loads, not deforming, remaining within the packaging envelope, being capable of tight manufacturing tolerances, and reducing cost and weight. The contextual factors that are discussed encompass social and societal impacts, ethical material sourcing, and sustainability. Deliverables include material recommendations, topology optimizations, performance analysis, and cost evaluations.

The main challenges of this project were the team’s limited knowledge of Finite Element Analysis (FEA), acquiring the accurate material property data, applying accurate constraints to the models, and estimating manufacturing and sourcing costs. The team addressed these challenges through research and collaboration with experts and resources throughout the University of Michigan.

The recommendations that the team has for material selection are shown in the table below, with least expensive at the top to most expensive at the bottom, all still being cheaper than the original components. The extensive cost analysis and comparison can be found in the engineering analysis portion of the report.

Table A: Material Recommendations Per Component

Ring Gear	Magnet Holder	Planet Carrier
Aluminum, 359.0, cast, T6	PTT (30% glass fiber)	PA66/6 (30% glass fiber)
Aluminum, C355.0, permanent mold cast, T6	PPA (60% glass fiber)	PA66/6 (35% glass fiber)
Aluminum, 354.0, cast, T6	PPA (50% glass fiber, lubricated)	PF (high strength glass fiber, molding)
Aluminum, 332.0, permanent mold cast, T5	PTT (30% glass fiber, flame retarded)	PTT (30% glass fiber)
Aluminum, 333.0, permanent mold cast, T6	PPA (50% long glass fiber)	PA66/6 (33% glass fiber, lubricated)

The team came to these recommendations through refining material properties within a large database called Granta EduPack. These properties were determined by load cases provided by Stoneridge as well as component interactions that indicate limits for particular components. This process is described more in detail in the engineering analysis section of this report. The team is confident in these recommendations due to the extensive verification process through FEA static structural analysis, random vibration, and hand calculations to name a few.

The team has completed the material selection process and has conducted topology optimization for the planet carrier and the magnet holder. This has all been provided in the following report.

ABSTRACT

The goals of this project are to reduce the cost and weight of the SmartBar actuator that is produced by Stoneridge, Inc. The team accomplished these by changing the materials of three parts, the magnet holder, planet carrier, and ring gear, as well as conducting topology optimization on them. The stakeholder requirements are ensuring a minimum lifetime, remaining within the packaging envelope, being capable of tight manufacturing tolerances, and reducing cost and weight. To verify that these were met, the team conducted several Ansys analyses to produce data for lifetime parameters, shock and vibration load case tests, linear fracture criterion, package envelope verification, cost, and weight. The team also considered manufacturing methods and tooling when minimizing material costs. The deliverables are the material recommendations and topology optimizations for the three parts, an associated analytical modeling tool created with simulation software, and an evaluation of performance, manufacturability, and cost considerations.

BACKGROUND

The system that the team is working on is the SmartBar actuator, which allows a sway bar to separate into two halves so that they can rotate about their shared axis. The sponsor of this project, and the owner of the design, is Stoneridge, Inc. Based out of Novi, MI, the company specializes in the design and manufacturing of electronic vehicle components such as actuators, valves, sensors, switches, connectors, camera systems, and infotainment. They then supply these products to several automotive, original equipment manufacturers. Stoneridge's main customer is Stellantis, so the Sway Bar actuator is on the Jeep Rubicon, Jeep Grand Cherokee, Ram Power Wagon, and more [14].

“Sway bars, also known as anti-roll bars, roll bars, anti-sway bars, or stabilizer bars, are U-shaped metallic pieces that are attached to the strut or control arm by each of the vehicle's wheels” [58]. Their purpose is to ensure that the tires, and therefore the vehicle itself, remain level and that the plane they create is parallel to the ground. A sway bar does this by acting as a torsion spring and twisting its ends, as shown in figure 1, so that when a wheel rises above the level plane, the bar compensates and returns to its horizontal position. The figure below displays a moment just before the sway bar corrects itself. This prevents tipping and improves traction control.

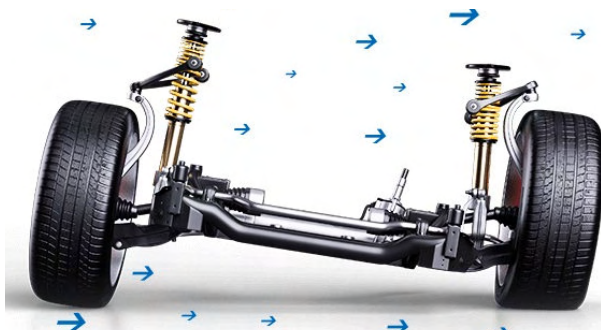
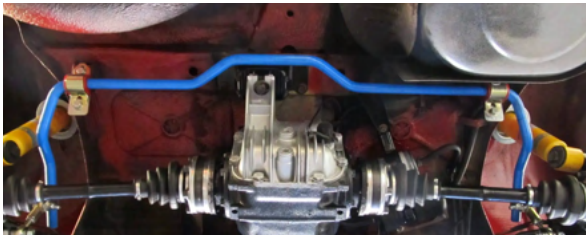
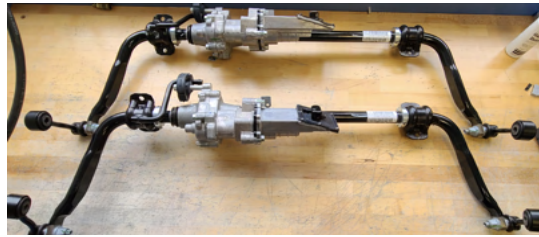


Figure 1. Sway bar preventing left wheel from rising above the other [67]

Sway bars are ideal for driving on even roads at high speeds. When driving over uneven ground, the wheels must be able to simultaneously be at varying heights so that the body of the car and the driver do not feel the shifting terrain [68]. This is why SmartBar actuators are included in vehicles that will be used for off-roading because they have a need for further suspension capabilities. A normal sway bar is displayed on the next page in figure 2a, and a SmartBar is displayed on the next page in figure 2b.



(2a) [68]



(2b) [14]

Figure 2. A sway bar is shown in blue in figure 2a (left) and two SmartBars are shown in figure 2b (right). The silver systems in the middle of the SmartBars are the SmartBar actuators. When installed in vehicles, the SmartBars will be in the same position that the sway bar is displayed in.

The mechanical components of the SmartBar actuator that comprise the transmission are shown below in figure 3, which is provided by Stoneridge.

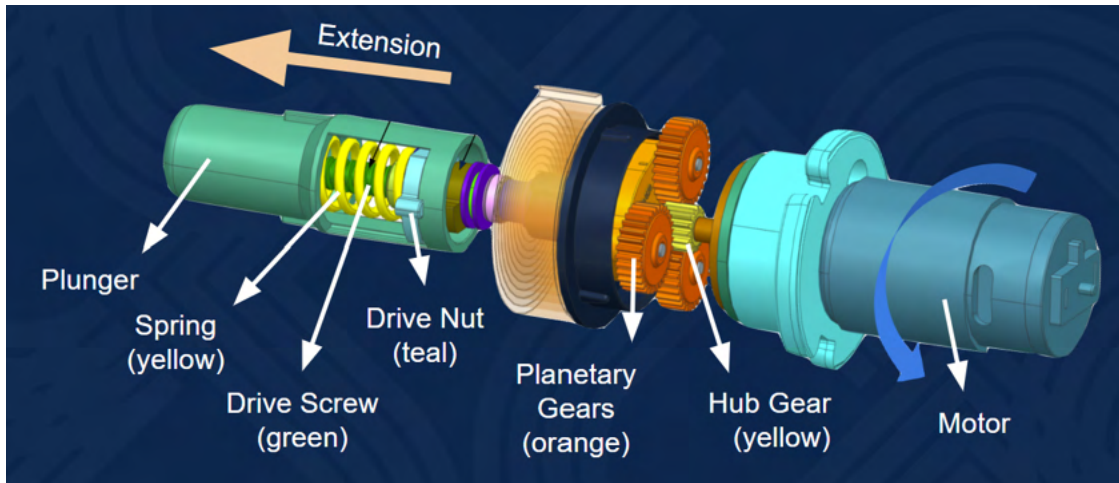
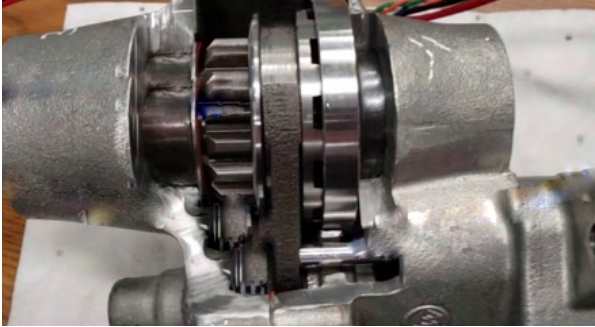
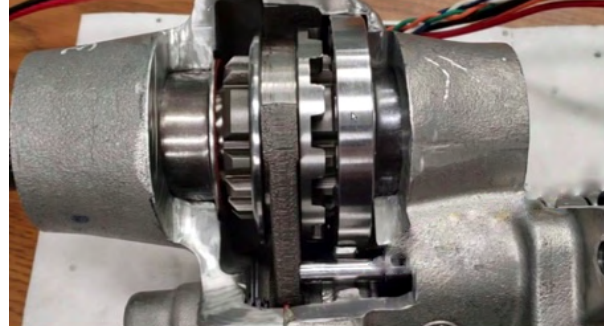


Figure 3. Stoneridge’s SmartBar actuator components that comprise the transmission and actuation mechanism. The drive nut moves within the window that the spring is visible through and simultaneously compresses the spring. This spring force causes the plunger to extend (in the direction of the arrow) [14].

The SmartBar actuator engages when a driver presses a designated button within their car, activating the system’s motor. This motor then rotates its transmission and a drive screw (within the spring in figure 3), which causes a drive nut to move linearly along the screw in the extension direction. By doing so, the nut axially drives a spring and plunger outward (the left direction in figure 3), until they contact one of the shaft collars and push it away from the other. When these collars are separate, they are no longer fixing the sway bar halves in place. This allows the halves to rotate about their axis so that the wheels can move vertically and reach different heights at the same time. This will be referred to as the “disengaged” or “unlocked” position. The engaged and disengaged positions of the shaft collar are shown in figure 4 on the next page. When the driver turns the Smart Bar off, the plunger retracts and the shaft collars reengage.



(4a) [14]



(4b) [14]

Figure 4. The left image shows the shaft collar in the engaged position, in which the sway bar halves are fixed and cannot rotate about their axis. The right image shows the disengaged position, in which the teeth are not meshed and the sway bar halves are disconnected.

Due to the cyclic loading that they experience, the SmartBar actuator and its components are susceptible to various failure modes. Therefore, the parts that the team is tasked with proposing material suggestions for, the magnet holder, planet carrier, and ring gear, must meet the requirements specified in the *Requirements and Specifications* section of the report. The three parts listed above are shown in figure 5.

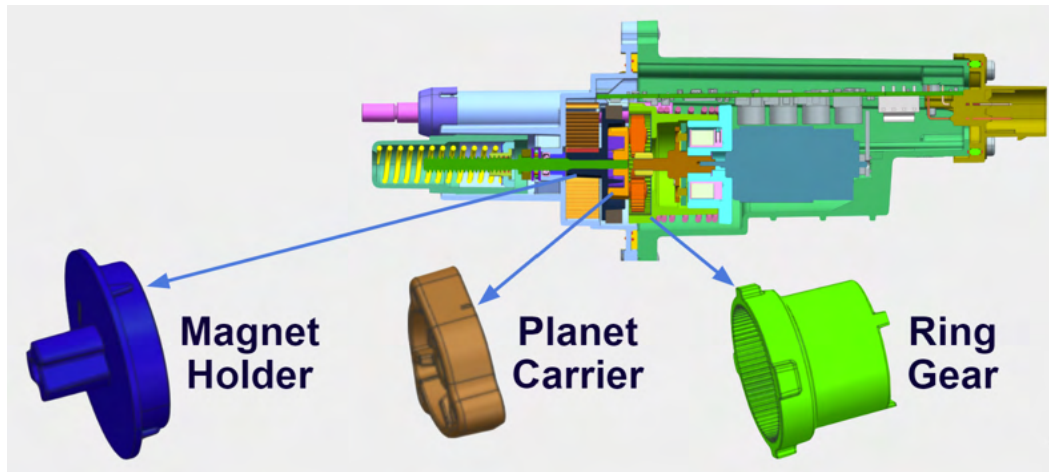


Figure 5. The general positions of the magnet holder, planet carrier, and ring gear are shown on a cross-section view of the SmartBar actuator [14]

In order to justify the alternative material proposals for these parts, their functions within the SmartBar actuator must be described. The magnet holder, which functions as named, is fixed to and therefore rotates with the drive shaft. Hall sensors, located around the outer diameter of the holder, signal to the controller that the plunger has extended enough to decouple the shaft collar. They do so by detecting changes in magnetic flux density when the magnets within the magnet holder pass them. The planetary gears are rigidly attached to the planet carrier, which is fixed to the drive shaft similar to the magnet holder. These gears are housed within the ring gear, and their teeth will be meshing.

PROBLEM DEFINITION DEVELOPMENT

There are currently various other mechanisms for the engagement and disengagement of sway bars on the market, but Stoneridge wishes to remain at the forefront. There have been no significant records of failure related to the three parts within the material investigation scope. The motivation of this project is therefore to increase the profitability of the SmartBar actuator. This system was first designed over 15 years ago, and the material of the magnet holder, planet carrier, and ring gear has remained a die cast Zinc known as Zamak 5 [14]. This material application has not been researched or updated since its design, and its acquisition from a different supplier makes it difficult to attain a cohesive reasoning for its use.

The team focused on defining the problem by assessing Stoneridge's needs. This process consisted of meeting with the project sponsor and the main design engineer of the SmartBar actuator to understand Stoneridge's primary goals. Through these conversations, the team determined that the main objective is to decrease the manufacturing costs of the magnet holder (currently \$0.67), planet carrier (currently \$0.32), and ring gear (currently \$1.20) through material selection while maintaining, or improving, its current functionality. After comparing the scope of this goal with the demands of MECHENG 450, the team chose to expand the problem statement by looking for alternate assembly optimization ideas. The team therefore refined the problem statement to be the following:

SmartBar actuators are used in offroading vehicles to disconnect two halves of a sway bar, allowing for smoother driving over uneven terrain. Stoneridge is currently ahead of its competitors in minimizing the cost and weight of its SmartBar actuator, but further reductions must be made in order to retain customers. Therefore, topology optimization must be performed and the materials of the magnet holder, planet carrier, and ring gear must be chosen while maintaining their original performance and sustaining load cases experienced on the motor.

Compiling five to ten materials that meet the stakeholder's requirements and reducing production costs of the three scoped parts, as well as completing the associated deliverables, would result in success as defined by Stoneridge. For the courses' metrics of success, the team must accomplish the following: compiling the before mentioned material list through use of finite element analysis (FEA), creating a tool that can be used for further material analysis, and both generating and conducting analysis on a chosen design optimization.

STAKEHOLDER ANALYSIS

Figure 6 on the following page showcases the team's primary, secondary, and tertiary stakeholders organized based on ecosystem map categories.

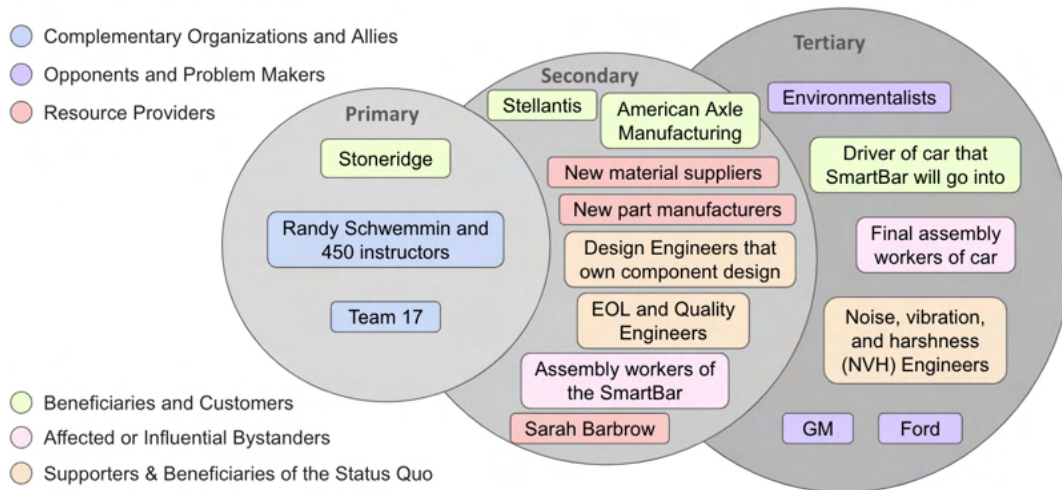


Figure 6. Stakeholder Analysis Diagram

Primary Stakeholders

The primary stakeholders of this project include Stoneridge as a Beneficiary and Customer, because they are the project sponsor whose problem the team is addressing. The team's individual section course instructor (Randy Schwemmin) and the MECHENG 450 course instructors are Allies. This is because they are supporting the team through feedback and providing necessary resources. This team is also considered a Complementary Organization/Ally since all members are invested in working together on the problem for the project sponsor.

Secondary Stakeholders

Secondary stakeholders include Stellantis and American Axle Manufacturing (AAM) who are both Beneficiaries and Customers of this project since they are both customers of the SmartBar systems. Stellantis owns the cars that the SmartBar actuator system is used in, and AAM is the company that assembles the SmartBar actuator with the two sway bar halves. Resource Providers include the librarian Sarah Barbrow, who will be helping with material research, new material suppliers, and new part manufacturers whom the team will be contacting to get cost estimates. Design Engineers who own the three components that the team is working on, End-of-Line (EOL) Engineers, and Quality Engineers are all Supporters and Beneficiaries of the Status Quo because introducing changes takes time for review and inspection of the parts. Assembly workers of the SmartBar actuator are considered Affected or Influential Bystanders because any changes that the team makes to the actuator will affect the assembly of the actuator with the modified components.

Tertiary Stakeholders

Tertiary stakeholders mainly comprise individuals/groups that have no direct impact on the design process or choices. Some tertiary stakeholders comprise of Opponents and Problem Makers, such as competitors to the customers like GM and Ford, who benefit from Stoneridge having more expensive products. Environmentalists also fall into this category because of the possible environmental implications that the changes might impose. End users of the product are the drivers of the cars that the SmartBar system will go into (drivers of Stellantis off-roading vehicles). They have no direct impact on the design process but will benefit from a lower SmartBar actuator cost, making them Beneficiaries and Customers. Final

assembly workers of the cars with SmartBars are Affected or Influential Bystanders since they may need to handle the SmartBar system for installation. Noise, Vibration, and Harshness Engineers are considered Supporters and Beneficiaries of the Status Quo since introducing changes consumes a lot of time for additional review and inspection of the parts that are already meeting noise, vibration, and harshness requirements.

Intellectual Property Agreement

The SmartBar actuator is owned and distributed by Stoneridge, so any material or design changes that the team proposes will be its internal property. Any conducted research, generated concepts, conclusions, deliverables, and resulting patents therefore do not belong to the team. The team willingly signed a formal contract with Stoneridge to confirm agreement to this relationship.

BENCHMARKING

Information Sources

A large portion of the project is research and analysis-based. The primary sources that the team utilized were designated Stoneridge contacts and the Stoneridge scholars who are students at the University of Michigan. The team scheduled 30 minute meetings every other week or as needed with both of these sources separately. Assumptions about component interfaces were verified by the relevant engineers working on the system, and calculations were reviewed by both a Stoneridge scholar and Professor Umbriac. The secondary sources included the instructional staff for MECHENG 450, professors of courses within the problem scope, Sarah Barbrow, past Stoneridge MECHENG 450 group reports, and any relevant articles or websites that the team found. In order to find FEA learning resources, the team met with MECHENG 305's Professor Huan, Professor Sienko, MECHENG 450 peer advisors, and CAEN staff. The team also utilized the Ansys Learning Hub tutorials to create a continuous learning plan. When beginning the material research stage, the team consulted Professor Love, a materials scientist who specializes in polymeric materials. He suggested the use of the Ansys Granta EduPack Material tool, and The team utilized this in addition to "Sources for Materials Information and Suppliers" on the MechE Capstone resource website [18] and any literature that discussed materials commonly used in the automotive industry, which have been cited below.

Coupling and Decoupling System Benchmarking

When innovating and improving a design, it is important to take into account similar approaches to accomplish the same functions. In this case, this was done by benchmarking the sponsor's SmartBar actuator against other disengaging/engaging sway bar mechanisms. However, after extensively searching and assessing other automotive designs it has become apparent that there are very few alternative designs/competitors on the market with even less available information about their design and application. To overcome this, the focus will be on other devices that can effectively engage and disengage two components in any system, which does not necessarily have to be in an automotive application. By generally describing the functionality of the product, the team is able to compare it to a wider variety of products and are able to benchmark critical characteristics between them, as seen in the previous section with the benchmarking approach. Table 1. presents key comparable features for each system.

The team noted the major specifications of each system for comparison. Separation Mechanism is important for understanding the basic function of each system. Cost, Weight, and Lifetime were categories that are important for understanding key features that make Stoneridge's SmartBar system

ahead or behind its competitors. It is also important for us to look into the materials that each system is made of since the problem scope focuses on internal component materials. This information is useful to observe if there are cheaper materials that make up one of the systems and can be used for further material research. This benchmarking will be used to brainstorm alternate design ideas for optimizing the actuator assembly.

Table 1: Benchmarking Coupling and Decoupling Systems

Coupling and Disconnect Systems	SmartBar Actuator (Stoneridge) [14]	Active Stabilizer Bar System - Rotary Actuator (BWI Group) [7]	Autolynx Sway Bar (Apex Design USA) [15]	Dodge Durango Diaphragm Clutch [37]	Solenoid Valve [1]	Pneumatic Cylinder [72]
Separation Mechanism	Motor is used to move a drive nut which extends the plunger	Uses a rotary actuator and a hydraulic pump to energize two solenoid valves	Turn of a knob on the top of the link restricts/allows vertical movement of the sway bar	Pressing a pedal compresses a spring, which pushes pressure plates off of a flywheel and removes friction	Coils around armature create a magnetic field that extends/retracts plunger	Inputs gas into a chamber to extend or retract plunger by exerting pressure on an internal plate
Cost	\$2941.67	\$2300	\$450	\$359.10	\$44.95	\$185
Weight	20 lbs	N/A	N/A	36 lbs	1.44 lbs	Varies on Dimensions
Lifetime	10 Years or 15,000 cycles	N/A	N/A	N/A	N/A	X Years or $\sim 12 \cdot 10^6$ cycles
Materials	Zinc Zamak 5, Stainless Steel, Bronze, Aluminum Alloy	Aluminum	Vulcanized rubber,	Steel, Carbon Kevlar	Brass, Stainless Steel, Polypropylene	Piston Rod - Chrome plated steel Tube material - Aluminum

Gaps, denoted by “N/A” within the table above, exist in the research for coupling and decoupling system benchmarking. This is because the information needed for comparison is not advertised by the distributing companies and therefore not easily accessible. Benchmarking Table 1 contains gaps primarily in the cost, weight, lifetime, and materials. Since this benchmarking will be primarily used for concept generation purposes, exact values for these categories are not necessary.

The systems above were chosen because of their similar functionality, with the only difference being their different application in a variety of vehicles. By benchmarking the different products the team hopes to understand what aspects of their designs are more effective than others and take away from their approaches ideas that could be incorporated into the general requirements, specifications, and later concept generation. The greater notes and takeaways for each system are presented below.

To elaborate more on the standard for comparison, Stoneridge's SmartBar actuator is powered by an electric motor and drives torque through a planetary drive train that later translates the rotational motion into a radial load through the application of a drive nut on the drive shaft to extend a plunger that engages/disengages the sway bar. The standout aspect of this design is its capability to effectively translate from rotational to linear motion within such a tight packaging envelope.

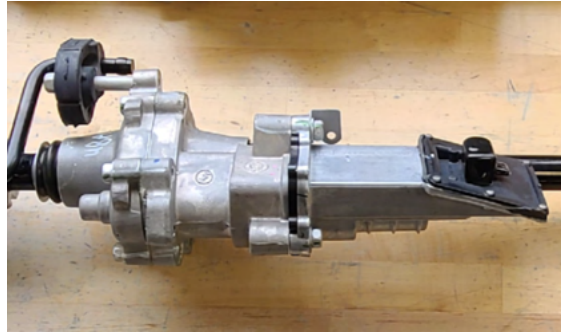


Figure 7. Stoneridge's SmartBar actuator [14]

The next competitor to Stoneridge's Smart Bar is the Active Stabilizer Bar System from BWI Group shown in figure 8 below, which also uses an actuator to rotate the two sway bar halves when activated [7]. This was included in the benchmark since it is the next closest sway bar disconnect mechanism to Stoneridge's design.



Figure 8. Active Stabilizer Bar System - Rotary Actuator (BWI Group) [7]

Another sway bar disconnect mechanism is the Autolynx Sway Bar, shown in figure 9 on the following page, which is manually installed by the user at both ends of the sway bar, fixing it to the body or chassis of the car [15]. The team included this system in the benchmarking because it provides an alternative way to restrict and allow freedom of movement to the sway bar without the use of an actuator.



Figure 9. Autolynx Sway Bar (Apex Design USA) [15]

The last three benchmarking systems are various locking and unlocking mechanisms that serve a similar purpose as the plunger mechanism in the Smart Bar actuator. This was done to better understand the functionality of the swaybar's driving subsystems, and how the same goal has been achieved in different circumstances. These alternative mechanisms are pictured in figures 10a, 10b, and 10c respectively.



Figure 10. Alternative disconnect/locking mechanisms. Pictured on the left (10a) is the Dodge Durango Diaphragm Clutch [37], the Solenoid Valve (10b) [1], and a Pneumatic Cylinder on the right (10c) [28].

Material Benchmarking

The team also conducted benchmarking of materials that are currently used for the ring gear, planet carrier, and magnet holder in Stoneridge's SmartBar actuator with other materials that are commonly used for gears and interfacing components. The current material used for the three components of focus is Die-cast Zinc Zamak 5. This benchmarking will continue to grow as the team does more material research and starts testing the different materials.

The benchmarking categories are derived from the project requirements and specifications, specifically the SmartBar’s performance throughout its lifetime so that it remains efficient and capable. With the intent of both costing down and reducing weight, the cost and density of each material are included for comparison. The remaining properties mentioned below are directly related to the performance of the parts under their maximum loading conditions. These include the thermal expansion of the materials during extreme temperature conditions as well as the lifetime due to the materials’ yield strengths and hardnesses. Note that toughness was not included because its value decreases significantly as temperature increases. Each of the material properties listed below implies an effect on the overall assembly performance, and should not be overlooked throughout the material selection process.

Table 2: Benchmarking Materials

Materials	Die Cast Zinc Zamak 5 (Current Material) [3][4][11][17]	Polyoxymethylene Homopolymer (Delrin) (POM-H) [5][12]	Nylon (type 6) [7][10][13][14]	Phosphor Bronze [1][2][9]	Polycarbonate (PC) [48] [49] [50] [51] [52]
Cost	\$4.03E-3 /cm ³	\$2.24E-3 /cm ³	\$0.55E-3 /cm ³	\$27.98E-3 /cm ³	\$3.36E-3 /cm ³
Density	6.60 g/cm ³	1.41 g/cm ³	1.15 g/cm ³	8.80 g/cm ³	1.20 g/cm ³
Stable Temperature Range	-40 to 369°C	-40 to 120°C	-40 to 93°C	-268 to 288°C	-40 to 137°C
Melting Temperature	370 to 410°C	172 to 184°C	215°C	880°C	280 to 320°C
Common Manufacturing Methods	Hot Chamber Die Casting, Machining	CNC Machining, 3D Printing, Injection Molding	Injection Molding	Hot Forging, CNC Machining, Casting, 3D Printing	Injection Molding, 3D Printing, CNC Machining
Yield Strength	269 MPa	72 MPa	83 MPa	450 MPa	39–70 MPa
Ultimate Tensile Strength	331 MPa	152 MPa	75 MPa	470 MPa	28–75 MPa
Brinell Hardness	91 BHN	N/A*	100 BHN	110 BHN	80 BHN
Coefficient of thermal expansion	2.74E-5 1/°C	8.46E-5 1/°C	6.30E-5 1/°C	1.78E-5 1/°C	6.66 E-5 1/°C
Raw Material Source	Zinc-Lead mines in China, Southern America. [16]	Synthetic, lab produced. Delrin is specific to DuPont. [23]	Coal and petroleum formed into fibers. [30]	Copper components naturally found in mines all throughout the world. [16]	Condensation of carbonic acid and bisphenol - lab made. [52]

Table 2 cont.

Material	Polyetheretherketone (PEEK) [31][53]	Polyethylene Terephthalate (PET) [63][54][51][45]	Mild Steel (AISI 1018) [58] [8][34]	Titanium [35][62] [64] [65][66]	6063 Aluminum Alloy [29][32]
Cost	\$0.12 /cm ³	\$1.10E-3 /cm ³	\$3.93E-3 /cm ³	\$3.47E-3 /cm ³	\$2.37E-3 /cm ³
Density	1.28 g/cm ³	1.38 g/cm ³	7.86 g/cm ³	4.51 g/cm ³	2.69 g/cm ³
Stable Temperature Range	N/A* to 250°C	-60 to 130°C	310 to 400°C	20 to 93°C	300 to 410°C
Melting Temperature	322 to 346 °C	267°C	1450°C	1660°C	660°C
Common Manufacturing Methods	Injection Molding, Additive Manufacturing, CNC machining	Injection Molding, Extrusion, Blow Molding, Thermoforming, 3D Printing	Forging, Tempering, Annealing, Case Hardening	Step-growth Polymerization, CNC Machining, 3D Printing, Injection Molding	CNC Machining, Extrusion, Sand Casting, Permanent Mold Casting, Die Casting
Yield Strength	91 MPa	40 MPa	370 MPa	1100 MPa	195MPa
Ultimate Tensile Strength	70 to 103 MPa	150 MPa	400 to 550 MPa	1170 MPa	241 MPa
Brinell Hardness	210 to 240 BHN	20 BHN	120 BHN	70 BHN	95 BHN
Coefficient of Thermal Expansion	5.00E-5 1/°C	7.02E-5 1/°C	1.20E-5 1/°C	0.86E-5 1/°C	2.34E-5 1/°C
Raw Material Source	Lab created with various organic synthesis methods. [8]	Lab made with PTA and EG along with the presence of a catalyst. [54]	Made from Carbon, Iron, Manganese, Phosphorus, and Sulfur, found in mines. [58]	Extracted using the Kroll process or Hunter process, mining. [11,35,65]	Aluminum (bauxite mining) with magnesium and silicon components (also found in mines). [4,10]

*Gaps denoted by “N/A” above exist in the research due to certain materials being newer and having less documented research regarding their material properties.

The materials in Table 2 are not the final recommendations, and they will serve to provide a baseline for future material research. The team chose to benchmark a broad range of materials that are used for various applications. Zinc Zamak 5 is the current material used for the ring gear, magnet holder, and planet carrier, so it was used as a baseline for further comparisons. With the goal of investigating the properties of a wide variety of materials, the team chose to benchmark different polymers which are usually lower in cost, such as Homopolymer Acetal, Nylon, Polycarbonate, Polyetheretherketone, and Polyethylene Terephthalate, as they are usually cheaper than metals. The team also considered metals, such as Bronze, Steel, Titanium, and Aluminum to gain a better understanding of the feasibility of using materials that are not as commonly used in the Automotive industry, or in the particular actuator system.

REQUIREMENTS AND SPECIFICATIONS

Stoneridge asked us to reduce the cost and weight of the ring gear, planet carrier, and magnet holder without impairing the functionality or packaging envelope of the individual parts and the overall product. To translate this task into engineering terms, the team focused heavily on understanding the function of each part, their interfacing components, and the final functionality of the assembled product. The team communicated frequently with the sponsor to understand the current standard of quality and performance for the SmartBar actuator. From this The team gathered quantifiable metrics of performance and tied them together with the general requirements.

The ranking of importance of the requirements was based on the idea that the renovated product should not be any less reliable, safe, or efficient than the current model. The current product's capabilities therefore need to be replicated or improved in the new/modified design by altering the components of interest. This was emphasized to us by both the sponsor as well as the ME 450 mentor, Randy Schwemmin. All of the requirements are defined and ensure a cheaper and lighter product with the same or improved standard of quality.

After working closely with both the project sponsor and mentor, Table 3, shown below, was made to rank the requirements from most to least important. It also describes the specifications and justifications behind each requirement. It is important to note that requirements ranked 1-3 are the “must haves”, or needs, in the project. Simply put, the team should not jeopardize the reliability and/or performance of the product in order to achieve the deliverables. The “nice to haves”, or wants, are requirements 4-6, ranked with 4 having the highest priority of the three. Requirements 4 and 5 are the overall goals of the project, but failure to achieve them will not intrinsically impact the functionality of the SmartBar actuator. All of the numerical values in Table 3 were either provided by Stoneridge or calculated using the results from the FEA and material research.

Table 3: Requirements and Specifications

Rank	Requirements	Specifications	Justification
1	Has a long lifetime before failure	<ul style="list-style-type: none"> - Withstands > 15,000 shift cycles* - Lasts > 10 years 	Components must be reliable over an extensive time period (values specified by the sponsor) to ensure customer safety and satisfaction.
1.1	Withstands shock and vibration load cases	<ul style="list-style-type: none"> - Withstands >135N +/- 15N axial load on plunger - Withstands > 60 shocks (11 ms shocks of 500 m/s²) - Withstands given vibrational load** - Safety Factor > 1.7 	Components must not fail in different environments and load cases (values specified by the sponsor) to ensure the quality of the product is preserved or improved.
1.2	Each part does not fracture	<ul style="list-style-type: none"> - Ultimate Tensile Strength > XX Pa 	Components must not fracture while under their normal use conditions (implied from Requirement 1).

Table 3 cont.

Rank	Requirements	Specifications	Justification
1.3	Each part does not deform	Coefficient of thermal expansion: Magnet Holder $\leq 9.318 \mu\text{strain}/^\circ\text{C}$ Planet Carrier $\leq 16.46 \mu\text{strain}/^\circ\text{C}$ Ring Gear $\leq 25.74 \mu\text{strain}/^\circ\text{C}$ Yield strength: Magnet holder $> 62.33 \text{ MPa}$ Planet carrier $> 29.98 \text{ MPa}$ Ring gear $> 35.72 \text{ MPa}$ 112 HV $<$ Hardness $< 178 \text{ HV}^{***}$ Young's Modulus $\geq 1 \text{ GPa}^{*}$	The components' resistances to deformation are imperative to their functionalities. The coefficients of thermal expansion were found through first principle calculations, and the yield strengths were found through Ansys and Von Mises. The hardness range was defined in relation to hardness of the planetary gears. The Young's Modulus requirements was defined as the threshold between soft and hard polymers [98].
1.3.1	Operates within robust environment temperature ranges	Does not seize/fail when operated between -40°C to 105°C	Components must be optimized for functionality under extreme temperature conditions (values specified by the sponsor) to ensure that variable weather does not cause failure.
2	Fits within specified packaging envelope ^{**}	Dimensions must be same as given in current drawings	Components must fit within their packaging envelope of current component design (values specified by the sponsor) to ensure that other functionalities within the assembly are not affected.
3	Manufacturing method of each part is capable of tight tolerancing	Tolerance $\leq \pm 0.001$ " for ring gear and planetary carrier Tolerance $\leq \pm 0.002$ " for magnet holder	Tolerance must be the same or tighter than listed in part drawings (values specified by sponsor CAD drawings).
4	Reduce Cost ^{**}	$< \$0.67$ for Magnet Holder $< \$0.32$ for Planet Carrier $< \$1.20$ for Ring Gear	New components should be cheaper than current components to ensure that Stoneridge remains ahead of its competitors (values specified by the sponsor).
5	Reduce Weight ^{**}	$\leq 36.01\text{g}$ for Magnet Holder $\leq 16.40\text{g}$ for Planet Carrier $\leq 86.37\text{g}$ for Ring Gear	New components should be lighter than, or the same as, current components because weight can be directly tied to cost (values specified by the sponsor).
6	Materials should be ethically sourced	Achieve Fairtrade Standards or meet equivalent requirements laid out by Fairtrade. [25]	Components or design changes should not include materials or require practices that have negative social or environmental implications.

* A cycle is defined as both the extension (disengagement of shaft collars) and retraction (engagement of shaft collars) of the plunger

** Power-spectral-density (PSD) loading data is located in Appendix D

*** The hardness specification only applies to the ring gear, as the range is that of the planetary gears' hardness

*' The Young's Modulus only applies to the planet carrier and magnet holder, as they must remain rigid for this application

**' This requirement was relaxed when brainstorming potential assembly optimizations

**' These requirements, unlike the prior ones, are wants rather than needs for functionality

As further analyses and ideas were explored between DR 2 and DR 3, Table 3 was amended. Requirement 1.2, the grayed out column, is no longer in consideration due to its overlap with the yield strength specification of requirement 1.3. None of the components can yield if they are to function as required, so the minimum yield strength will intrinsically account for the minimum ultimate tensile strength. The specification value was therefore not specified. It is also worth noting that requirement 1 will be verified by Stoneridge. This is discussed further in the Verification and Validation Plans section.

Specification Assessment Plans and Challenges

Some difficulties that the team encountered when assessing the engineering specifications included researching accurate material property values and estimating manufacturing and sourcing costs. The team also had numerous knowledge gaps for FEA due to inexperience. While conducting the analyses, the team needed to simultaneously learn the Ansys software, request technical assistance if stuck on a problem, and refresh knowledge on material behavior. The team also had challenges when looking for material property values to compare with the specifications, especially for materials that are newer and have less associated documentation. This required extensive research, and the team eventually began using the Ansys Granta EduPack instead of sourcing information from various databases. When estimating the costs of manufacturing and sourcing materials, the two main challenges were compiling a realistic estimation of costs and communicating with suppliers, as they had little to no incentive to give us information in a timely manner. The team therefore conducted research on various manufacturing methods for this task, and the results are discussed further in the *Cost Analysis* subsection. Despite these challenges, the team found the specification values for coefficient of thermal expansion, minimum yield strength, hardness, and minimum Young’s Modulus. Some of the specifications involved calculations that required review and use of past theory, and these are discussed in the Engineering Analysis section.

ENGINEERING DESIGN STANDARDS

Table 4. Relevant Standards

Standard	Standard Description	Relevance
ISO 1328-1:2013 [2]	Sets flank tolerance definitions for cylindrical gear teeth	The team is changing the manufacturing methods for the ring gear.
SAE J1950 [2]	Guidelines for corrosion testing for ground vehicles	Components in the system must not corrode before a lifetime requirement of >10 years.
ISO 6336-5 [5]	Calculation of Load Capacity of Spur and Helical Gears - Part 5: Strength and Quality of Materials	The team will need to calculate the load on the gears to use for stress analysis.
AGMA 2000-A88 [12]	Gear Classification, Materials, and Measuring Methods for Unassembled Gears	The team will need to evaluate the heat treatments, materials, and hardness ranges for the generated designs.
ANSI/AGMA 6123-A06 [12]	Design Manual For Enclosed Epicyclic Gear Drives	Components the team is optimizing are part of a planetary gear train and must follow standards for manufacturing, assembly, thermal rating etc.
ISO 10825 [2]	Gears – Wear and damage to gear teeth – Part 1: Nomenclature and characteristics	The team must consider the ways that the components might fail

Table 4 on the previous page presents the engineering standards that are relevant to the project. These standards will be important for us to follow to ensure the designs are safe and are of high quality. These standards are chosen with relevance to the primary design requirements. They address the rules that the team must follow for material selection, gear characteristics, and manufacturing of the components.

DESIGN PROCESS

Design Process Structure

To fulfill the needs of the project sponsor and meet the requirements for the design, the team will follow a structured design process. The major phases of the design process will include Problem Definition Development, Requirements and Specifications Development, Concept Exploration and Material Research, Solution Development and Verification, and Final Solution Proposal. These phases are presented in figure 11.

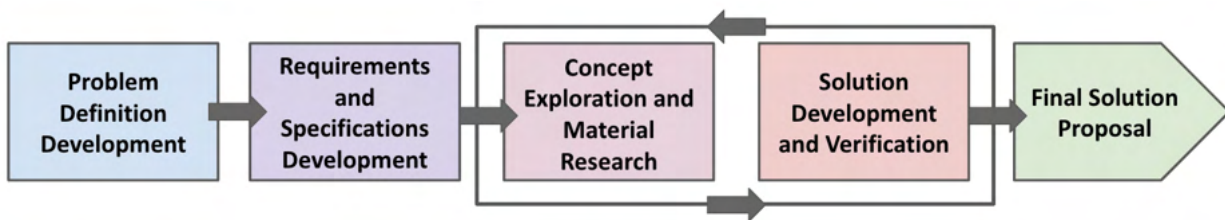


Figure 11. Model of the design process phases.

The team has followed the model above and is finalizing the solution proposal for the project. Concept Exploration was thoroughly explored as to find alternative methods to reduce both weight and cost of the components assigned. Approaches for concept exploration include brainstorming, functional decomposition, and concept screening. Material research will take place at the same time to ensure that Stoneridge's primary objective, to receive alternative materials for the three given components, is met. More behind the design exploration process and results can be found in the Project Scope Expansion section. Solution Development and Verification focused on ensuring that the designs meet all the design requirements, including manufacturing and cost reduction assessments. The team used simulation software (Ansys) to perform FEA on three cases: the current baseline system with its original geometry and materials, a system with the original geometry and new selected materials, and a system with the optimized geometry and the new selected materials. This will be done to compare the performance of the altered systems to that of the baseline. The final step of the design process will be the Final Solution Proposal, in which the team will give options of materials for both the original and structurally optimized (topology) geometries of the ring gear, magnet holder, and planet carrier.

The design process follows the ME 450 Capstone Design Process Framework (in figure 12 below), with emphasis on Problem Definition, Concept Exploration, and Solution Development and Verification since the Need Identification and Realization are out of scope for this class [18].

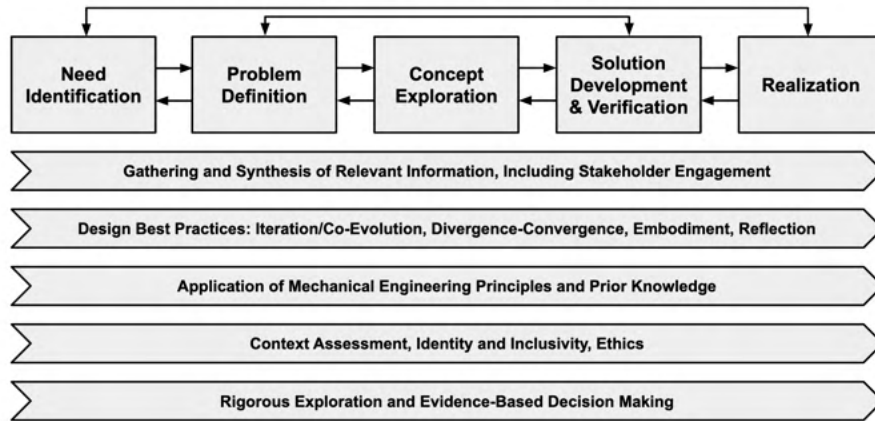


Figure 12. ME 450 Capstone Design Process Framework [18]

The design process differs slightly from the ME 450 Framework because Concept Exploration and Material Research fall into the same stage of the process. This is because the SmartBar project focuses heavily on material research for the three components of focus, which is why the team combined the research with concept exploration activities to stay on track with the course milestones.

Due to the nature of the project, the team’s design process references Blessing’s model from the Models of Designing, Wynn and Clarkson text. This model represents a cyclical, activities-based approach which closely aligns with the team’s chosen design process. This is because the team will conduct the same analysis process on many different materials in order to iteratively test [73]. Figure 13 (a) presents a diagram of this model from Wynn and Clarkson text [73]. It will include finding the cost and manufacturing methods for each material. These will be repetitive activities that the team will complete in the Solution Development and Verification phase. The team’s design process also references Cross’s Model (Figure 13 (b)) because it includes feedback from the Generation and Evaluation phases. This is included in the team’s model using cyclic arrows between the Concept Exploration and Material Research and Solution Development and Verification phases [73]. The team experienced these phases to be highly iterative which is why there are cyclic arrows.

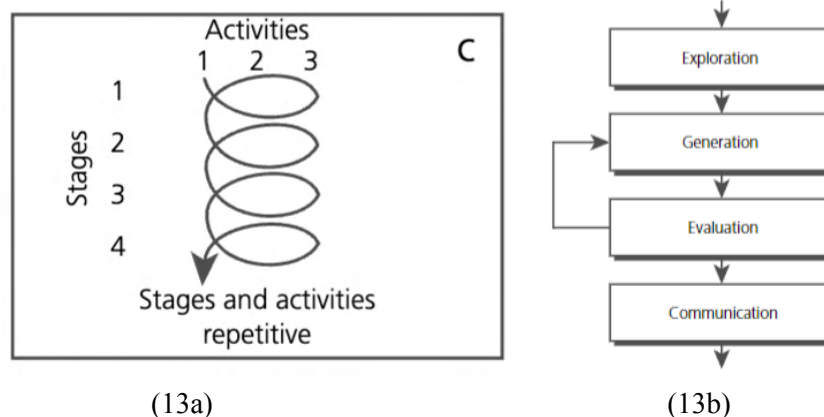


Figure 13: Figure 13a (left) is from the Wynn and Clarkson text and depicts a stage-based repetitive activity model. Figure 13b (right) is a diagram of Cross’s Model from the Wynn and Clarkson text, which also addresses the nonlinear design process and cyclic nature of the generation and evaluation phases [73].

The design process differs slightly from Blessing's model, as not all of the stages have a set of repetitive activities that the team must complete, such as the Problem Definition Development phase. This is represented in the model (Figure 11) which has cyclical arrows for the Concept Exploration and Material Research and the Solution Development and Verification phases. The design process aligns closely with Cross's model [73]. The Wynn and Clarkson text explains that exploration consists of defining the problem, while generation includes concept exploration, and evaluation consists of testing the concepts [73]. This is very similar to the design outlined in figure 13b. The team's process only differs because there is an individual stage for Requirements and Specifications.

DESIGN CONTEXT

Throughout the design process, it is important to assess and understand the contexts in which the solution will be implemented and whom it will affect. A previous section of the report discussed stakeholders and the impacts that this project will have on them and the effect they will have on the project.

The social and societal incentives for this project are complicated because the end users will not be directly interacting with the end product. At a large scale, however, if the team is able to reduce the cost of the SmartBar actuator by a significant amount, Stoneridge may be able to sell their components at a lower price. This could then result in Stellantis selling the cars at a more affordable price.

The largest social impact the team has identified so far is the sourcing of the materials that will be chosen to go into production. The project sponsor has outlined that the goal of this modification is to reduce cost of production, and did not address social impact, so it is clear that the priorities lie with reducing cost. This means that the team must take into account if the materials are sourced ethically and what the costs are of producing with other materials that aren't just monetary. For example, the current material used is die cast Zinc Zamak 5. "Several studies regarding environmental and health risks in connection to Zinc mining in China have been published [that discuss natural] lead-Zinc mines, not only Zinc mines. They conclude that Zinc, lead and cadmium are released into the surrounding environment, polluting soil and crops, thus posing health risks to humans [including illnesses like] 'metal fume fever'[16]." When exploring alternatives to the current material, it is vital to understand the source of these components. It is unclear where the zinc used in current production comes from directly, but when recommending a material this ethical dilemma will be heavily taken into consideration, with the intention of sourcing materials from safe and ethical environments.

In terms of sustainability, it is important to understand the lifetime of this equipment. The SmartBar is required to last for 10 years, so it is not a part that should need to be replaced or have any single use components. In the material exploration, the team will look into how each material is disposed of at end of life (e.g. recyclability) and what that associated cost would be. The system itself, when used, does not emit pollutants or consume any resources besides electricity. The production of the components depending on the manufacturing processes could, however. The team will explore sustainable options in materials, from sourcing to end of life, but it is uncertain whether those solutions will be entertained. The personal ethics of the team align on wanting to think sustainably and use this opportunity of selecting a material and optimizing the assembly to do so in a way that would positively impact the world. Unfortunately, this brings us into an ethical dilemma along with an issue in the power dynamic between us, the class expectations, and Stoneridge's goals. The majority of for-profit companies would select the best performing assembly and material that is the cheapest no matter the impact. This does not align with the team's ethical values, however due to the distribution of power within the circumstances, the team will

not be the ultimate decision makers in this scenario. An aspect that may be a further point to explore in order to incentivize alignment of ethical decisions and fiscally responsible ones could be the potential of government subsidies or tax write offs that may be available to Stoneridge should they choose this path.

The University of Michigan - College of Mechanical Engineering has a curriculum that a student must undergo in order to be awarded with a degree, which makes a degree from this program quite valuable. A part of this is the rigor of curriculum within each course, especially within design based classes with such an open ended scope. In this class, the team has a sponsor with certain expectations that must be met, and they would like the problem solved as specified. Stoneridge also owns all of the intellectual property that may be created in this project. The course instructors, however, would like us to broaden the scope in order to undergo the full design process required to pass this course. This disconnect and both parties having power over the team is important to acknowledge. The team has already begun working with the instructors to help mitigate this disparity.

MATERIAL SELECTION

Concept Generation

Additional materials need to be researched to determine materials to test on Ansys. The team planned to determine these materials by first analyzing the first iteration benchmarking in Table 2. This table is a list of common materials used in automotive and actuator applications. The team planned to observe the top priority requirements and find materials that are comparable or are better for meeting the requirements compared to Zinc Zamak 5. For example, pure titanium has a stable temperature range of 20 to 93°C, which does not meet Requirement 1.3.1 (refer to Table 3). The team will therefore not focus any further research on titanium and ensure that future possible material alternatives strictly comply with the specifications relative to their requirements. However, titanium alloys are still under consideration, as they have varying stable temperature ranges. A similar approach was planned to be taken for the other currently benchmarked materials and their material properties. The team initially planned to consider this method to be the first filter (Filter 1) for converging the concept generation. The flow chart with these steps are presented in figure 14. Table 5 below is a tool that the team created to more efficiently benchmark the applicability of alternative materials with Zinc Zamak 5 by using material characteristics that can be easily researched from available literature online. Thus it makes the approach of filtering/iterating through hundreds of materials more feasible.

Figure 14 on the following page presents a comprehensive overview of the initially planned process described for concept generation and concept selection.

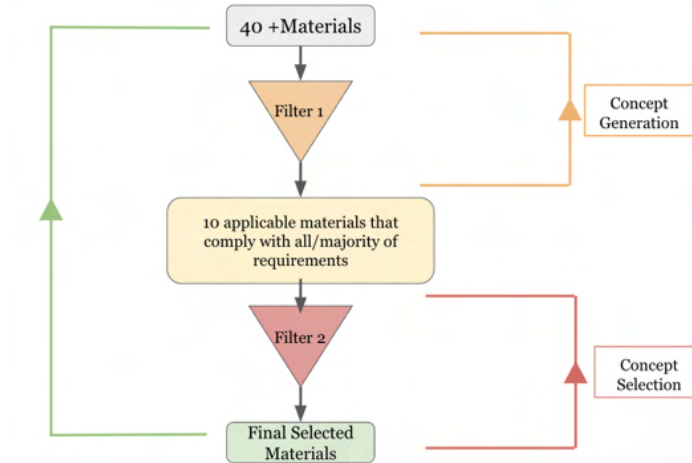


Figure 14. This figure comprises the concept generation and selection plan that the team will take to select materials for testing. Filter 1 uses the requirements listed in Table 5. Filter 2 uses Ansys to determine the rest of the requirements (presented in Table 6) and will further narrow down the best materials which the team will present to Stoneridge.

Table 5. Filter 1 - Material Characteristics

Material Characteristic	Conjoined Requirement	Justification
Yield Strength	Requirement #1.1 & Requirement #1.3	Yield Strength is very influential in the behavior of the components under varying loads. Since load cases will be constant in all analyses, the impact of this property will be comparable with alternatives.
Coefficient of Thermal Expansion	Requirement #1.3	The coefficient of thermal expansion is a quantitative value that can be directly compared to other alternatives given that the tolerances for temperature are constant for all thermal analyses.
Stable Temperature Range	Requirement #1.3.1	Ensuring that the material is stable within the tolerances provided by the sponsor is a simple way of understanding where it stands against their alternatives.
Cost	Requirement #4	Raw material sourcing is one of the main contributors to final part cost. Therefore, it will heavily influence the outcome of fulfilling the requirement. It is a quantitative value that can be directly compared to alternatives.
Density	Requirement #5	Density of the material is the only factor that will dictate the outcome of fulfilling the requirement. This is due to geometries being constrained in the problem scope of material selection. The direct relationship allows for simple comparison of alternatives.

Concept Selection Process

The team planned to continue to iterate the concept generation process until a list of ten or more alternative materials meet all or the majority of the requirements. These remaining requirements will be determined from the Ansys simulation testing and are shown in table 6. This table serves as the tool for Filter 2 presented in the concept generation and selection diagram in figure 14.

Table 6. Filter 2 - Testing Approach for Requirements

Requirement #	Testing Approach
1	Ansys Analysis: Static Analysis
1.1	Ansys Analysis: Shock and Vibration Load Case Tests
1.3.1	Ansys Analysis: Steady-State Thermal Analysis at max/min operating temperatures
2	Ansys Analysis - CAD Simulation will validate packaging envelopes
3	Limited quantity trial run from manufacturer for capability and tolerancing assessment
4	Ansys Analysis: Cost analysis for each component
5	Ansys Analysis: CAD Simulation will define weight of each part
6	Analysis of ethical sourcing methods to ensure Achieve Fairtrade Standards are met

Given the nature of the problem scope and deliverables, the engineering analysis is heavily intertwined with the concept selection process. This is because some of the requirements were derived from Ansys simulation test results as shown from the testing approaches in Table 6. Further details on the concept selection process that the team used is detailed below.

To most accurately define the performance of the materials within the defined geometries of the given parts, FEA (Finite Element Analysis) was performed with Ansys software. This enabled the team to apply specific and realistic constraints onto the parts with their relative loading conditions acting on them from their interfacing parts. The Ring Gear, Planetary Gear Carrier, and Magnet Holder had several FEA Analyses conducted on them to benchmark the performances of the suggested material alternatives as listed in Table 2. After obtaining the final specification values from FEA, the team conducted a cost analysis. A pugh chart was then used as the method to compare these final requirements, in addition to the rest of the already defined requirements.

The Material Concept Generation and Concept Selection Process described above were the initial plans for finding a top list of materials. After researching material selection tools, the team discovered the Granta EduPack Material Selection tool. This tool was used to filter the list of materials to a list of 10-20 top applicable materials for the magnet holder, planet carrier, and ring gear. As previously mentioned, the concept generation process and engineering analysis phases in the project greatly overlapped. A more extensive discussion of the Granta EduPack tool that was used for the material selection process is described under the *Engineering Analysis* section for *Material Selection Using Granta EduPack Material Filtering Tool*.

PROJECT SCOPE EXPANSION

Concept Generation

In order to promote a productive brainstorming session, the team first individually came up with 20 ideas each and brought them to the team meeting. As a team, methods like design heuristics and morphological charts with functional decomposition were used to provoke more creative ideas. The team will highlight the collaboration on these methods, but the individual documentation of the concept generation can be seen in the *Individual Concept Generation* section of the Appendix. A large emphasis was placed on the subfunctions of the actuator, addressing these with each concept generation method used. This actuator has many, but the key subfunctions were the ability to detect whether the collars are engaged or not, if there was a safety feature that would lock when no power was connected, and if it succeeds in permitting free rotation between the two halves when the collars are in an unlocked position. When the team came together to combine the ideas and begin to come up with more, the ideas generated were classified into addressing one or more of those subfunctions. There was also a star assigned to the concepts that addressed material selection as well, as that is something the problem statement calls for in addition to the design concepts.

The first method the team used to generate concepts was a morphological chart, shown in Table 7 below. As taught in the course learning blocks, “the morphological chart is a method to generate ideas in an analytical and systematic manner [where] various functions and sub-functions of a product can be established (or "decomposed") through a function analysis” [90]. Below shows one morphological chart with functions of the magnet holder being the main analysis point.

Table 7. Morphological Decomposition Chart

Sub-functions	Works with the hall sensor to track rotational movement of the components.	Rotates with the drive screw	Must withstand vibration and shock loads, and torque load from the drive screw
1	Proximity sensor for the drive nut	Merge drive screw with magnet holder	Shock absorbing (rubber) coating on the magnet holder
2	Limit switch connected to magnet holder	Shrink fitting between drive screw and magnet holder interface	High yield strength material
3	Use a motor with an encoder	Key fitting between drive screw and magnet holder	Lubricant for smooth torque transfer
4	String potentiometer to measure linear translation distance	Dovetail joints	Add additional bearing and bushing that will withstand the axial and torsional loads from the drive screw
5	Pressure sensor connected to the spring	Threaded connections	Add additional reinforcements (brackets) for stability

The next method the team want to highlight is design heuristics, which is “an idea generation technique [that] allows us to capture unique information about strategy use that has not been captured

in previous prescriptive approaches to idea generation” [77]. This approach provides a list of 77 different prompts that make the designer think about the problem and solution from a different perspective. One of the design heuristics that inspired new concepts was number 63, *substitute way of achieving function*. From that heuristic, the team was able to come up with over 8 different sensor ideas like proximity sensors, encoders, linear actuators, as well as different mechanical aspects like a lock or braking system to stop the gear train that can be unlocked with a force like a seat belt. Another heuristic The team used was to 20, *change the geometry of the system*, sparking one of the most promising ideas: exploring topology. This topic is discussed further later in the following subsection, *Topology Optimization*. A diagram of all the concepts generated using the design heuristics methods is presented in Figure 15.

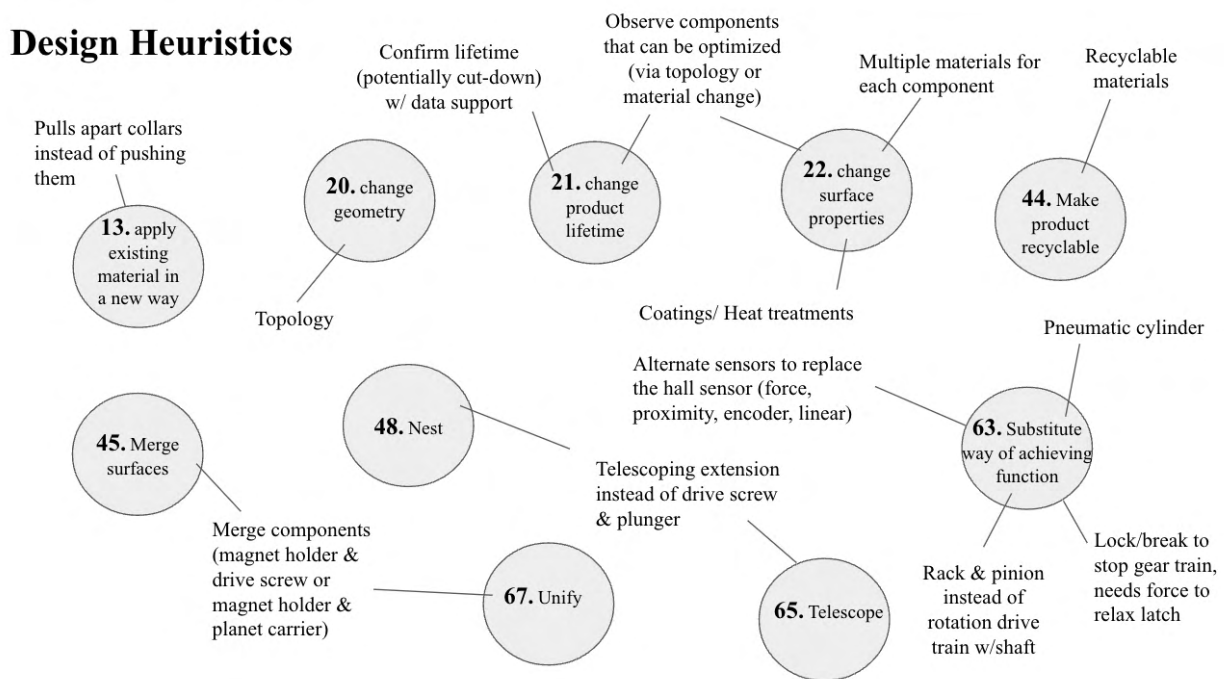


Figure 15. Using design heuristics, the team was able to use divergent thinking to generate a wide variety of unique contacts.

Topology Optimization

Topology optimization is the altering of the distribution of material within a defined domain or component, while still considering loads, constraints, boundary conditions, and manufacturing as well as reducing cost [84]. The team’s goal will be to balance the decrease in material costs with the potential increase of manufacturing and tooling costs. This can be done through mathematical models and algorithms on various software, but the team has decided to use Ansys. An example of what topology optimization could look like on an arbitrary gear is shown on the following page in figure 16.

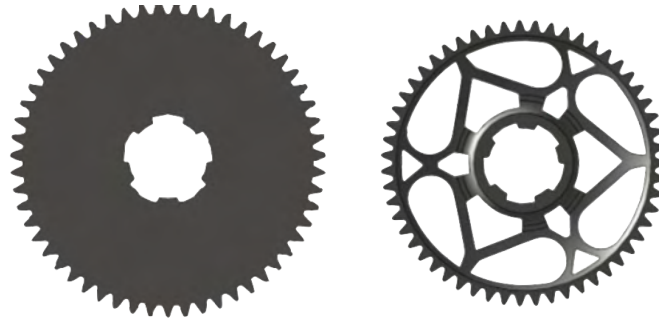


Figure 16. An example of topology optimization in which material is removed from non-crucial areas of a gear. Crucial features, such as the teeth and shaft hole, remain. [85]

Concept Selection Process

Once the generated concepts were compiled, the team narrowed them down using concept screening, evaluation, and selection. The team first utilized concept screening by applying a series of filters to the preliminary 160 ideas in order to organize them. The first of these was a “gut check”, which involved removing concepts that would obviously not work due to reasons such as not being technically feasible or not aligning with the project requirements [18]. This removed around 100 of the generated concepts. The team then examined the remaining ideas and combined ones that had similar methods of action, which left around 12 concepts remaining and is shown in the *Individual Concept Generation* section of the Appendix. The team then conducted concept evaluation, in which the remaining solutions were examined in relation to the design requirements. The main requirements considered were the impacts on the lifetime and current SmartBar packaging envelope and design, as a change to any encasing components would likely mean that several other parts would require alterations. Using these methods, the team decided on the four best concepts to move forward with into concept selection.

Some of the reasoning included that topology optimization will reduce weight and keep the parts within their current envelopes. It is a definitive route to reducing weight, while causing the least impact on the rest of the assembly. The team also chose replacing the hall sensor and current gear train as options because they allow for further concept generation, remove several components, and could reduce the system cost and weight. The team thought that merging components would decrease cost by combining manufacturing processes. It is worth noting that the team’s first concept idea when the project was assigned was using topology optimization due to a member’s individual research. This concept was not fixated on, but it remained an option throughout the concept selection process, as it aligned closely with the project requirements. This is proven by the following discussion.

The team utilized a Pugh chart, Table 8 below, in order to compare the four design optimization concepts against each other. Each concept was given a score of -1, 0, or 1, with 0 corresponding to a neutral impact on the criteria and -1 and 1 corresponding to a negative and positive impact. The criteria is derived specifically from the requirements and specifications, Table 3 above, and the rows with no relevant scoring information are grayed out. Further information on the concepts below are included in the *Pugh Chart 2 Concepts* section in Appendix A.

The sub-requirements of the “Has a long lifetime before failure” requirement were lumped into the parent for simplicity. The weighting for the criteria was decided using team discussion and the existing

requirement and specification rankings. Requirements for the operation of the device were ranked the highest, as they are necessary for both the course’s and sponsor’s scopes. Reducing cost and fitting within the packaging envelope are desired but not fully necessary, so they were given a slightly lower weight. The Stoneridge sponsor emphasized reducing cost over weight, tolerancing of the scoped components is not crucial, and ethical material sourcing is not fully up to the team’s discretion, as discussed in the *Design Context* section. Therefore, these criteria were ranked the lowest for concept selection. As seen from the chart, topology optimization had the most total points, so the team decided to move forward with it as a design optimization. However, in order to complete the concept development steps that are required for the scope of the course, the team also decided to move forward with replacing the hall-effect sensor as a second design optimization.

Table 8. Pugh Chart for Preliminary, Broad Design Optimization

Criteria	Weight (1-5)	Topology Optimization	Replacing Hall-Effect Sensor	Replacing Planetary Gear Train	Merging Components
Safe for assembler and end user	5	0	0	0	0
Has a long lifetime before failure	5	0	0	0	0
Fits within specified packaging envelope	4	1	-1	-1	1
Reduce cost	4	0	1	0	0
Reduce weight	3	1	1	0	0
Manufacturing method of each part is capable of tight tolerancing	3	-1	0	0	-1
Materials should be ethically sourced	2	0	0	0	0
TOTAL		4	3	-4	1

Updated Requirements and Specifications

The requirements and specifications for the topology optimization concept will remain the same as the original list in the *Requirements and Specifications* section. This is because the components will be functionally the same, so they will align closely with the material selection requirements. However, the requirements and specifications table for specifically the sensor selection will include the additional rows shown on the following page in table 9. This updated list, in addition to the original, was used in the process described in the next section to both generate and select relevant sensor replacement options.

Table 9. Sensor Specific Requirements and Specifications

Ranks	Requirements	Specifications	Justification
1	Collar can be engaged and disengaged	Extends and retracts the plunger XX mm +/- XX mm	Plunger should still be capable of accurate extension and retraction parameters to ensure the repeatability and reliability of the SmartBar is preserved or improved.
2	Switching mechanism sets motor constraints at retracted and extended plunger positions	- Extension - Motor shaft rotates XX times CCW - Retraction - motor shaft rotates XX times CW	To accurately displace the collars, motor parameters must be defined and applied in a repeatable way.
3	Wires/sensor components must not obstruct the functionality of other parts	- Wiring < XX m in length - Wiring < XX m in diameter	The component must remain within its specified packaging envelope to ensure that there are minimal failure modes/altercations between sub-assemblies.
4	Accurate	- Accuracy error of 0.5% [78]	Must have a small margin of error to ensure that the plunger is consistently within its specified parameters.
5	Precise	- ± 1 mT [78]	Precision is extremely important to ensure repeatability in the system, acting as a preventative for possible failures in function.

The requirements ranked 1 and 2 are system functions that must be accomplished despite any sensor changes. Requirement 3 is a need that must be met in order to not disturb other components within the system. Accuracy and precision are the lowest priority because the system could still function without them, but they are necessary for proper functioning. The specification values in Table 9 that are depicted as XX's will not be filled, as these added requirements are only for sensor selection, and they will not be considered going forward. Having a failsafe in case of loss of power was also considered as a sensor specific requirement, but there is already a secondary failsafe sensor that mechanically detects when the ring gear spring is in its engaged and disengaged positions.

REPLACING HALL EFFECT SENSOR

Concept Generation

The first Pugh chart concluded that in order to expand the project scope The team should explore topology or replace the hall effect sensor. In order to understand what the options were for replacing the hall sensor, as that is a broad design change, the team repeated a very similar process as the scope expansion concept generation in order to come up with more specific ideas of how The team could achieve a similar result with a different mechanism. For this concept generation, The team used mainly functional decomposition and determined the necessary functionality of the hall sensor (current design). These criteria are shown below in Table 10.

Concept Selection Process

This concept generation process resulted in fewer concepts than the previous due to the more limited scope. Therefore, the team only needed to combine similar ideas in order to narrow down the selection. The resulting concepts are shown below in the sensor-specific Pugh chart, Table 10. The scoring scheme is similar to the preliminary Pugh chart above, but the -3 through 3 values were based on a comparison to actual values of a hall-effect sensor. Real values were also found for the five sensor concepts, but they were translated to the stated scoring scale in order to compare. A 0 corresponds to a similar criteria value, more negative corresponds to a less optimal value, and more positive corresponds to a more optimal value. The hall sensor's total score is 0 and sets the baseline for all other sensors. The criteria are derived from a combination of the original and sensor-specific requirements and specifications, and the rows with no relevant scoring information are, once again, grayed out. The green criteria are the sensor-specific requirements mentioned previously in Table 9. The relative weights for the additional sensor specific criteria were decided using team discussion and the ranking reasoning within the *Updated Requirements and Specifications* subsection of the *Project Scope Expansion* section. More detail on the concepts below can be found in Appendix B.

Table 10. Pugh Chart for Sensor Selection

Criteria	Weight (1-5)	Current Design - Hall Sensor [78]	Motor with encoder [79]	Proximity sensor for drive nut [80]	Limit switch [81]	String potentiometer [82]	Pressure sensor [83]
Has a long lifetime before failure	5	20 years	-2	-1	-2	-2	-1
Safe for assembler and end user	5	RPN < 100	0	-1	0	-2	-1
Collars can be engaged and disengaged	5	N/A	N/A	N/A	N/A	N/A	N/A
Switching mechanism sets motor constraints at retracted and extended plunger positions	5	N/A	N/A	N/A	N/A	N/A	N/A
Fits within specified packaging envelope	4	60 x 12 x 5 mm	-2	-3	-1	-2	-3
Wires / sensor components must not obstruct functionality of other parts	4	wireless, connected via pins to PCB board	-2	-2	-1	-2	-2
Reduce cost	3	\$1 each	-3	-2	-1	-3	-2
Reduce weight	3	45 g	-3	-2	3	-2	-1
Accurate	3	0.5%	0	-1	-2	1	-1
Precise	3	± 1 mT	0	-2	-1	0	-3
Manufacturing method of each part is capable of tight tolerancing	2	N/A	N/A	N/A	N/A	N/A	N/A
Materials should be ethically sourced	1	stainless steel	-1	-1	0	1	0
Total			-45	-52	-21	-47	-51

The most critical criteria were a long lifetime and safety, so these played a larger role in the scoring of the Pugh chart. As shown in Table 10 above, the hall-sensor clearly has the highest total score, as the other five concepts have very negative values. The team felt that the Pugh chart was comprehensive of all of the necessary design elements, so the hall sensor will be used rather than a replacement. Therefore, the only design optimization that the team will pursue is topology optimization.

Topology Optimization Alpha Solution

The analysis that must be done for topology optimization is running a software algorithm on the magnet holder, planet carrier, and ring gear with both their original material and the final chosen 5-10 proposed materials. The team used SolidWorks for the preliminary iteration due to its simplified FEA interface and each member's familiarity with it, but Ansys will be used for all future iterations. This involved applying various arbitrary loads and constraints to a part, the planet carrier in this case, as The team do not currently have the exact load values that will be applied for the final analyses. Equal, arbitrary loads were applied radially, in the clockwise direction, to the three planetary gear holes. The team then applied an arbitrary torque to the center shaft hole and set each hole as a critical geometry. The team used these arbitrary constraints in order to gauge general behavior in specific areas to have a better idea of expected failure modes. This first iteration is shown below in figure 17. The middle and right planet carriers have had a 25% mass reduction applied to them, and the right has had an additional color scale applied to indicate which material is alright to remove.

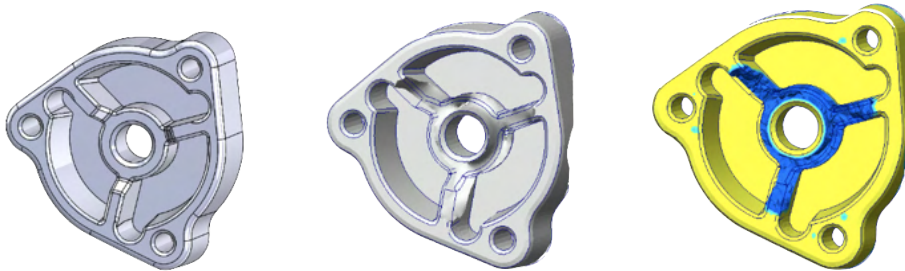


Figure 17. The original, unedited planet carrier is shown on the left, the planet carrier with a 25% mass reduction is shown in the middle, and the middle carrier is shown on the right with colors indicating which material is necessary to keep. Yellow indicates the material that must remain, and blue indicates material that could be removed while maintaining original functionality.

Topology optimization only involves removal of material, so the layout of the magnet holder, planet carrier, and ring gear within their subsystems will not differ.

The team chose this concept due to moderate sponsor influence to not make large design changes as well as the time constraints of the course. However, this selection was supported by use of a Pugh chart, so it is the optimal solution for the team to pursue in this context. It is also worth noting that no numbers during material selection were fudged or inaccurate, and the analyses were conducted with integrity. The selected concept of topology optimization is defined in a similar manner as the material selection project component, and the optimized parts will be analyzed using FEA accordingly.

ENGINEERING ANALYSIS

All of the following engineering analyses were performed in order to conduct accurate simulations with appropriate forces and constraints. The first portion defined the baseline yield strength for each of the components's materials through applying calculated loads. The second portion then used FEA to confirm each material's performance. This was completed with the goal of providing to Stoneridge a list of materials that meet all of the requirements and specifications but that also have a reduction in cost and weight.

Material Selection Alpha Solution

As this project has seemingly two paths of discovery, the first FEA iteration is also the alpha solution when it comes to the material selection. Based on this first iteration the team was able to collect excellent insight into failure modes of the components and which characteristics. The team can set limits to produce a more refined list of potential alternative materials.

Material Selection Using Granta EduPack Material Filtering Tool

The team chose to use the Granta EduPack material database in order to filter through 1930 metals and 974 polymers to find potential alternative materials. This software was used in the MECHENG 450 course curriculum, so the team had familiarity with the interface and was able to quickly learn to filter through this database, deriving the requirements from the information the team collected from the alpha solution. This source for material information is trusted not only because this resource was used in MECHENG 450, but also because Granta EduPack is a software company owned by Ansys. Ansys is a highly trusted company when it comes to simulation software and widely used by companies across the world and is constantly updated, so the team knows that the sourcing of the information within the database is consistent and comparable throughout different materials.

Table 11: Material Selection Requirements for Granta EduPack

Property	Value	Justification
Magnetic Type	Non-magnetic	Hall sensors transduce magnetic fields, and having ferrous materials may cause interference to this system's accuracy
Density (max)	6749.99 kg/m ³	≤ Current Zinc Zamak 5 component density, assuming no volume change
Service Temp. Range	-40°C to 105°C	From Stoneridge's provided specifications
Manufacturing process	Polymers: Injection Molding Metals: Die Cast	Limited process options to these due to part geometry and mass production capability
Yield Strength (min)*	Planet Carrier: 29.98 MPa Magnet Holder: 62.33 MPa Ring Gear: 35.72 MPa	Derived from static FEA principal stresses based on maximum load cases. Safety factor of at least 1.7 (2) was used.

Thermal Expansion Coefficient (CTE)*	Planet Carrier: 16.46 $\mu\text{strain}/^\circ\text{C}$ Magnet Holder: 9.318 $\mu\text{strain}/^\circ\text{C}$ Ring Gear: 25.74 $\mu\text{strain}/^\circ\text{C}$	Based on part interfaces and related part CTEs, specifically on press fit/ slip fit and gear mesh interfaces.
Hardness**	112-178 Vickers	Only used for the ring gear. This range is the same as the provided hardness range of the planet gears that interface on the ring.

* The values differ depending on component

** The hardness specification only applies to the ring gear, as the range is that of the planetary gears' hardness

In Table 11, various values are listed which were used in order to refine the results of nearly 3000 materials in order to produce a list of applicable materials to test in FEA. Some of these properties have an asterisk denoting that the value varies based on the component. This is the case for yield strength because it is derived from the load cases applied on the specific geometry of each part. Similarly, the coefficient of thermal expansion and the hardness limitations are based on the properties of the parts that the selected component interfaces with. Hardness was only considered on one of the components, the ring gear. This is because the geometry of gear teeth requires a hardness consideration due to the nature of the force direction and concentration on gear teeth. Therefore, a significant difference in hardness could cause one gear to deform or even fracture the other gear. The other parts had no geometries interacting with an impact force, so hardness was not considered. The yield strength and CTE calculations will be described more in depth in the coming sections of Engineering Analysis. The team was sure to incorporate stakeholder feedback in the decisions that were made, mainly on the limiting of the manufacturing process. The team spoke to the stakeholders and lead engineers responsible for the actuator, and confirmed that injection molding and die casting were familiar processes used by Stoneridge. Therefore, based on the geometries and production quantities of the components, they would be comfortable limiting processes to solely those two methods. Additionally, the team was encouraged to explore polymers only for the planet carrier and magnet holder after the team provided evidence to the necessity of hardness requirements for the ring gear.

First Principles Force Analysis for FEA

To select materials that will meet the requirements and specifications, the ring gear, planet carrier, and magnet holder will need to be appropriately modeled with the loads that they will experience during their performance. These loads will be determined using first-principles force analysis on each component. A diagram of the components of the planetary gear train and the associated rotation directions of each component are presented in figure 18. Counterclockwise is denoted by CCW and clockwise is denoted by CW.

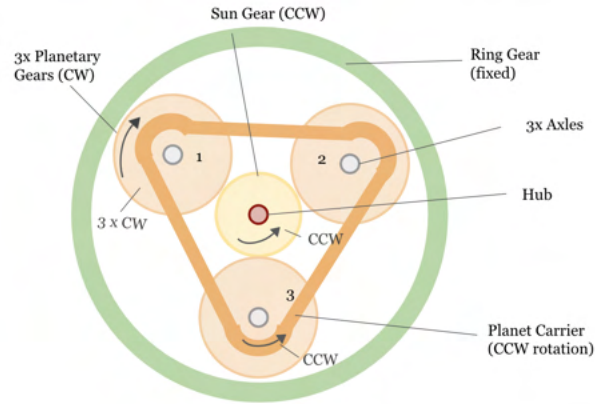


Figure 18. The ring gear, sun gear, planet gear, and planet carrier are presented with their associated rotation direction.

The rotation direction of the sun gear (CCW) was provided to us by Stoneridge. It is driven by the motor connected via the hub which rotates in the CCW direction when looking at the plunger end. Consequently, each planet gear moves in the opposite direction (CW). The three planet gears together move in the CCW direction. The planet carrier moves along the CCW direction via the three axles that connect the planet carrier to the planet gears. The ring gear is fixed and does not rotate.

The output spring force to fully extend the plunger is $135\text{N} \pm 35\text{N}$ (F_{spring}) as specified by Stoneridge. As the spring compresses, this force pushes against the plunger to extend it forward. The location of this force is shown in figure 19.

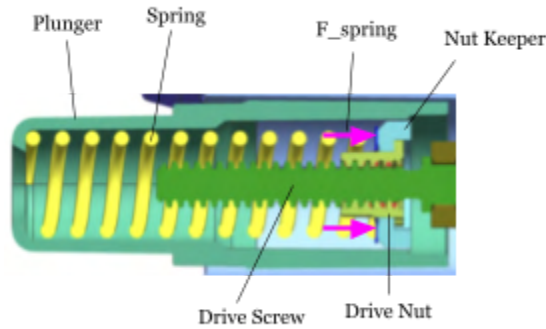


Figure 19. The load F_{spring} is shown at the location the drive nut will experience the load. A cross-sectional view of the major components at the plunger end of the actuator is depicted.

The spring force (F_{spring}) pushes against the drive nut keeper which also pushes against the drive nut. These forces result in a torque experienced by the drive screw by the drive nut. Figure 20 shows the connection between the drive screw and the magnet holder.

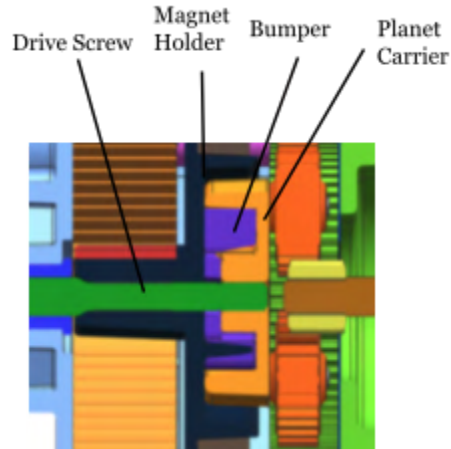


Figure 20. A cross-sectional view drive screw, magnet holder, bumper, and planet carrier is depicted. The drive screw is rigidly connected to the magnet holder and is slip fit to the planet carrier center.

All first principle analysis will be derived from the plunger at full extension, where all other components in the system are held stationary. The drive screw is rigidly attached to the magnet holder by a press fit. This is one of the primary external torques acting on the magnet holder. Therefore, it is essential to calculate this torque to use for further Ansys simulations. Equation 1 is used to determine the torque to overcome thread friction and to push the spring. The torque will be analyzed at the maximum force that the drive screw will feel by the plunger, which occurs at full extension [86]. This is the most relevant force to test at since testing at the maximum force will provide worst-case scenario results for the simulation testing. Additionally, The team included a safety factor (SF) of 2 on this output force. All force analysis was performed using a F_{spring} at the maximum load (170 N) multiplied by the SF of 2. This met Stoneridge's requirements, as it was larger than their specified minimum value of 1.7.

$$T_{DS} = \frac{Fd_m}{2} \frac{(l + \pi f d_m)}{\pi d_m - fl} / (\eta_{efficiency}) \quad (1)[86][103]$$

T_{DS} is the torque on the drive screw (Nm), F is the maximum axial compressive force (F_{spring}) equal to $170N * SF$ (N), d_m is the diameter (m), l is the distance the nut moves parallel to the screw axis when the nut is given one turn (m), f is the coefficient of friction between ULTEM 4001 and Stainless steel (0.1 - 0.3), and $\eta_{efficiency}$ is the efficiency of a drive screw and drive nut interaction (86, 97). The Matlab code of the calculations and all associated values for these variables are listed in Appendix F. The magnet holder also experiences forces from the bumper interaction onto the magnet holder as the two components rotate. As seen in figure 20 on the previous page, The bumper is located between the planet carrier and magnet holder. It sits between three nubs that extrude out of the magnet holder.

Using the torque from the drive screw, which will be the same torque the magnet holder feels, the forces on each nub ($F_{Bumper/MH}$) could be determined using the following equation:

$$F_{Bumper/MH} = (T_{DS/MH}/d_{DS/Nub})/3 \quad (2)$$

Where $T_{DS/MH}$ is the torque onto the magnet holder from the drive screw (Nm), calculated from Eq. 1 and $d_{DS/Nub}$ is the approximate distance from the center of the drive screw hole to one of the nubs (m). There is a factor of $\frac{1}{3}$ since there are 3 nubs where the torque from the drive screw is evenly distributed.

Using gear force analysis principles, a free body diagram (FBD) of the magnet holder was constructed and is shown in figure 21. For all notations, the component that is acting on the part in the FBD is denoted first. The component that the force is applied onto is denoted second. For example, $F_{DS/MH}$ indicates the force from the drive screw (DS) onto the magnet holder (MH).

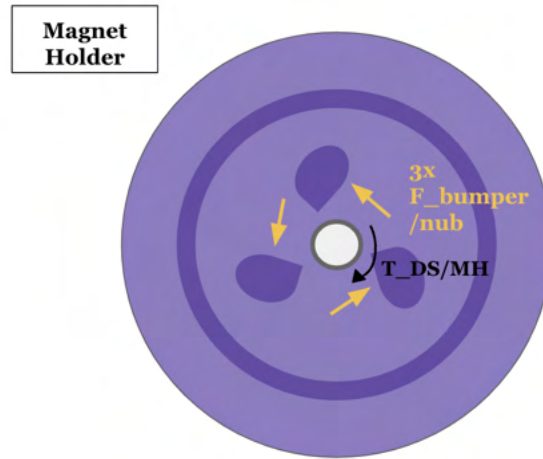


Figure 21. A cross-sectional view of the magnet holder is depicted. The external torque experienced on the magnet holder by the drive screw ($T_{DS/MH}$) is labeled. The external force of the bumper onto the magnet holder nubs ($F_{bumped/nub}$) is labeled.

As previously mentioned, the torque on the drive screw (T_{DS}) is the same torque that acts on the magnet holder ($T_{DS/MH}$) from figure 21. This torque and the forces felt on the nubs of the magnet holder will be used in the Ansys simulation for loads acting on the magnet holder.

To determine forces on the planet carrier, the team observed the tolerance of the fits between the drive screw and axles that interface with the planet carrier. It was determined that there is a tolerance gap of 0.1 mm between the drive screw shaft and the planet carrier. Because of this, a slip fit between the drive screw and the planet carrier was assumed. Therefore, there is no external torque felt on the planet carrier from the drive screw at the interfacing hole. As discussed before and seen in figure 20 above, there is a bumper that sits between the magnet holder and the planet carrier. The planet carrier has 3 flat faces that interact with the bumper. Using force analysis, the flat surfaces on the planet carrier will feel the same force by the bumper that the magnet holder feels (denoted by $F_{Bumper/PC}$). This relationship is presented below using Eq. 3.

$$F_{Bumper/PC} = F_{Bumper/MH} \quad (3)$$

Using this relationship, the reaction forces from the axles onto the planet carrier was derived. The axles are press fit into the planet carrier and drive it CCW, resulting in a bending moment at each location

where the axle interfaces with the planet carrier. It can be assumed that the torque from the drive screw onto the magnet holder is the same torque acting on the bumper since the magnet holder, bumper, and planet carrier all move together as one unit [86]. Therefore the sum of the moment produced by the three axles onto the planet carrier must counteract the torque from the drive screw onto the bumper (equal to $T_{DS/MH}$). Knowing this, the following equations were used to determine the forces acted by the axles onto the planet carrier and their components in the x (Eq. 5) and y (Eq. 6) directions. These component forces were used as the forces experienced at the axle holes in Ansys for Static Analysis.

$$F_{axle/PC} = \frac{1}{3} (T_{DS/MH} / d_{DS/PC}) \quad (4)[86]$$

$$F_{axle/PC(x)} = F_{axle/PC} \cdot \cos\left(\frac{\pi}{3}\right) \quad (5)[86]$$

$$F_{axle/PC(y)} = F_{axle/PC} \cdot \sin\left(\frac{\pi}{3}\right) \quad (6)[86]$$

The variable $d_{DS/PC}$ is the distance from the center of the drive screw hole to one of the axles on the planet carrier (m). $F_{axle/PC}$ represents the force felt at one of the axle holes on the planet carrier (N), represented by a multiplication factor of $\frac{1}{3}$ in Eq. 4. Through right triangle geometric analysis and approximating each axle be 120 degrees away from each other, the angle at which the force from the axles act on the planet carrier was determined. The derivation of this angle is shown in Appendix I. An FBD of the planet carrier with its associated forces is shown in figure 22.

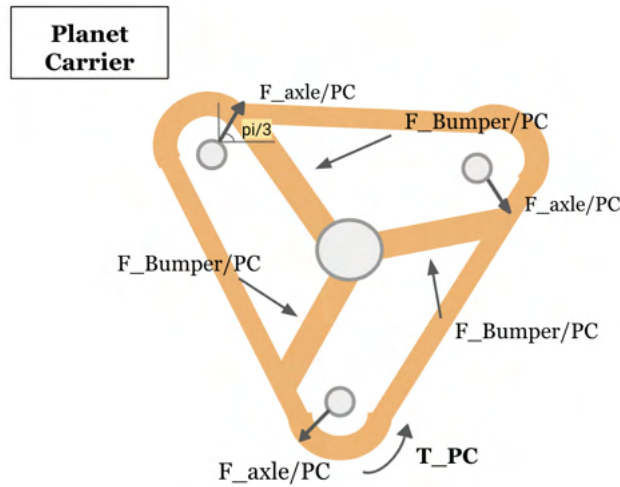


Figure 22. FBD of the planet carrier is shown. The associated torque at the center where the drive screw is located, as well as the reaction torques from the axles that connect to the planet gear are labeled. The reaction torques from the axles onto the planet carrier (PC) are denoted by $T_{axle/PC}$. The forces felt from the bumper are denoted by $F_{Bumper/PC}$.

The component forces $F_{axle/PC(x)}$, $F_{axle/PC(y)}$, and the forces by the bumper onto the planet carrier are used as the forces experienced on the planet carrier in Ansys for the Planet Carrier Static Analysis Model.

To determine the loads on the ring gear, further decomposition of the forces felt throughout the planetary gear system was needed. These forces were determined using planetary gear torque equations. As previously discussed, since the magnet holder and planet carrier move as one unit, an assumption that the planet carrier feels an overall torque (T_{PC}) that is equivalent to $T_{DS/MH}$ was made. Using this relationship, the torque of the sun gear was determined, and the forces from the sun gear onto the planet gear were derived using the following equations:

$$T_S = (T_{PC} * \frac{S}{S+R}) \cdot \frac{1}{\eta_{gear\ efficiency}} \quad (7)[86]$$

$$F_{SP1(t)} = \frac{1}{3} \left(\frac{2 * T_S}{d_s} \right) \quad (8)[86]$$

$$F_{SP1(r)} = F_{SP1(t)} \cdot \tan(\theta_{PA}) \quad (9)[86]$$

Where T_S is the torque of the sun gear (Nm), S is the number of teeth on the sun gear, R is the number of teeth on the ring gear, d_s is the pitch diameter of the sun gear (m), θ_{PA} is the pressure angle of the gears (20 degrees), and $\eta_{gear\ efficiency}$ is the efficiency of the gear mesh interactions (0.95) [103]. $F_{SP1(t)}$ is equal to the tangential force by the sun gear onto one planet gear and $F_{SP1(r)}$ is the radial force by the sun gear onto one planet gear. A factor of $\frac{1}{3}$ is used in Eq. 8 to represent only one of the three planet gears. An FBD of the sun gear is shown below in figure 23.

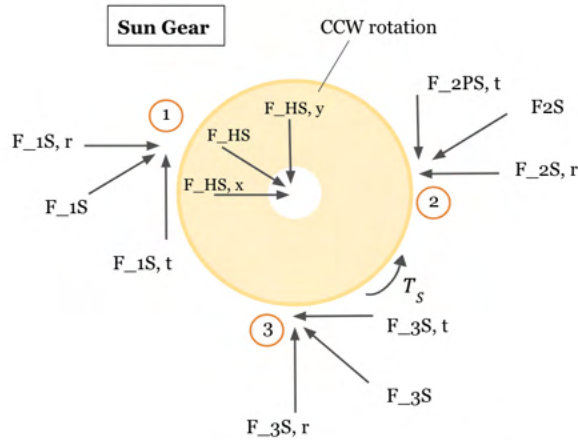


Figure 23. FBD of the sun gear. F_{1S} is the reaction force felt on the sun gear from planet gear 1. Similar denotations for labeling are used for reaction forces felt on the sun gear from planet gears 2 and 3. F_{HS} is the reaction force felt on the sun gear from the hub shaft. The values for F_{HS} were not necessary to calculate for force analysis, but are included in the diagram for completeness.

The forces from the sun gear on the planet gears derived above and the reaction forces from the ring gear onto the planet gears are presented in figure 24. The radial force direction is denoted by “r” and the tangential force direction is denoted by “t”.

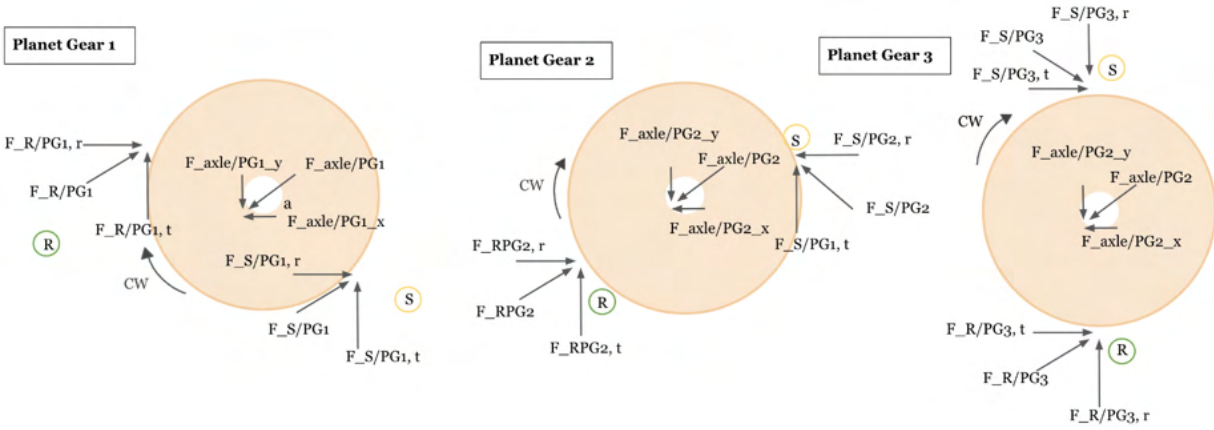


Figure 24. Planet carrier gears feel the force from the driven sun gear and the reaction force from the forces they impose on the ring gear. $F_{R/PG\#}$ and $F_{S/PG\#}$ (with # equal to 1, 2, or 3) denotes the reaction forces from the ring gear onto the planet gear and sun gear onto planet gears. Forces from the axles onto the planet gears are represented by $F_{axle/PG\#}$.

To determine the forces on the ring gear, a force balance on each planet gear is necessary since the forces from the ring gear onto the planet gear ($F_{R/PG1}$) will be equal and opposite to the forces felt on the ring gear by the planet gears ($F_{PG1/R}$). Only an analysis on one planet gear is necessary since each planet gear will produce the same force onto the ring gear with only a difference in location along the gear teeth. The forces in the x and y directions were evaluated. Force balance equations in each direction are indicated by Equations 10, 11, and 12.

$$0 = F_{axle/PG1(x)} - F_{R/PG1,r} - F_{S/PG1,r} \quad (10)[86]$$

$$0 = F_{axle/PG1(y)} - F_{R/PG1,t} - F_{S/PG1,t} \quad (11)[86]$$

$$F_{R/PG1,t} = \text{sqrt}((F_{R/PG1,r})^2 + (F_{S/PG1,r})^2) \quad (12)[86]$$

The forces $F_{axle/PG1(x)}$, $F_{S/PG1,r}$, $F_{axle/PG1(y)}$, and $F_{S/PG1,t}$ are all known, and therefore the forces on the ring gear $F_{R/PG1,r}$ and $F_{R/PG1,t}$ can be directly solved. The $F_{axle/PG1(x)}$ force is equal to the force from the axle onto the planet carrier. This happens when the planet gear is held stationary at maximum extension of the plunger because it will feel a force from the axle onto the gear in the opposite direction of the gear rotation. The distributed forces from the planet gears are presented in the FBD of the ring gear in Figure 25 below.

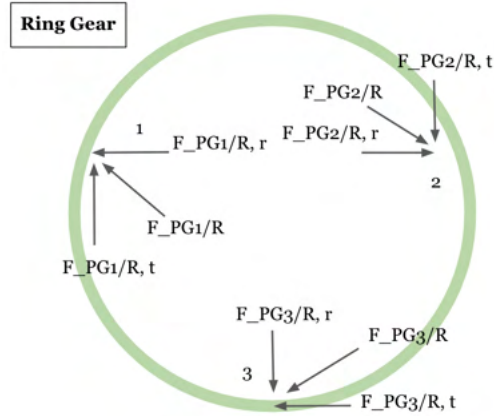


Figure 25. FBD of the ring gear is shown. All forces from the planet gear onto the ring gear are labeled.

The ring gear also feels forces on the opposite end of its gear teeth. Figure 26 below shows the end of the ring gear and 3 small extrusions where the ring gear is fixed into place.

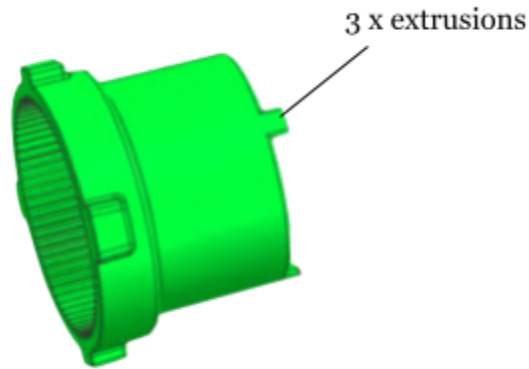


Figure 26. Ring gear image with a callout at extrusions where torque is felt and forces were determined for FEA Ansys modeling.

Using force analysis to determine the torque felt by the ring gear, the forces at each extrusion were determined. The following set of equations were used:

$$T_{RingTeeth} = 3 \cdot F_{R/PG1,t} \cdot d_{RingTeeth} \quad (13)$$

$$F_{RingExtrusion} = \frac{T_{RingTeeth}}{3 \cdot d_{RingExtrusion}} \quad (14)$$

where $T_{RingTeeth}$ is the total torque from the three planetary gears onto the teeth of the ring gear (Nm) and $F_{RingExtrusion}$ is the force (N) felt tangentially on each of the ring extrusions labeled above in figure 26. The variable $d_{RingTeeth}$ is pitch diameter of the ring gear (m) and $d_{RingExtrusion}$ is the diameter between extrusions at the back of the ring gear (m). These, in addition to the forces by the planetary gears onto the

ring gear teeth, are all the forces felt on the ring gear. These forces were then used in the Ansys Static Analysis Model for the ring gear.

Ansys Simulation Workbench Setup

Following the completion of the first principles analysis, all necessary parameters for an accurate simulation had been defined. All forces, torques, and material properties were assessed using Ansys' Workbench software, which was chosen given its capabilities to provide accurate simulation results. More importantly, the software was capable of running Static Structural Analysis, Modal Analysis, Random Vibration Analysis, and Structural Optimization (Topology) Analysis, in that order given that they are dependent on the Static Analysis results. Having access to all of these simulations within the same domain proved to be extremely beneficial given the nature of Finite Element Analysis simulations, as iterations between tests and materials were much more time efficient.

To begin the Finite Element Analysis of the components, the team had to choose the correct tools and implement the geometries of the parts onto Ansys Workbench. Geometries for the Magnet Holder, Planet Carrier, and Ring Gear were all imported using .stp files provided to the team by Stoneridge. Having imported the geometries into the Workbench, the following step was to incorporate the correct simulations in the right order, since they are dependent each other's results. As can be seen below in figure 27, simulations were selected from the Toolbox on the left hand side of the screen and then dragged onto the workbench work area. Ansys is capable of sharing precise data such as geometries, materials, and simulation results amongst other simulations and can also be seen in figure 27 to be done through purple and pink links between the simulations as they flow from left to right.

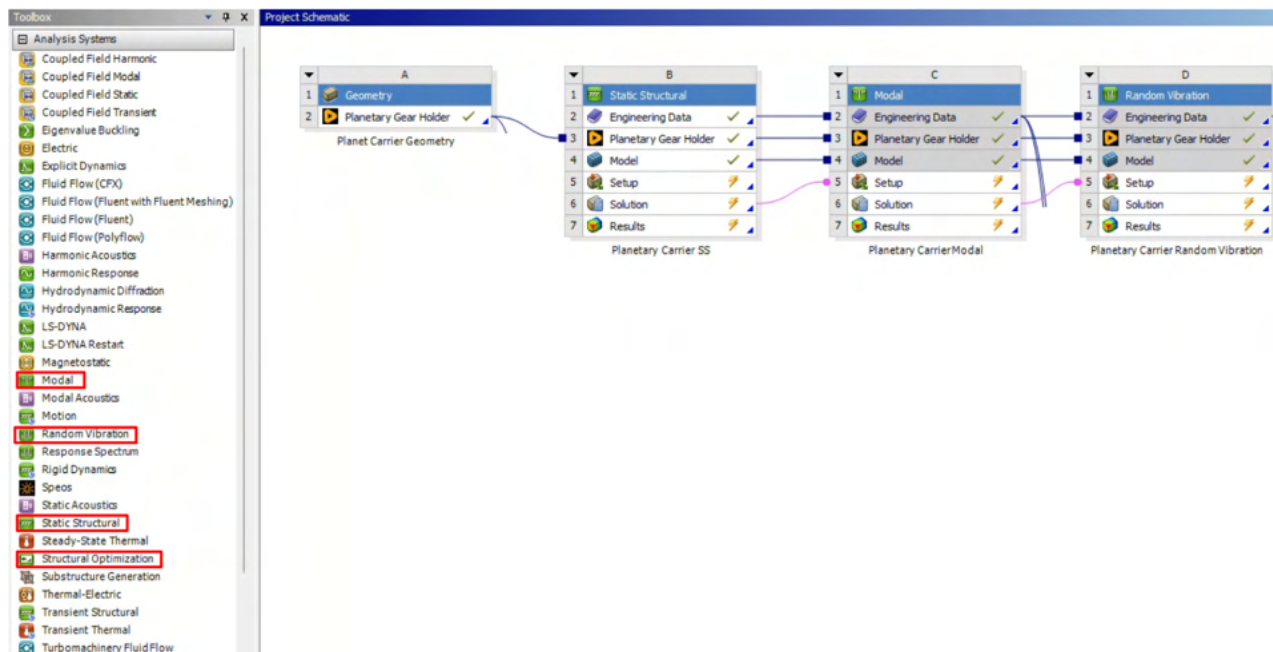


Figure 27. Screenshot of the Ansys workbench for the Planet Carrier's Static, Modal, and Vibrational FEA. Ansys Toolbox can be seen on the left and the chosen simulations are highlighted in red boxes. Beginning with the geometry, purple and pink wires flowing from left to right show that engineering data, geometries, and simulation results/solutions are shared through all simulations for their specific component.

As the analyses progressed, data was continuously used interchangeably specifically for the “Engineering Data” stage of the initial Static Structural analysis on the planet carrier. This is due to the fact that all relative materials were first imported into that first simulation, and could be easily shared amongst all simulations instead of manually importing them every time. This resulted in a very interconnected flowchart for all of the components analyses, as can be seen below in figure 28.

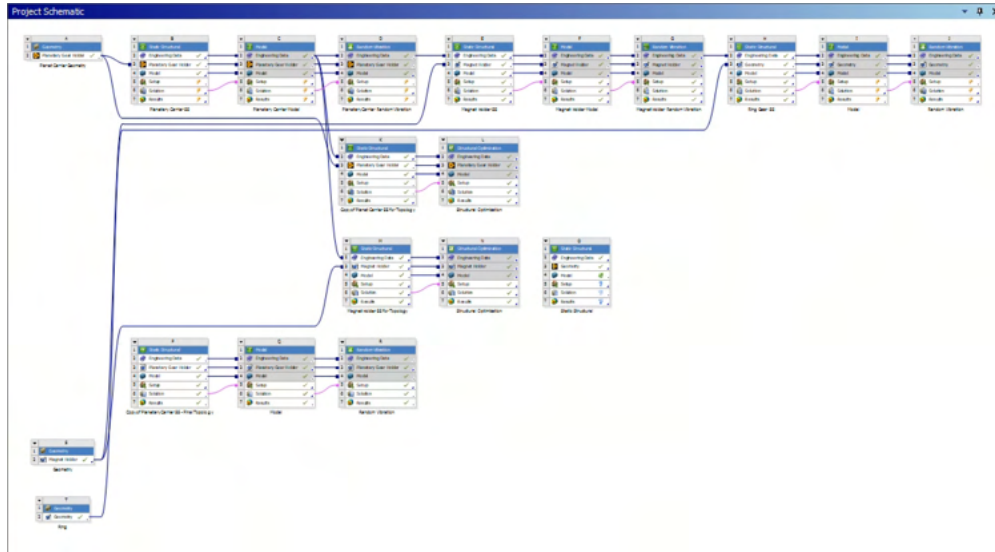


Figure 28. Screenshot of the final Ansys Workbench flowchart for all components. The workbench shows that all relative analyses have been done for each of the components.

Convergence Testing

The size of the finite element mesh largely influences the results of FEA. A smaller mesh size increases accuracy in the analysis results, and a larger mesh size decreases accuracy. However, a smaller mesh size also increases analysis time [89]. The team chose to use convergence testing in order to find an optimal mesh size for the FEA that was conducted. There are various methods for convergence testing, but the team followed the process described below.

Convergence testing involves comparing the results of a chosen analysis, Static Structural analysis in the team’s case, when the mesh size is varied. A mesh should be at least two elements thick at any given point in a model [89], so for example, because the magnet holder’s thinnest wall is approximately 1.50 mm, the starting mesh size needed to be 0.75 mm or less. Once this initial mesh size was chosen and analyzed, the simulation was then repeated, approximately halving the mesh each time until the result had less than a 10% difference from its previous iteration. The team specifically examined the maximum principal stress solution value, as the stresses were a key value that needed to be recorded. These values, in addition to their associated mesh sizes and percent differences, are included in the table in Appendix G. The mesh sizes in the green rows of the table were used for the remainder of the FEA for their respective parts.

Static Structural Analysis

In order to translate the load cases provided by Stoneridge to material requirements, the team had to conduct static analysis within the Ansys software. As shown above in the First Principles Section, the maximum load cases, with an added safety factor, were evaluated at the interfaces of the three specific components that were selected for this project throughout the drive train. These individual three parts had

different forces felt on them that had to be modeled independently for each of the parts. As seen above in the Workbench Setup, each part was individually modeled. First principle forces were then applied to each component to retrieve information about the material performance.

Following the application of accurate loads and constraints, the model was then simulated at its optimal mesh size found during convergence testing. The results showed maximum stress concentrations, principal stresses, and deformations as can be seen below in figure 29. These quantitative results were recorded for every iteration of material, and were additionally used to identify possible failure modes and opportunities for topology optimization.

All simulations done below were done on the current material for production Zinc Zamak 5, and the maximum principal stresses found through this analysis were used to determine the minimum yield strength requirement for the material of each component; this process is shown below in the Finding Baseline Yield Strength Values section of the report. This simulation was then repeated for each material passed using the Granta EduPack settings mentioned in the previous section. Below in figure 29, the “Static Structural” portion of the tree is visible, as well as the analysis solution selections to gather the correct information to derive the minimum yield strength for material selection. Along with that are the Modal and Random Vibration portions of this tree. These sections were also set up in the workbench mentioned above and the Vibrational Analysis section below of this report discusses further what information this test provides.

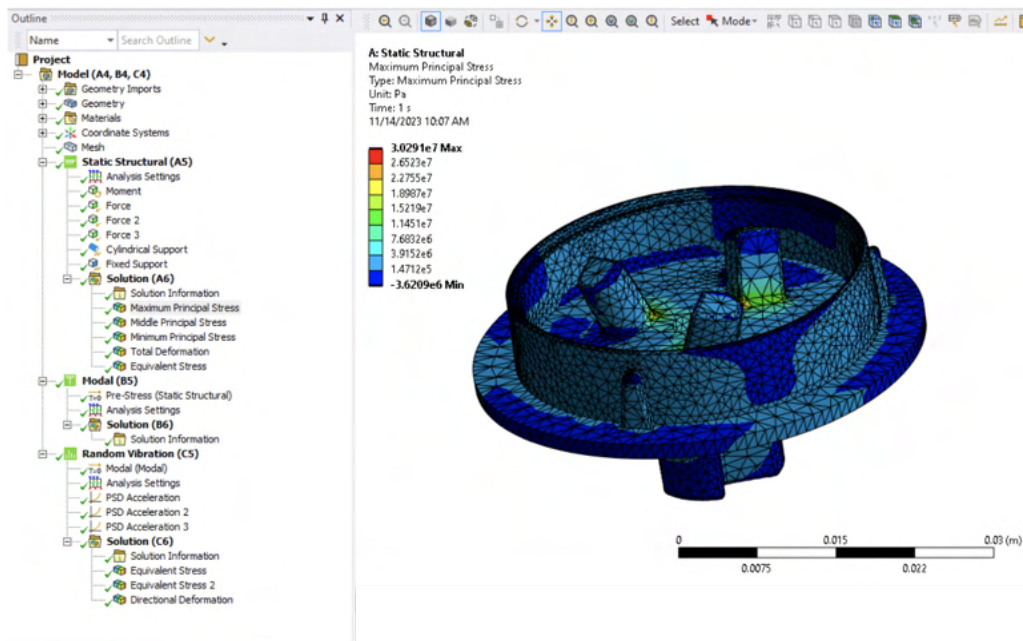


Figure 29. Static Analysis Mechanical Dashboard on Ansys displaying results for Maximum Principal Stresses on the Magnet Holder.

To ensure that there is clarity, the team has written a general walkthrough of the process for the original geometries and material of the components below.

Planet Carrier Analysis

Firstly, the planet carrier was simulated to experience loads at its three shaft holes due to the reaction forces of the planetary gear shafts, and its inner nub surface areas given the reaction forces experienced from the magnet holder as seen in figure 22. Their respective vectors and geometries are shown below in figure 30. Given that the center shaft hole is a slip fit between the drive screw and planet carrier, a cylindrical support was defined at that interface to be fixed in the radial and axial directions, but free in the tangential given that it can rotate freely. The holes for the planet gear shafts were defined to be fixed supports, given that they are press fit to one another.

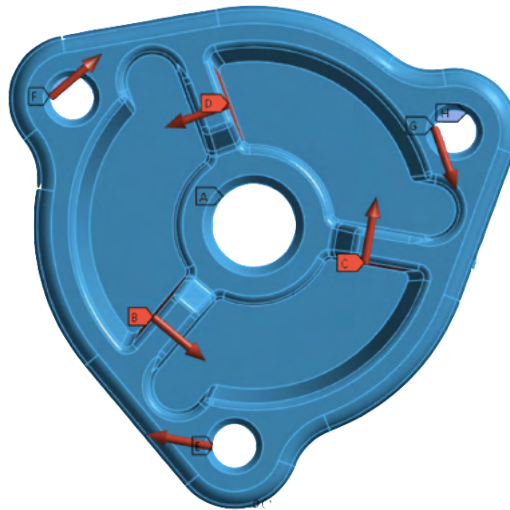


Figure 30. A screenshot of Ansys Static Structural Simulation with highlighted and defined force vectors and constraints on the Planet Carrier CAD model.

Following the application of said parameters, the simulation was run and resulted in the solutions shown on the next page in figure 31.a and figure 31.b.

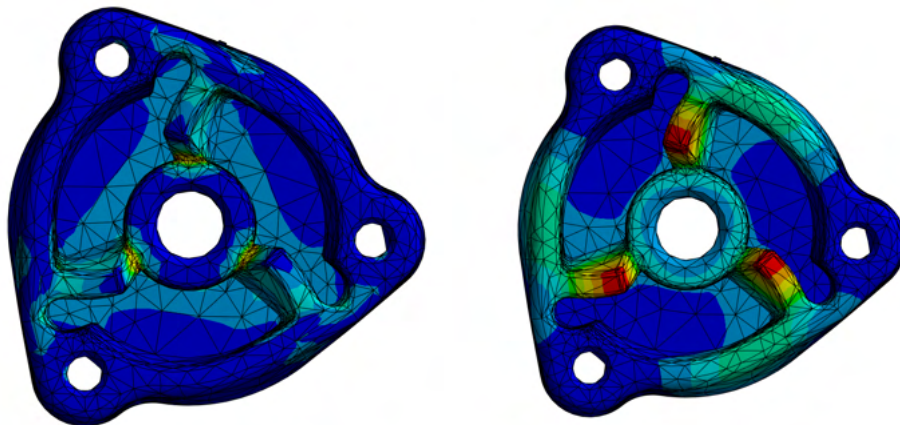


Figure 31.a (left) and Figure 31.b (right). Figure 31.a shows a screenshot of the planet carrier's static structural simulation results for equivalent stress. It can be seen that there is a stress concentration at the interconnected edge or “rib” feature between the drive screw shaft hole and the outer edge. Figure 31.b shows the maximum deformation results for the same simulation, from which the maximum concentration occurs on the top edges.

Magnet Carrier Analysis

Secondly, the magnet carrier was simulated to experience loads at its internal interfaces, shown in red, given that these are the same reaction forces that were applied to the planet carrier. Since the magnet holder is press fit to the drive screw, this means that the rotational motion generated from the previously described loads will create a torque about that inner shaft hole interface, as can be seen in figure 21. The press fit relationship between the two components was defined as a cylindrical support about that same drive screw shaft hole interface, fixed in the axial, radial, and tangential directions. The applied loads and constraints on the magnet holder's geometry can be seen below in figure 32.

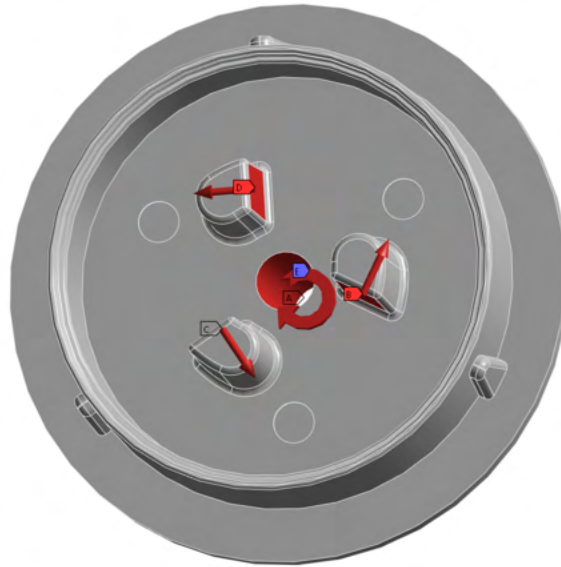


Figure 32. A screenshot of Ansys Static Structural Simulation with highlighted and defined force vectors and constraints on the Magnet Holder CAD model from an isometric view. The “nubs” applied force is shown in red and indicated with letters B,C,D

Following the application of said parameters depicted in figure 31, the simulation was run and resulted in the solutions shown below in figure 33.a and figure 33.b.

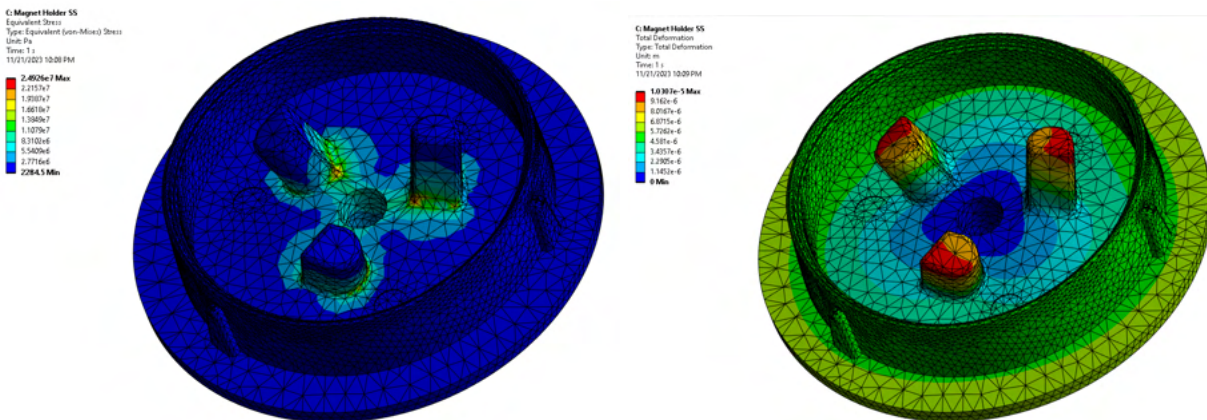


Figure 33.a and Figure 33.b. Figure 33.a on the left shows a screenshot of the magnet holder's static structural simulation results for equivalent stress. It can be seen that there

is a stress concentration at the bottom curved edge of the nubs. Figure 33.b on the right shows the maximum deformation results for the same simulation, from which can be seen that it occurs on the top-sided edges of the nubs.

Ring Gear Analysis

Lastly, the ring gear was simulated slightly differently than the other two components. One of the differences is that not all of its surfaces were assigned the same mesh size. The ring gear's long and large geometry resulted in far too long simulation times for a fine-quality mesh. Therefore the team used the "Mesh Sizing" tool to select faces of interest and assign them a much finer mesh relative to the rest. Doing so allowed the team to have a high-quality mesh for the teeth on the ring gear which were of interest, and a very coarse mesh for the rest of the component, as can be seen below in figure 34. This proved to provide accurate results and time-efficient simulations.

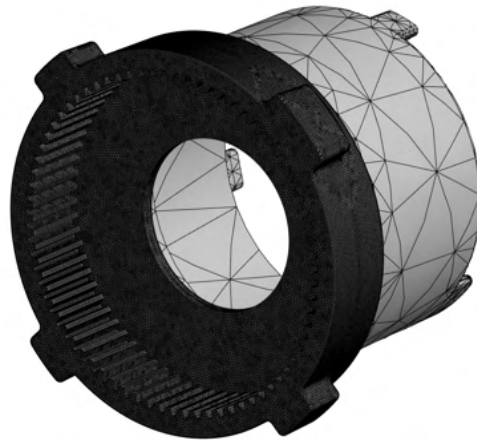


Figure 34. Screenshot of the Static Structural simulation's mesh refinement done on the teeth of the ring gear from an isometric view.

The ring gear was simulated to experience three-point loads at teeth during static equilibrium, which are applied from the planet gears as they rotate about the sun. Three reaction forces were also applied to the extrusions at the back end of the ring gear since they are inserted into slots to rigidly attach them to the rest of the body, which is also why they were defined as rigid constraints. Loads and constraints can be seen below in figure 35.

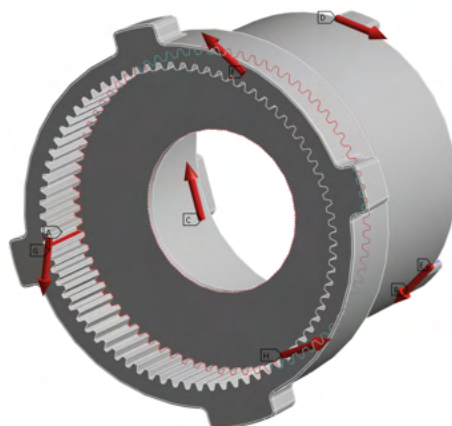


Figure 35. A screenshot of Ansys Static Structural Simulation with highlighted force vectors, their respective geometries, and constraints on the Ring Gear CAD model from an isometric view.

The parameters applied to the ring gear in the simulation were simplified based on the static equilibrium load cases from the first principles analysis. The approach was a final alternative since the team was not able to accurately simulate a distributed stress from the planet gears over every tooth on the ring gear. This was due to difficulties translating pre-defined parameters and relationships between several geometries and components such as gear meshes and gear ratios from Solidworks into Ansys. It is important to note that all solutions from the simulations would have been the same for either approach (modeling forces on one tooth vs distributed on multiple teeth) since the loads experienced by an individual tooth would be relatively the same for both cases, which is why the team followed through with said parameters. Following the application of said parameters, the simulation was run and resulted in the solutions shown below in figure 36.

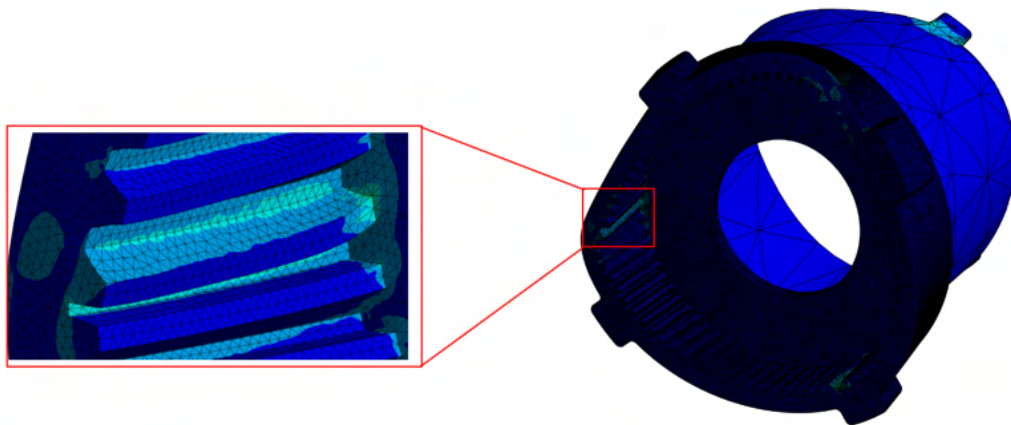


Figure 36. A screenshot of the ring gear's static structural simulation results for equivalent stress. Given the fine mesh, an augmented image was included to show the stress concentrations experienced at the base of the teeth.

Finding Baseline Yield Strength Values

Through conducting Static Structural analysis on the planet carrier, magnet holder, and ring gear, the baseline yield strength specification values were found. To do this calculation, the team first added the maximum, middle, and minimum principal stresses to the solution output. This list is shown below in figure 37.

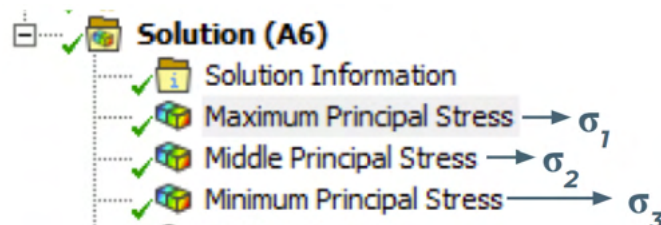


Figure 37. An easy-to-read depiction of the solutions that were output from the Static Structural analysis. The principal stresses were assigned as σ_1 , σ_2 , and σ_3 .

The maximum values for each of these three results were then arbitrarily plugged into the Von Mises equation as σ_1 , σ_2 , and σ_3 . This is shown as Equation 15 below, and it provides the critical stress value, σ_v , at which yielding begins in a ductile material with complex loading [100].

$$\sigma_v = \sqrt{\frac{(\sigma_1 - \sigma_2)^2 + (\sigma_2 - \sigma_3)^2 + (\sigma_3 - \sigma_1)^2}{2}} \quad (15)$$

The Von Mises Criterion, which is shown below in Equation 16, was then applied [100]. σ_{yield} is the yield strength, and this equation is simply stating that its value must be larger than the critical stress value if the material is to not yield when the specified load is applied.

$$\sigma_{yield} > \sigma_v \quad (16)$$

The team then multiplied this yield strength by 2 to account for a conservative safety factor, and the result was used as the baseline yield strength that the component's material must have in order to meet the given requirements. It is worth noting that Zinc Zamak 5 was utilized for these analyses, but the principal stresses were found solely from the loading conditions and the material used should therefore not affect the resultant values. This process was repeated for each of the three components, and their final minimum yield strengths were listed in the specifications for requirement 1.3 within Table 3.

Thermal Analysis - CTE

The CTE values were analyzed by observing the tolerances between slip fits and press fits. The objective was to ensure the slip fit would remain a slip fit and the press fit would remain a press fit at the maximum high and low operating temperatures (-40°C and 105°C). To narrow down the list of materials generated by the Granta EduPack Material Selection tool, maximum values for the coefficient of thermal expansion (CTE) were determined. Additionally, the CTE for the ring gear was also analyzed for two cases. The first case was to ensure the gear teeth tip diameters are less than 0 thousandths of an inch so that there is overlap, and the gears still mesh together after any expansion or shrinkage that could occur at different temperatures. The second case was to ensure that there is a tolerance of greater than 0 thousandths of an inch for the tip and root clearance at the maximum high and low temperatures for gear meshing. An assumption was made to use greater than or less than 0 for the baseline of the two cases in order to find CTE values that will satisfy both cases. The minimum CTE of the two cases was chosen as a conservative value to use in Granta EduPack for material selection filtering. A depiction of this tolerance for the ring and planet gears is shown in figure 38 below.

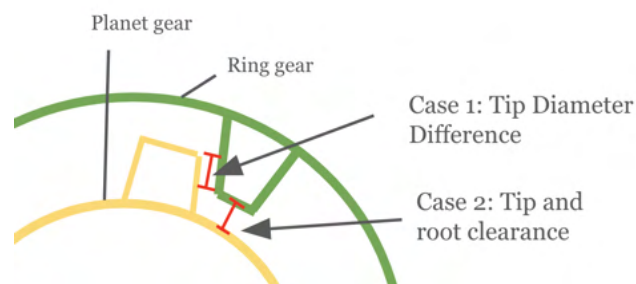


Figure 38. Depictions of the two dimensions are used to find the required CTE at the maximum high and low temperatures to maintain proper gear meshing and rotation.

The main interactions that were observed include the press fit between the drive screw and magnet holder, slip fit between the drive screw and planet carrier, press fit between the planet carrier and axles, and ring gear teeth interaction with planet gear teeth. For every interaction, there is one known CTE for the part that will remain the same material (drive screw, axles, and planet gears). For the known material, Eq. 17 was used to determine the change in diameter it will experience at the maximum high and low temperatures (Δd). The part interactions analyzed are shown below in Figure 39.

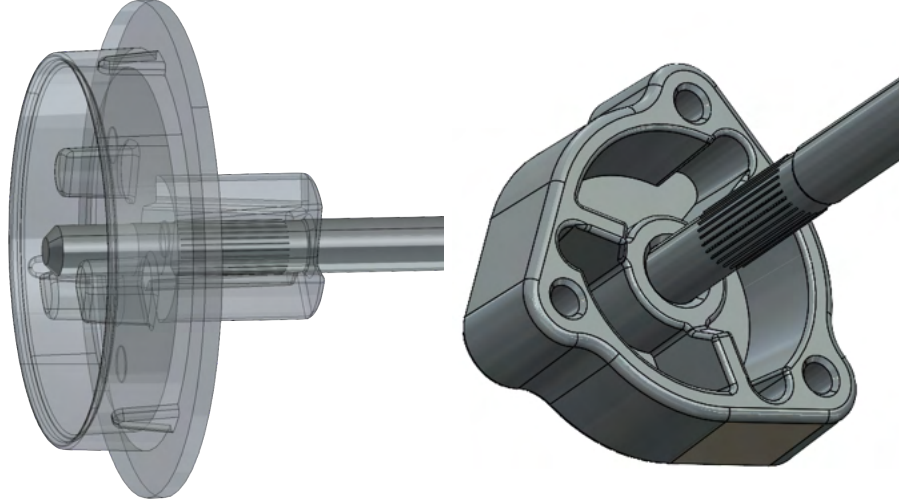


Figure 39. The image on the left is the magnet holder and drive screw press fit interaction. The image on the right is the planet carrier and drive screw slip fit interaction.

The following equations present the process used to determine the new material CTE boundaries. Eq. 17 and Eq. 18 provide the changes in the diameter of the part with a *known* material and the part that will have a *new* material. Eq. 19 sets up the relationship between the tolerance between the two materials. A table for the interferences for each interaction that was analyzed can be found in Appendix H. These values were determined using the Machinists Handbook for reference of press fit and slip fit standard tolerances and multiplied by a safety factor of 2 [101]. Eq. 20 substitutes Eq. 17, Eq. 18, and Eq. 19 into one equation which can be rearranged to solve for α_{new} .

$$\Delta d_{known} = d_{known} \cdot \alpha_{known} \cdot \Delta T_{known} \quad (17)[102]$$

$$\Delta d_{new} = d_{new} \cdot \alpha_{new} \cdot \Delta T_{new} \quad (18)[102]$$

$$(d_{new} + \Delta d_{new}) - (d_{known} + \Delta d_{known}) \leq \text{or} \geq \text{tolerance} \quad (19)[102]$$

$$(d_{new} + d_{new} \cdot \alpha_{new} \cdot \Delta T_{new}) - (d_{known} + d_{known} \cdot \alpha_{known} \cdot \Delta T_{known}) \leq \text{or} \geq \text{tolerance} \quad (20)[102]$$

The Δd is change in diameter due to expansion or shrinkage, d is the original diameter distance (m), α is the CTE (microstrain/°C), and ΔT (°C) is the change in temperature from the maximum high/low temperatures to an approximated room temperature of 25°C. The calculations are provided in Appendix H.

Solving for α_{new} each part allowed the team to have one more identifying parameter for the Granta EduPack material selection tool. These CTEs were validated by using the exact material properties for the top filtered materials for each part. Each of the interfacing components was checked for slip fit and press fit interactions at the maximum and minimum temperatures to ensure that they remain slip and press fit where necessary. MATLAB was used to complete the calculations and the code is provided in Appendix H under *First Principles - Thermal Analysis - CTE Validation*. Results from this testing show all press fits and slip fits remain as such at operating temperatures of -40°C and 105°C.

Thermal Analysis - Stress

The team also looked at the stress effects of thermal expansion. The governing equation (Eq. 21) below was used to solve for the effect of stress on the magnet holder from the drive screw and planet carrier from axles [86]. Such as the pressure from the drive screw onto the magnet holder at -40 C and 105 C. This analysis was only completed on press fit interactions since this contact can result in stress on the parts at various temperatures depending on expansion or shrinkage. The calculations were completed in MATLAB and the code is provided in Appendix H under *First Principles - Thermal Analysis for Stress*.

$$P = \frac{\delta}{\frac{d \left(v_i - \frac{d^2 + d_i^2}{d^2 - d_i^2} \right)}{E_i} - \frac{d \left(v_o - \frac{d^2 + d_o^2}{d^2 - d_o^2} \right)}{E_o}} \quad (21)[86]$$

The notation “i” references the shaft (drive screw or axle) which has known materials and “o” is for the hub whose material is not known and will change (magnet holder and planet carrier). The variables in the equation above include d which is the nominal diameter of the hub (mm), the outer diameter of the hub d_o (mm), the internal diameter of the shaft d_i (mm), the Young’s Modulus (E) (GPa), and Poisson’s ratio for the shaft v_i and the hub v_o .

For the ring gear, bending stress on the gear teeth was calculated at maximum temperatures using the Lewis Bending Stress equation for gear teeth below in Eq. 22:

$$\sigma_t = \frac{K_v W_t}{FmY} \quad (22)[118]$$

Where K_v is the dynamic factor (dimensionless) which is equal to 1 since stresses are evaluated at static conditions, W_t is the tangential load on the gear teeth (N), F is the face width (mm), m is the module (mm), and Y is the Lewis form factor (dimensionless) determined from the gear teeth number [118].

These stress values were normalized to the yield strength of the material. The team will be assessing each material for thermal stress effects using a pass/fail system. This is because the main focus for material selection is cost and density. Thermal stress analysis is completed to ensure that the parts do not fail and will function as normal under worst-case environmental conditions.

Vibrational Analysis

To meet requirement 1.1 which specifies the part must withstand PSD loading conditions as specified by Stoneridge, a vibration analysis was performed on Ansys. Stoneridge provided power spectral density (PSD) data (see Appendix D) which was inputted as tabular data under the Random Vibration analysis

system [96]. The system was modeled under the same static loads used in the static analysis FEA in addition to the vibrational loads. Figure 40 presents the Ansys Mechanical Workbench setup.

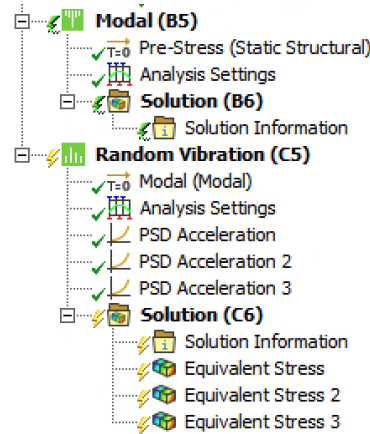


Figure 40. Following Ansys recommended setup for vibrational analysis, PSD Data was inputted for the vibrational loads on each component in the X, Y, and Z directions. Equivalent stress data was collected to compare each material.

Maximum stresses were recorded from the output equivalent stress solution from Ansys. Data was obtained from a scale factor of 3 Sigma, which indicates a probability of 99.73% that the resulting stress will occur on the part. Maximum stresses for the filtered list of materials for each part (magnet holder, ring gear, and planet carrier) were collected to record in the material selection pugh charts seen in Appendix E. The maximum stresses were converted to percentages by normalizing them to the material’s yield strength. This allows for easy comparison between each material based on how much stress the material feels compared to their own yield strength. The results of the percentages for the magnet holder are shown in Figure 41 below.

Criteria	Weight	0.095% max T 0.071% min T	PTT (30% glass fiber)	PTT (30% glass fiber, flame retarded)	PTT (30% glass fiber, 15% PTFE)
Withstands specified vibrational load profile (% of yield)	Pass / Fail	0.23%	0.06%	0.08%	0.07%
Criteria	Weight	PPA (60% glass fiber)	PPA (50% long glass fiber)	PPA (50% glass fiber, lubricated)	LCP (50% glass fiber)
Withstands specified vibrational load profile (% of yield)	Pass / Fail	0.04%	0.03%	0.04%	0.06%
Criteria	Weight	LCP (45% glass fiber)	LCP (40% glass fiber)	LCP (30% glass fiber)	LCP (15% glass fiber)
Withstands specified vibrational load profile (% of yield)	Pass / Fail	0.07%	0.07%	0.06%	0.03%

Figure 41. Vibrational loads as normalized percentages for each material. This is the narrowed list of materials and vibrational results for only the magnet holder.

The team will be assessing each material for vibrational load resistance using a pass/fail system. This is because the main focus for material selection is cost and density. Vibrational analysis is to ensure that the parts do not fail and will function as normal under worst-case environmental conditions.

Shock Analysis

To meet Requirement 1.1, a shock analysis was initiated. Shock information provided by Stoneridge (see Appendix D) was input into Ansys Shock Analysis. Each part was placed under static loads from the Ansys Static Analysis with the addition of 60 total 11-ms shocks of 500 m/s². Due to issues with the Ansys shock system setup, the team was unable to produce consistent results for stresses or deformation due to shock. The team met with MECHENG 305 FEA Expert Professor Huan from the University of Michigan to discuss the shock results who explained that shock simulation was out of his scope. Therefore, verification of the team’s methods could not be achieved and we cannot provide accurate shock simulation results. The team recommends Stoneridge use its Shock Test fixture to examine the behaviors that result from the shock loads the SmartBar System will feel. More details on the verification and validation process for shock analysis are described in the *Verification and Validation Plans* section of this report below.

Topology Optimization

To meet the cost and weight reduction requirements, the team conducted topology analysis by first applying the same loads and constraints used in the static analysis FEA. The team then chose to reduce mass by a preliminary value of 5%, while still maintaining or reducing the equivalent stresses experienced by each component. This mass reduction was a first iteration, as the generated topology model was then opened in Solidworks for ease of design for manufacturability. The team removed material, where it was specified as non-crucial by the topology analysis, within Solidworks and smoothed the resulting geometry so that it could be die cast or injection molded. The model was then transferred back into Ansys to verify that the equivalent stresses and component mass met the specifications. The geometry changes were made such that a die or mold could be created to fit them. The Ansys Workbench setup and the results of this optimization are discussed in the Final Topology Optimizations section.

FINAL MATERIAL SELECTION

Cost Analysis

The unit price for each part was determined by finding the tooling/labor/overhead cost for the parts. Stoneridge provided the team with unit costs for each part. The unit costs are listed in Table 12 below for the original material Zinc Zamak 5.

Table 12. Unit Costs

Part	Unit Cost (\$)
Magnet Holder	0.67
Planet Carrier	0.32
Ring Gear	1.203

After completing all engineering analyses discussed above, a final list of materials for each part was made. The Granta EduPack Material Selection tool provides unit cost per volume of material. This value was used since the volume for each of the analyzed parts is fixed. Using the fixed volume retrieved from Ansys Dimensions, the unit costs of the new material for each part were calculated using Eq. 23.

$$\text{Unit Cost Per Volume} * \text{Volume} = \text{Unit Cost of Material} \quad (23)$$

Using Granta EduPack, the unit price per volume for Zinc Zamak 5 was retrieved. Using the known volume for Zinc Zamak 5, the team then calculated the unit cost for the material. To obtain an estimate of important manufacturing and labor costs such as the tooling/labor/overhead (TLO) cost per unit, the unit cost of material was subtracted from the overall unit costs in Table 12. Using these values the percentage of TLO for each part was calculated using Eq. 24 below. For every material, the unit cost per material was divided by 100% minus the TLO percentage to obtain the overall unit cost per part for each material (Eq. 26).

$$\frac{\text{Unit Cost of Zinc Zamak 5} - \text{Total Unit Cost}}{\text{Total Unit Cost}} * 100\% = \% \text{ TLO} \quad (24)$$

$$100\% - \% \text{ Tooling} = \% \text{ of Material Cost} \quad (25)$$

$$\frac{\text{Unit Cost of Material}}{\% \text{ Material Cost}} = \text{Total Unit Cost (TLO + material)} \quad (26)$$

The percentage of TLO was calculated to be 33.12 % and the percentage of material cost was calculated to be 66.88%. An example of this process is shown below in Table 13.

Table 13. Unit Price Calculation Example for an Alternate Ring Gear Material

Material	Max price of range from EduPack (USD/m³)	Volume of part	Unit Cost of Material (\$)	Unit price with TLO (\$) (zinc is from Stoneridge)
Aluminum, 359.0, cast, T6	1.08E+04	1.31E-05	0.14	(0.14/ 33.12%) = 0.427

This process was repeated for each material list for the magnet holder, planet carrier, and ring gear. The material lists were then ranked in price from lowest to highest. The density of each material is also highlighted and color-coded to be lightest in color for lowest density materials as shown in Figure 42 below. This was done to easily present the results for each material based on cost and density since Stoneridge is focused on reducing cost. Figure 42 is an example of a ranked list for the ring gear.

Ring Gear										
Metals (Die Cast)										
Material	% cost reduction from unit price (price difference /original price)	Max price of range from edupack (USD/m ³)	Volume of each part (m ³)	Price per volume(\$)	Unit price with TLO (\$)	Density	weight	% cost of price of material	% cost of TLO on component	
Aluminum, 359.0, cast, T6	64.47%	1.08E+04	1.31E-05	0.14	0.427	2.70E+03	0.0353862	33.12%	66.88%	
Aluminum, C355.0, permanent	63.16%	1.12E+04	1.31E-05	0.15	0.443	2.74E+03	0.03591044	33.12%		
Aluminum, 354.0, cast, T6	62.17%	1.15E+04	1.31E-05	0.15	0.455	2.81E+03	0.03682786	33.12%		
Aluminum, 332.0, permanent	61.51%	1.17E+04	1.31E-05	0.15	0.463	2.80E+03	0.0366968	33.12%		
Aluminum, 333.0, permanent	61.19%	1.18E+04	1.31E-05	0.15	0.467	2.80E+03	0.0366968	33.12%		
Aluminum, 390.0, die cast, F	61.19%	1.18E+04	1.31E-05	0.15	0.467	2.76E+03	0.03617256	33.12%		
Aluminum, A390.0, permanent	61.19%	1.18E+04	1.31E-05	0.15	0.467	2.76E+03	0.03617256	33.12%		
Aluminum, A390.0, permanent	61.19%	1.18E+04	1.31E-05	0.15	0.467	2.76E+03	0.03617256	33.12%		
Aluminum, EN AC-48000, ch	61.19%	1.18E+04	1.31E-05	0.15	0.467	2.71E+03	0.03551726	33.12%		
Aluminum, 319.0, permanent	60.86%	1.19E+04	1.31E-05	0.16	0.471	2.82E+03	0.03695892	33.12%		
Aluminum, 336.0, permanent	57.24%	1.30E+04	1.31E-05	0.17	0.514	2.74E+03	0.03591044	33.12%		
Aluminum, 336.0, permanent	57.24%	1.30E+04	1.31E-05	0.17	0.514	2.74E+03	0.03591044	33.12%		
Aluminum, A332.0, cast, T6	57.24%	1.30E+04	1.31E-05	0.17	0.514	2.73E+03	0.03577938	33.12%		
Zinc-aluminum alloy, ZA-27, c	25.99%	2.25E+04	1.31E-05	0.29	0.890	5.05E+03	0.0661853	33.12%		
Zinc Zamak 5	0.00%	3.04E+04	1.31E-05	0.40	1.203	6.75E+03	0.0884655	33.12%		

Figure 42. Spreadsheet used to calculate the unit price of the ring gear depending on the material.

The setup for the final ranked lists for the magnet holder, planet carrier, and ring gear can be found in Appendix J.

Comparison of Capable Materials

The team formatted the final lists of materials for each of the three components as pugh charts. Because all of the requirements aside from lowering cost and weight are necessary for the SmartBar Actuator to function, they were given a pass or fail label rather than weight for each criteria. In Figure 43 below, a pugh chart for the ring gear is given. The remaining pugh charts for the ring gear as well as the other two components can be found in Appendix E.

Criteria	Weight	Zamak 5	Aluminum, 359.0, cast, T6	Aluminum, 354.0, cast, T6	Aluminum, A390.0, permanent mold cast, F	Aluminum, 390.0, die cast, F	Aluminum, A390.0, permanent mold cast, T6
Reduce cost from \$1.20	2	\$1.20 (0)	\$0.43 (5)	\$0.46 (5)	\$0.47 (5)	\$0.47 (5)	\$0.47 (5)
Reduce weight from 86.37g	1	86.37 g (0)	35.34 g (5)	36.83 g (5)	36.17 g (5)	36.17 g (5)	36.17 g (5)
Withstands >135N +/- 15N axial load on plunger (% of yield)	Pass / Fail	12.40%	10.11%	9.22%	11.87%	9.43%	7.65%
Withstands specified vibrational load profile (% of yield)	Pass / Fail	0.70%	1.32%	1.28%	1.47%	0.93%	0.95%
Does not seize/fail when operated between -40°C to 105°C (% of yield)	Pass / Fail	2.31% max T 2.30% min T	2.38% max T 2.37% min T	1.83% max T 1.82% min T	2.32% max T 2.30% min T	2.23% max T 2.22% min T	1.65% max T 1.64% min T
Has a Vickers Hardness value between 112 and 178 HV	Pass / Fail	115 HV	115 HV	115 HV	120 HV	127 HV	150 HV
Tolerance \leq +/- 0.001" for ring gear and planetary carrier	Pass / Fail	(+/-) 0.001" for finished part (die casting)	(+/-) 0.001" for finished part (die casting)	(+/-) 0.001" for finished part (die casting)	(+/-) 0.001" for finished part (die casting)	(+/-) 0.001" for finished part (die casting)	(+/-) 0.001" for finished part (die casting)
Is ethically sourced	N/A	Zinc-Lead mines in China, Southern America. [16]	Aluminum (bauxite mining) with magnesium and silicon components (found in mines). [4,10]	Aluminum (bauxite mining) with magnesium and silicon components (found in mines). [4,10]	Aluminum (bauxite mining) with magnesium and silicon components (found in mines). [4,10]	Aluminum (bauxite mining) with magnesium and silicon components (found in mines). [4,10]	Aluminum (bauxite mining) with magnesium and silicon components (found in mines). [4,10]
Does not seize/fail when operated between -40°C to 105°C (% of yield)	N/A						
Has a Young's Modulus \geq 1 GPa	N/A						
Tolerance \leq +/- 0.002" for magnet holder	N/A						
TOTAL		0	15	15	15	15	15

Figure 43. One of two pugh charts for the ring gear. The green boxes indicate that a material passes the respective criteria.

To fill the charts, the team utilized the cost analysis method from the previous subsection in order to populate the cost row, and calculated the weights using the densities found from the Granta EduPack material database. The cost values in the figure above are the total unit costs including the TLO costs. The static structural, thermal, and vibrational analysis results were then inputted into their respective rows as percentages of the yield strengths. This was done in order to show the materials' strengths relative to each other as well as the original. As stated in the *Material Selection Using Granta EduPack Material Filtering Tool* subsection, the manufacturing processes were limited to injection molding for polymers and die

casting for metals. Note that the planetary gear’s drawing had tolerances as small as 0.001”, but injection molding can reach this specification. However, these materials were marked with yellow boxes in Appendix E. The ethicality associated with using each material was also assessed, and brief comments are provided in Figure 43. This criteria was neither weighted nor treated as a pass or fail, because the team found “ethically sourced” to be a subjective requirement. The information is therefore solely for Stoneridge’s use and its application is up to the discretion of the company.

The green box indicates that a material passes the given criteria, and a red box indicates that a material fails. If a material has at least one red box, it should not be considered for use. The criteria of “Does not seize/fail when operated between -40°C to 105°C” was used for both the planet carrier and magnet holder, but was neglected for the ring gear in this pugh chart format. This is because the team already conducted calculations, found in the *Thermal Analysis - CTE* subsection, to ensure that all of the above materials were acceptable for the application on the basis of thermal stability.

The cost was weighted as a 2 because it is Stoneridge’s main priority, and weight was weighted as a 1 because it needs to be the same or less than its current value. Both were then given values from 0 to 5, which follow a linear scale in relation to each row’s largest and smallest values. This did not include the cost and weight of Zinc Zamak 5, as those numbers were significantly larger than those for the other materials. The total scoring in the bottom row shows which materials will be favorable when prioritizing cost and weight, but further validation should be done by Stoneridge before any material changes are implemented. This will be discussed in the Verification and Validation Plans section. The five cheapest materials for each component are summarized in Table 14 below.

Table 14. The materials are listed with the least expensive at the top and the most expensive at the bottom. They are all still cheaper than the original components.

Ring Gear	Magnet Holder	Planet Carrier
Aluminum, 359.0, cast, T6	PTT (30% glass fiber)	PA66/6 (30% glass fiber)
Aluminum, C355.0, permanent mold cast, T6	PPA (60% glass fiber)	PA66/6 (35% glass fiber)
Aluminum, 354.0, cast, T6	PPA (50% glass fiber, lubricated)	PF (high strength glass fiber, molding)
Aluminum, 332.0, permanent mold cast, T5	PTT (30% glass fiber, flame retarded)	PTT (30% glass fiber)
Aluminum, 333.0, permanent mold cast, T6	PPA (50% long glass fiber)	PA66/6 (33% glass fiber, lubricated)

FINAL TOPOLOGY OPTIMIZATIONS

Planet Carrier and Magnet Holder Optimizations

The team produced final topology optimizations for both the planet carrier and the magnet holder. Following the method described in the *Topology Optimization* subsection, both components were iterated through the process until optimal results were achieved.

As mentioned in the Topology Optimization section, Structural Optimization (topology) simulations were built on the Static Structural Simulation solutions for the original geometries of both the magnet holder

and planet carrier. The solutions were imported into the structural optimization simulation by linking the two in the workbench, as can be seen below in Figure 43.

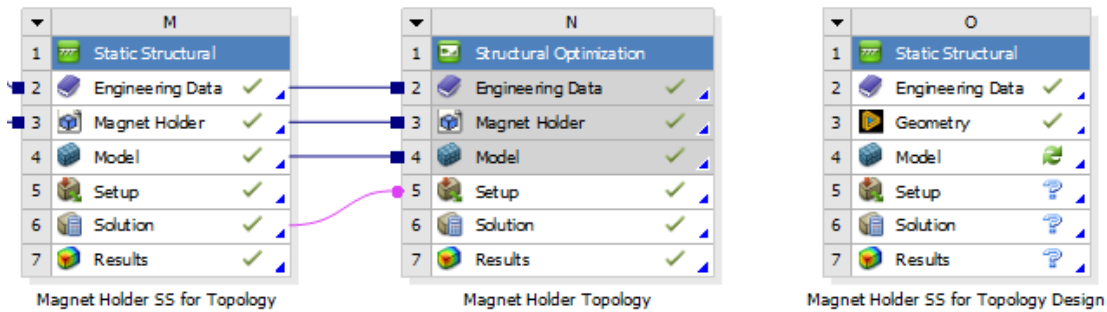


Figure 43. Screenshot of the Ansys Workbench showing how the solutions from the Static Structural Analysis were imported into the Structural Optimization Analysis for the Magnet Holder.

After importing the original geometries, load cases, and solutions the structural optimization simulation was run under the constraints mentioned in the Topology Optimization section. The solutions from the structural optimization simulations for both the planet carrier and magnet holder can be seen below in Figure 44.a and Figure 44.b.

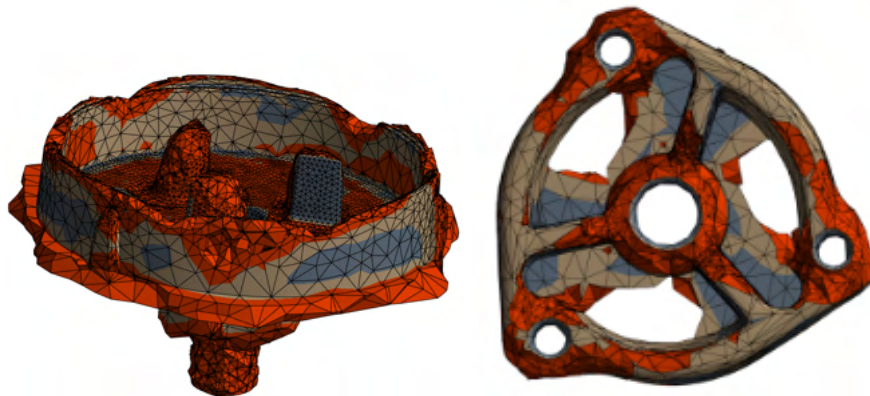


Figure 44.a and Figure 44.b. On the left is Figure 44.a, which shows the solution for the magnet holder from the Structural Optimization simulation. On the right is Figure 44.b, which shows the solution for the planet carrier from the Structural Optimization simulation.

The results generated from the simulation were to be redesigned on Ansys' SpaceClaim Software, but given the time constraints on the project and the learning curve for the software, the team opted to instead redesign the original model on Solidworks. The team deeply analyzed the results, taking note of what geometries were optimized and how. For the magnet holder, the simulation opted to remove mass from the outer edges and inner surface that holds the magnet. As for the planet carrier, the simulation completely removed mass from the areas in between the nubs since they experienced minimal stress distribution.

Building off of the results, the team did their best to replicate the design changes shown in Figure 44.a and Figure 44.b by sketching on the original geometries on Solidworks. The planet carrier had volume removed in the same spot where the topology said it would be optimal to remove, and the team designed

the extrusions in the shape of tear drops to prevent stress concentrations at any edges. Similarly, The magnet holder had volume reduced on the circular extruded surface that is meant to hold the magnet in the Y-axis only. Although the simulation opted to remove the majority of the mass from the same extruded surface in the X-axis, the team decided that it would be best to only follow through in the Y-axis given that the implications of reduced mass on these surfaces are not completely known yet, and will be further assessed in the final report. The final design for topology optimized geometries can be seen below in Figure 45a and Figure 45b.

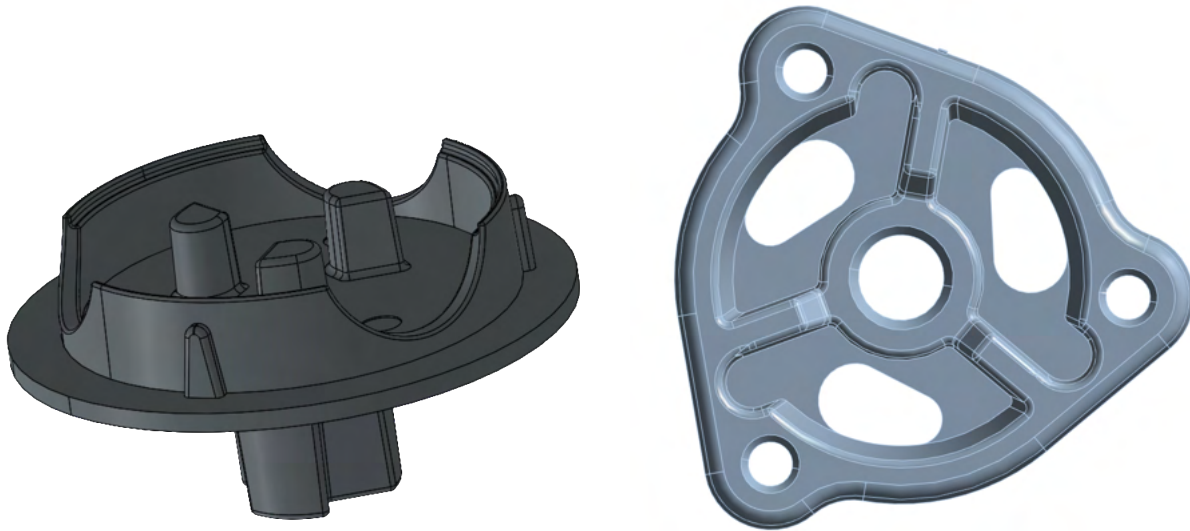


Figure 45.a and Figure 45.b. On the left is Figure 45.a which is the optimized geometry for the magnet holder, with circular extrusions on the outer surface to prevent stress concentrations. On the right is Figure 45.b, which is the optimized geometry for the planet carrier. The circular extrusions can be seen in between the nubs.

Lastly, the new geometries were imported again into the Ansys workbench to ensure that the components and materials meet and exceed the requirements and specifications. An example of the new geometries being validated again on Ansys can be seen below in Figure 46.

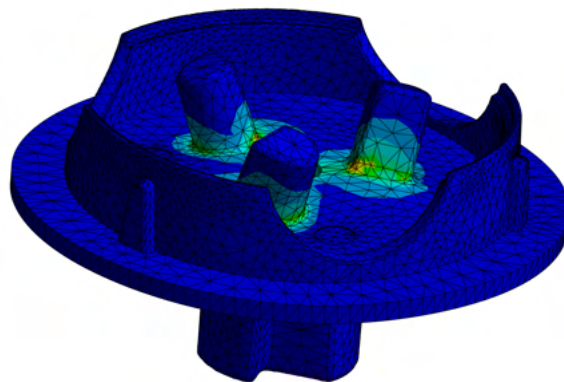


Figure 46. Screenshot of the second iteration Magnet Holder being tested to ensure they still meet specifications and requirements.

Final Topology Optimized Geometry Material Selection

The final step in the process is to also propose an optimal material with each new design for the components, since their new geometries may create different stress and deformation behaviors. The optimized solutions can be applied to any of the top materials, but given the time frame of the project, the team decided that it would be most time-efficient to only simulate the top five best-performing materials shown in Table 14. Table 15a and Table 15b below demonstrate the simulation results for both the magnet holder and planet carrier respectively. It is important to highlight that 4.61% of mass was reduced in the optimized design of the magnet holder, directly reducing the cost of raw material required for the component. It was also able to achieve a maximum stress reduction of 2.19% relative to its original geometry simulation results, making the component even more durable and efficient. Similarly, the optimized planet carrier reduced mass by 3.96%, greatly reducing the cost of raw materials for the component. Unlike the magnet holder, it was not able to reduce the maximum stresses but was still capable of maintaining very similar stresses to those experienced by the original geometries. Only the stress reduction percentage was mentioned in the results because failure is heavily dependent on the maximum principal stresses as they are the largest in magnitude throughout all simulations.

Table 15a. Final simulation results for the Magnet Holder’s top five respective material alternatives.

Magnet Holder - Topology Optimized Design					
Material	Max. Principal Stress (MPa)	Max Vibrational Stress (MPa)	Deformation (mm)	Mass Reduction %	Stress Reduction %
PTT (30% glass fiber)	24.41	0.087	0.0201	4.61	2.17
PPA (60% glass fiber)	24.52	0.095	0.0102	4.61	2.19
PPA (50% glass fiber, lubricated)	24.52	0.092	0.0127	4.61	2.19
PTT (30% glass fiber, flame retarded)	24.41	0.085	0.0186	4.61	2.17
PPA (50% long glass fiber)	24.52	0.084	0.0115	4.61	2.19
Zamak 5	24.88	0.376	0.0024	4.61	2.11

Table 15b. Final simulation results for the Planet Carrier's top five respective material alternatives.

Planet Carrier - Topology Optimized Design					
Material	Max. Principal Stress (MPa)	Max. Vibrational Stress (MPa)	Max. Deformation (mm)	Mass Reduction %	Stress Reduction % (Static)
PA66/6 (30% glass fiber)	15.31	2.25	0.000134	3.96	-0.33
PA66/6 (35% glass fiber)	15.29	1.67	0.000109	3.96	-0.28
PF (high strength glass fiber, molding)	15.22	5.65	0.000048	3.96	-0.17
PTT (30% glass fiber)	15.33	4.74	0.000077	3.96	-0.35
PA66/6 (33% glass fiber, lubricated)	15.29	3.33	0.000011	3.96	-0.28

Both components would be manufactured via injection molding given the suggested materials, and the implications have been assessed through an FMEA analysis as seen in Appendix K. The broader issue for this solution would be the need for entirely new tooling which would imply an additional cost. However, given that the components would be transitioning to a new material at the benefit of reduced cost and weight, it could be argued that the shift to this manufacturing method will pay itself over time.

Exclusion of Ring Gear

The team did not conduct topology optimization on the ring gear due to its geometrical constraints. It is composed of two major sections, the first being the ring gear teeth and the second being a thin walled cover for a portion of the system's motor. The teeth would not perform as intended if material were removed from them, the motor cover is already as thin as what is structurally acceptable, and its remaining features are crucial to its functionality. In addition, a change could also impact the component's ability to be die cast. Refer to Figure 34 for a visual of the ring gear.

VERIFICATION AND VALIDATION PLAN

Table 16. Verification and Validation Plans per Specification

Rank	Specification	Verification	P/F	Validation
1	Withstands > 15,000 shift cycles*	Ansys Analysis: SN Curve	TBD	Stoneridge cyclic tests*
	Lasts > 10 years	Ansys Analysis: Strain Life Parameters	TBD	Stoneridge cyclic tests*
1.1	- Withstands >135N +/- 15N axial load on plunger	Ansys static load test with random vibration test	PASS	Stoneridge shock and vibration cyclic testing*
	Withstands > 60 shocks (11 ms shocks of 500 m/s ²)	Ansys static load test with shock test	TBD	Stoneridge shock and vibration cyclic testing*
	Withstands given vibrational load**	Ansys static load test with random vibration test	PASS	Stoneridge shock and vibration cyclic testing*
1.3	Coefficient of thermal expansion: Magnet Holder $\leq 9.32 \mu\text{strain}/^\circ\text{C}$ Planet Carrier $\leq 16.46 \mu\text{strain}/^\circ\text{C}$ Ring Gear $\leq 25.74 \mu\text{strain}/^\circ\text{C}$	Granta EduPack	PASS	Tolerance evaluation of each material + Stoneridge cyclic testing at boundary temperatures*
	Yield strength: Magnet holder > 62.33 MPa Planet carrier > 29.98 MPa Ring gear > 35.72 MPa	Granta EduPack	PASS	Stoneridge cyclic tests under operating loads and conditions*
	112 HV < Hardness < 178 HV	Granta EduPack	PASS	Stoneridge cyclic tests for wear*
	Young's Modulus $\geq 1 \text{ GPa}$	Granta EduPack	PASS	Stoneridge cyclic tests under operating loads and conditions*
1.3.1	Does not seize/fail when operated between -40°C to 105°C	Granta EduPack	PASS	Thermal Stress Analysis + Stoneridge cyclic testing
2	Dimensions must be same as given in current drawings	CAD geometric evaluation	PASS	Stoneridge verification of component packaging envelope

Table 16. Verification and Validation Plans per Specification Cont.

Rank	Specification	Verification	P/F	Validation
3	Tolerance $\leq \pm 0.001''$ for ring gear and planetary carrier Tolerance $\leq \pm 0.002''$ for magnet holder	Research for Injection Molding and Die Casting	PASS	Stoneridge assessment of manufacturing methods
4	< \$0.67 for Magnet Holder < \$0.32 for Planet Carrier < \$1.20 for Ring Gear	Cost analysis	PASS	Supplier quotes
5	$\leq 36.01g$ for Magnet Holder $\leq 16.40g$ for Planet Carrier $\leq 86.37g$ for Ring Gear	Material density and current volume analysis	PASS	Weight measurement of final manufactured parts at Stoneridge
6	Achieve Fairtrade Standards or meet equivalent requirements laid out by Fairtrade. [25]	Research	TBD	Stoneridge assessment

*Refer to Figure 47 for Stoneridge’s cyclic test process

Above in Table 15 is the requirements and specifications table, now with the addition of how the solution will be or has already been validated and verified to meet these criteria. Next to the verification column, there is a PASS/FAIL column meaning that the team has already conducted the verification method, and the solution has passed that testing or the N/A means that the test has not occurred yet. Stoneridge has provided the team with shock cases, and they were simulated in a very similar manner to the previous tests, however through a gut check, these values were insignificant by orders of magnitude. Due to the limitations on the time frame of this course, the team was unable to confirm the validity of these values, therefore the team is recommending Stoneridge to conduct shock testing to ensure the recommendations withstand those cases as well. The team also recommends Stoneridge to conduct lifetime testing. Below in Figure 47 you can see the existing test plan that Stoneridge consistently uses, which will be addressed later in this section. Finally, the ethical sourcing requirement needs rigorous research to confirm that the materials the team is recommending are suitable to be used in a sustainable manner. This will be discussed further in the next steps section of the report, however this will be the final step of the team's verification of the proposed materials. Every other recommendation the team can confidently say passed due to engineering analysis.

The rightmost column contains the validation methods for each of these components. Because the team was working the majority of the time with simulations, nearly every validation method listed was a physical test that Stoneridge would need to conduct for the recommendations to be valid to them.

The first three criteria list the Ansys static load test and random vibration test as their verification method. This is because the static and random vibration simulations on Ansys use the load cases provided by Stoneridge and the vibrational loads with a safety factor on both. This means that the simulations run by the team could verify that the material selected or the part change selected, if run through this successfully, could be compared on how well it can withstand the shock and vibration load cases and not

deform as well, as those values listed were derived from the simulation too. These simulation methods and results are provided in the corresponding sections of the Engineering Analysis and Solution section of the report, which address the engineering process and any assumptions made within the verification. In order to validate that these simulations are accurate, the recommended test is Stoneridge's existing cyclic tests. The team has been notified by Stoneridge of existing tests and equipment, shown in Figure 47 below, and this is one that the team would recommend is run on the proposed materials in order to validate their performance. It is also recommended that these are chamber tested at the temperature extremes as well. The temperature range requirement was confirmed by running the static tests at these ranges, as well as the hand calculations of the coefficient of thermal expansion in the corresponding engineering analysis section above. The team is extremely confident that none of these parts exceed the packaging envelope because of CAD geometric analysis as well as the only geometric changes were removal of material from the same dimensions. The weight analysis was done using Ansys volume tools as well and used the densities given in the Granta EduPack. This is similar to what was done for cost, as the raw values were sourced from the EduPack as well, but the unit cost was extrapolated through the analysis shown earlier in the report. The manufacturing methods were limited to die casting for metals and injection molding for polymers, this tolerance and decision is discussed as well in the engineering analysis section.

All of the completed verification methods done by the team are outlined in greater detail within the engineering analysis section of this report. The solutions comply with each of these specifications and requirements, and the team has high confidence in these results due to Ansys simulations being a trusted industry standard verification tool and that the simulation and assumptions were verified by an expert, MECHENG 305 FEA Professor Huan, along with convergence testing to validate the precision of the results of the simulation itself. The validation necessary for these simulations the team will also have high confidence in because Stoneridge has conducted these tests before, shown in their plan in Figure xx below, and they are necessary in order to physically prove that the assumptions made are robust enough to translate the conclusions made from the team's results, and if any material properties that have not been explicitly defined cause any unforeseen issues in the actuator.

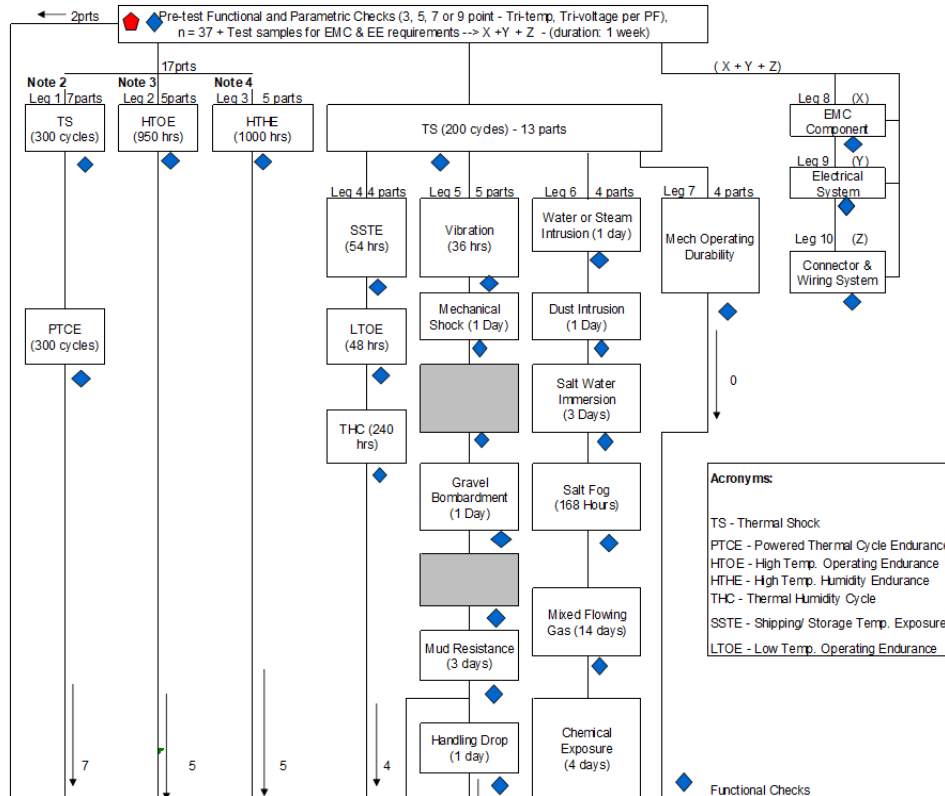


Figure 47. Current Stoneridge baseline PV Test Flow Diagram for the SmartBar Actuator, Including all Test Legs

DISCUSSION

Problem Definition

With additional time, the team would aim to verify vibration and shock analysis results by reviewing the Ansys Workbench with experts. The team would choose to expand the problem definition even further by exploring alternate ways the magnet holder and planet carrier can be topology optimized. Analysis for static loads, shock, and vibration would be completed and compared between multiple topology-optimized designs. The team found that topology decreased weight, and sometimes improved stress concentrations on the part. Therefore, exploring the benefits of topology optimization is worth pursuing in the future with more time.

Reflection

After starting with little to no experience in Ansys, the team spent time thoroughly reviewing Ansys software and its various applications. The team became well acquainted with Ansys tools and how to apply them for the purposes. The team also learned to utilize the material selection tool in Ansys which helped aid the entire material selection process. Overall, the learning curve for Ansys started as the biggest challenge, however after obtaining resources from the internet and watching Ansys tutorials, the team's comfort and confidence in using the program increased.

Concept generation and engineering analysis was a very similar process and tended to bridge into one entire process. The team was able to work on engineering analysis and Ansys simulations in tandem.

While some members of the team focused on learning Ansys, others focused on first principles analysis. Splitting up the work in this way allowed for better time management and the ability to complete all project tasks by DR#3 presentation and report. Another important lesson learned includes the value of literature and reference textbooks. Searching online for textbooks, or using textbooks/standards available heavily guided the team when completing the first principle analysis work.

Design Critique

The only direct design aspect of our solutions was through the topology optimization. The strengths of this solution is that it can be iteratively run to reach theoretically accurate results which can validate early concepts and design changes. This also saves Stoneridge time and resources by not having to invest in physical prototypes and testing. The weakness in this approach is that while making the component more aesthetic and easier to manufacture, the transition between the generated solutions and the interpreted results leads to loss of effectiveness in final solutions. An example of this is the planet carrier being optimized to reduce mass by 5% in simulations, but after design interpretations the final solution had a mass reduction of 3.96% as seen in Table 15b, having a 1.04% loss in mass reduction in the process. This could be improved through several design interpretations between topology simulations and the original geometry to reduce as much mass as possible relative to the solution parameters.

Having completed the design process, the team should not have attempted to learn the SpaceClaim software that Ansys provides to redesign optimized components. This is because it proved to be very difficult to learn and was therefore an inefficient use of the team's time. It was more intuitive to the team to translate the topology optimization results to SolidWorks and redesign the component based on those interpretations instead.

Additionally, applying surface conditions at the interfaces between the components could have generated more accurate solutions. For example, the team did not apply assembly constraints within Ansys, so the software relied solely on the default available constraints. Taking this next step would provide a model with slightly different interfaces, which may be more or less accurate depending on the quality of the assembly.

Challenges

Although the team became more comfortable with Ansys throughout the duration of the project, there were still several challenges related to the software that arose. One major challenge the team faced included completing shock load testing. Issues with the model occurred on Ansys and meaningful results could not be obtained. If this issue cannot be resolved, the team recommends Stoneridge use its Shock Test Fixture to produce shock test results. Another challenge included limited computer capabilities regarding CPU and RAM. The CAEN computers available for the project were unable to run the optimal mesh size for the ring gear that was determined from the convergence test of the ring gear. The team overcame this challenge by choosing a slightly smaller mesh size to run for the ring gear. The quality of the mesh was checked using the Mesh Quality feature in Ansys. Another challenge the team experienced was long wait times for simulation runs. Some simulations took over an hour to complete. It was pivotal to plan out days for simulation runs and ensure there was enough time to complete all necessary tests. The team took advantage of the long simulation times by completing first principles or report writing during wait times.

The team also faced challenges regarding finding accurate values for cost. Getting an estimate for the cost of each manufacturing process, tooling, and service employers was difficult to obtain through research. To

combat this issue, the approach discussed in the *Cost Analysis* section was taken. Finding a general price for tooling/labor/overhead based on existing metal and plastic materials supplied to Stoneridge served as the best method to estimate unit costs.

Potential challenges for manufacturing methods of the final proposed plastics for the planet carrier and magnet holder, and the final proposed metals for the ring gear are outlined in depth in the Failure Mode Effects and Analysis (FMEA) discussed in the following Threat Analysis section and presented in Appendix K.

Threat Analysis

Various simplifications were made throughout the engineering analyses, so the team completed a Failure Mode Effects and Analysis (FMEA) to account for potential shortcomings of the components. The team created a Risk Priority Number (RPN) ranking scheme by defining and then multiplying each failure mode’s severity value, occurrence value, and detection value. This is shown in Figure 48 below.

Value	Severity	Occurance	Detectibility
1	- Unnoticeable / No impact on component functionality	- Extremely unlikely that failure will occur	- Almost always detectible in-house
2	- Component still functional, but has minor issues that impacts < 25% of end users	- Relatively low amount of failures	- Relatively high amount of failures are detected in-house
3	- Component still functional, but has minor issues that impacts < 50% of end users	-	-
4	- Component still functional, but has minor issues that impacts < 75% of end users	-	- Relatively low amount of failures are first detected by end users
5	- Component's secondary function is impaired	- Relatively moderate amount of failures	- Relatively moderate amount of failures are first detected by end users
6	- Component loses secondary function	-	-
7	- Component's primary function is impaired	-	-
8	- Component loses primary function	- Relatively high amount of failures	- Relatively high amount of failures are first detected by end users
9	- Failure mode affects safety and functional requirements with a warning	-	-
10	- Failure mode affects safety and functional requirements without warning	- Relatively very high amount of failures / almost guaranteed	- Almost impossible to detect failure mode prior to releasing product to end users

Figure 48. Risk Priority Number (RPN) definition table

Severity, occurrence, and detection were defined on a scale from 1 to 10, and their associated meanings were. The boxes with a dash fall under the definition that is above them. The team completed an FMEA

for each of the three components as well as the expected manufacturing processes, injection molding and die casting. The FMEA for the ring gear is shown below in Figure 49, and the remainder of the FMEAs are in Appendix K.

Ring Gear										
Function	Potential Failure Mode	Potential Effect(s) of Failure	Severity	Potential Cause(s) of failure / Mechanism(s) of Failure	Occurance	Process Controls	Detectability	Risk Priority Number (RPN)	Recommended Actions	Responsibility
Houses the motor	- Collection of debris or disruptive objects on/ in the motor	- Negatively impacts the efficiency and capability of the motors	6	- Out of specification tolerances of interfacing components (ring gear and motor housing) create gaps/ entrances for debris/ dust	2	- End of line (EOL) part quality inspections - Proper assessment of Cp & Cpk tests from supplier for component	4	48	- Ensure manufacturer/ supplier are capable of ensuring quality parts	Stoneridge
Allow planetary gears to rotate about the sun gear	- Fracture/ Cracking - Component Deformation - Tooth Wear	- Inefficient torque transmission between planet carrier and magnet holder - Gear slippage	9	- Material hardness mismatch between the ring gear and planet gears - Loads enacting on teeth of the ring gear exceed the capabilities of the selected material (acting stress is larger than the tensile strength)	2	- Material testing / Material selection reassessment - Design review for load capabilities	2	36	- Ensure manufacturer/supplier are capable of ensuring quality parts - Cyclic life testing at varying temperatures for nominal loads	Stoneridge
Die cast manufacturing - Form Desired Geometry	- Cold Shut	- Weak structural integrity of components	8	- Premature solidification	2	- Flow simulation, process optimization	2	32	- Improve mold design, increase molten metal temperature	Stoneridge
Die cast manufacturing - Fill mold with material	- Misruns	- Incomplete parts that are unusable	8	- Low temperature, slow pouring	2	- Temperature control, pour rate adjustment	1	16	- Optimize temperature and pour rate, preheat the die	Stoneridge
Die cast manufacturing - Eject Cast Part	- Ejector Marks	- Surface defects, part rejection	4	- Improper ejection settings	1	- Ejection mechanism adjustment, lubrication	1	4	- Calibrate ejection pins, apply appropriate lubrication	Stoneridge

Figure 49. Failure Mode Effects and Analysis (FMEA) table for ring gear

The table includes the functions that will potentially be affected, as well as their failure modes, effects of failure, causes of failure, process controls, and recommended actions. These functions were then assigned a final RPN, which was calculated with Equation 27 below, and the highest risk was highlighted in yellow.

$$severity\ value * occurrence\ value * detectability\ value = RPN \quad (27)[104]$$

The highest risk items in the FMEA will provide a priority ranking for the validations that Stoneridge should conduct. For example, the impact of debris will be mitigated by Stoneridge’s seal testing procedures and the potential for wear or deformation will be mitigated by their cycle testing.

REFLECTION

Greater Context and Impacts

As mentioned in the *Design Context* section, the project is tied to public health and safety as the materials being selected for the components are sourced differently. The current material, die-cast Zinc Zamak 5, has associated environmental and health risks, especially from Zinc mining which can release harmful elements like lead and cadmium which can cause health issues to workers and damage their local agriculture. In a global context, the optimized topology design and material selection could make the product more affordable for end-users. The social impacts of the use and disposal of the product were assessed through the recyclability of alternative materials and disposal methods. Similar to the global context, the economic impacts associated with manufacturability would imply altering the cost of the product in vehicles and impacting their affordability. Lastly, several tools such as stakeholder maps, FEA, and GrantaEdupack were used to find ethical solutions in a time efficient manner as well as be able to benchmark alternative solutions to one another.

Inclusion and Equity

As mentioned in the *Design Context* section, the power dynamics are complex, shaped by the different interests and authority of the stakeholders involved. Stoneridge holds significant influence due to their role as the financial and strategic driver of the project, prioritizing cost reduction in production. This focus contrasts with the team's ethical and environmental concerns, particularly regarding the sustainable sourcing and life cycle of materials. The team, composed of members with a strong inclination towards sustainable practices, faces a power imbalance as their decision-making is constrained by the sponsor's priorities. Additionally, the dynamics between the team and the end users, who do not directly interact with the product, create a disconnect in priorities and perspectives, with the end users likely more focused on the final product's performance and cost rather than its environmental impact.

The power dynamics are further complicated by the educational context of the project, as the University of Michigan sets certain academic standards and expectations. The ME 450 Instructional team also influenced the project's scope and depth, potentially diverging from the sponsor's commercial objectives. The team's challenge lies in balancing the needs and wants from the different stakeholders in their respective positions of power. This was done so by consistently communicating with all stakeholders and understanding their perspectives on certain decisions before taking action. Emphasizing balancing the sponsor's focus on cost, the team's own ethical considerations, and the academic requirements set by the university.

Cultural, privilege, and identity differences within the team and between the team and the sponsor add another layer to these dynamics. These differences led to varied approaches to problem-solving and decision-making, influencing how the team prioritizes and integrates different viewpoints. However, the team's capacity to fully incorporate these diverse perspectives into the final design is limited by the influence of the sponsor, highlighting the often-complicated nature of power relations in collaborative projects where multiple stakeholders with differing priorities and levels of influence are involved.

Ethics

Ethics were thoroughly discussed throughout the *Design Context* section. To quickly summarize, the team faced ethical dilemmas in finding capable materials that are sourced ethically and capable of meeting the requirements and specifications. To manage this, the team proceeded to evaluate all of the best alternative

materials whilst simultaneously keeping record of their environmental impacts and sources methods to hand over to Stoneridge to evaluate. After thorough research, the team found several polymer alternatives that met the criteria, achieving a positive shift in ethical sourcing given the differences in metal and plastic sourcing as seen in the material selection pugh charts in Appendix E. Note that several of the materials use various fillings, which have additional ethical considerations. For example, glass fibers or glass fillings are lab-made, but because they are sourced from sand, they are highly sustainable [109]. Carbon fiber fillings are also lab-made and have long lifetimes, but their creation is highly energy intensive and there is no simple recycling method [117]. Alternatively, mineral fillings, such as mica or calcium carbonate, are mined or found in quarries throughout various regions of the world [114, 115, 116]. The use of this information in relation to material sourcing will be left to the discretion of Stoneridge.

RECOMMENDATIONS

Stoneridge asked for a streamlined way to determine alternate materials for their parts. The team has outlined a method that can work well for any alternate material selection application. The team recommends that Stoneridge take this approach to apply in the future. The Granta Edupack tool is a valuable starting place to search materials for certain applications. As outlined in our results, Ansys serves as an important tool to check stresses and deformation to parts. However, the shock and vibration analysis will need to be addressed by Stoneridge, as the team was unable to verify the results obtained from Ansys due to time and resource constraints. The team still recommends Stoneridge use Ansys because it provides a way to incorporate static loads with random vibration and shock test simulations. The results and setup, including all applied load and constraints, should be verified by an FEA expert since there are limited resources about Ansys simulation setups available online. Once completed, Stoneridge will have one streamlined approach to test for static load stresses, vibrations loads, and shock loads.

Important system-level recommendations include doing a thorough cost analysis using quotes from manufacturers to confirm unit costs for each part with material changes. This should include determining accurate values for tooling/labor/overhead for each proposed material. Another important consideration will be the sourcing of each material to be sustainable and ethical when choosing an alternate material. The sourcing of each material is provided in the final pugh charts for each part in Appendix E for Stoneridge to reference. All validation tests described in the Verification and Validation section of the report should be completed after selecting a material to ensure the part performs as expected. Refer to Appendix K for a thorough risk analysis (FMEA) related to the manufacturing processes for plastics and metals, as well as specific risks associated with the planet carrier, magnet older, and ring gear. Recommendations to address each risk are also provided in the FMEA tables.

CONCLUSION

The team focused on reducing the cost and weight of the SmartBar Actuator, both by proposing new materials for the magnet holder, planet carrier, and ring gear, as well as by topology optimization. The top stakeholder requirements, which have been translated into quantifiable engineering specifications, include ensuring a minimum lifetime, withstanding specified loads, not deforming, remaining within the packaging envelope, being capable of tight manufacturing tolerances, and reducing cost and weight. The design context also heavily relies on ethical material selection due to the social and societal implications and end-of-life disposal options. Concept generation and selection were done for both the first iteration

material selection process and potential design improvement. Deliverables included material recommendations, topology optimizations, performance analyses, and cost evaluations.

The top five material recommendations for each component, from least to most expensive, are listed in the Engineering Analysis section. These were chosen using the Granta EduPack material database in conjunction with extensive verification done by hand and with FEA. The main challenges were forming a new knowledge base in FEA, creating accurate FEMs, and estimating costs. The team conducted and recommended for Stoneridge various validations in order to ensure that the material selections were based on solid conclusions from the simulations.

ACKNOWLEDGEMENTS

The team would like to thank Stoneridge for providing both the capstone project opportunity and support throughout the semester in order to complete it. Thank you to Harish Chowdhary Athipatla and Mark Brankovich, the team's company contacts, as well as Stoneridge Scholar, Kevin Kaya, for an invaluable experience. The team especially wants to acknowledge Randy Schwemmin for providing his time as well as direction and feedback at every step of the project timeline.

The team finally would like to thank the MECHENG 450 instructional team, Sarah Barbrow, Professor Umbriac, Professor Huan, and Professor Love for their time, support, and willingness to help.

APPENDIX A

Individual Concept Generation

The concept generation used by the team. It shows each member's individual contributions that were then all combined for concept selection and further generation processes.

Concept 1 - planet carrier

Concept 2 - make the entire system smaller

Concept 3 - use gear with splines to connect

Concept 4 - planet carrier expansion

Concept 5 - planet holder made of 2 parts

Concept 6 - planet holder that has

Concept 7 - set gears that are connected

Concept 8 - planet holder made of 2 parts

Concept 9 - planet holder that are connected

Concept 10 - use the manufacturing technique

Concept 11 - planet holder made of 2 parts

Concept 12 - planet holder made of 2 parts

Concept 13 - planet holder made of 2 parts

Concept 14 - planet holder made of 2 parts

Concept 15 - use rollers (coating)

Concept 16 - use a different gear design

Concept 17 - planet holder made

Concept 18 - planet holder made

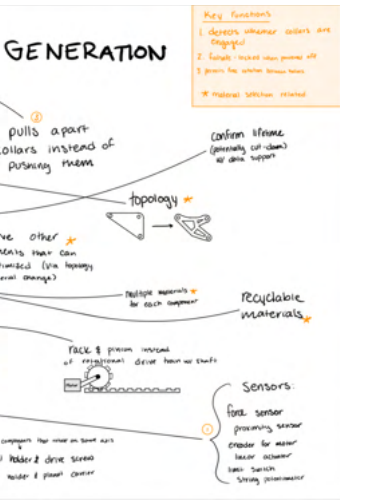
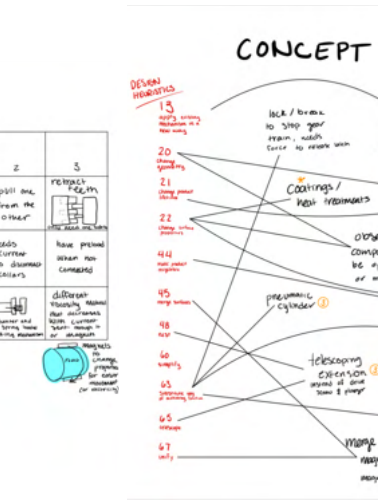
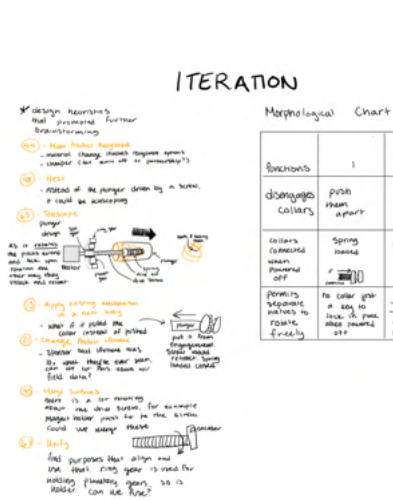
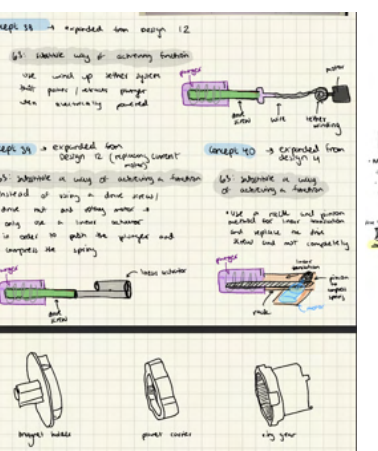
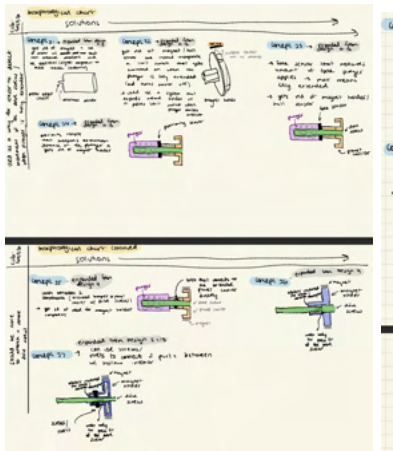
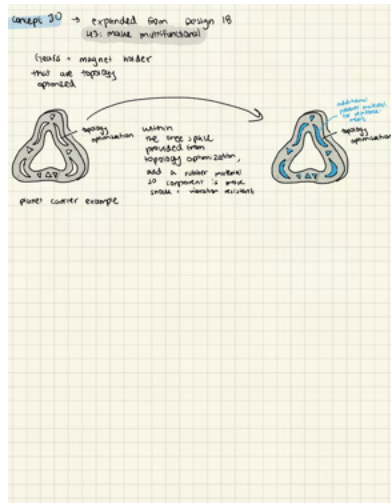
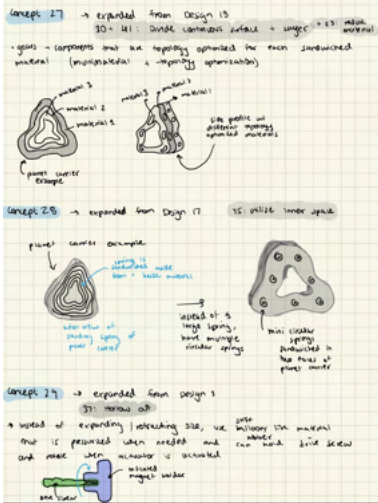
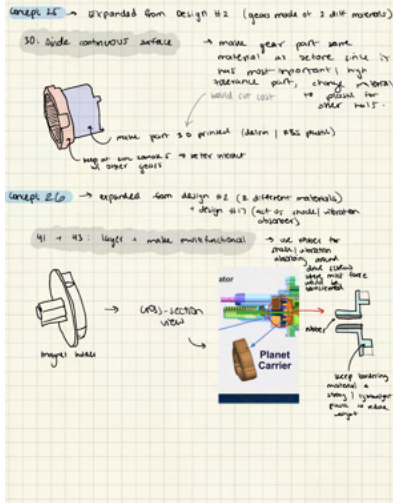
Concept 19 - observe other looking mechanisms

Concept 20 - add an additional part

Concept 21 - expanding team design

Concept 22 - expanding on design

Concept 23 - expanding team design






APPENDIX B

Sensor Selection Pugh Chart Concepts

Table with the details of each sensor analyzed in the pugh chart, including an image and short description.

Concept	Image	Description
Hall Sensor (current design) [92]		<p>The Hall-Effect sensor is sensitive to magnets. The output state is held until a magnetic flux density reversal falls below B_{rp} causing it to be turned off. [92]</p>
Motor with Encoder [93]		<p>A motor encoder is a rotary encoder mounted to an electric motor that provides closed-loop feedback signals by tracking a motor shaft's speed and/or position. Various motor encoder configurations are available such as incremental or absolute, optical or magnetic, and shafted or hub/hollow shaft, among others. The type of motor encoder used depends upon many factors, particularly motor type, the application requiring closed-loop feedback, and the mounting configuration required. [93]</p>
Proximity Sensor for drive nut [80]		<p>"Proximity Sensor" includes all sensors that perform non-contact detection in comparison to sensors, such as limit switches, that detect objects by physically contacting them. Proximity Sensors convert information on the movement or presence of an object into an electrical signal. [95]</p>

<p>Limit Switch [81]</p>		<p>A limit switch is an electromechanical device operated by a physical force applied to it by an object. Limit switches are used to detect the presence or absence of an object. These switches were originally used to define the limit of travel of an object, and as a result, they were named Limit Switch. [94]</p>
<p>String Potentiometer [82]</p>		<p>A String potentiometer can be used to measure steering angle or linear travel. Features a 500mm travel using a stainless steel cable, and a M8 3P analog signal connector that easily connects to our plug and play harness system [82]</p>
<p>Pressure Sensor [91]</p>		<p>Pressure sensors are extremely useful devices that measure the physical pressure of gasses or liquids via a sensor and output signal. Pressure is defined as the force required to stop a fluid from expanding, typically displayed as force per unit area. [91]</p>

APPENDIX C

Benchmarked Materials

Some of the benchmarked materials that were found prior to the team's discovery of Granta EduPack's large material database and filtering system.

Materials	41xx Steel – Chromoly Steel	Grade 303 Stainless Steel	Grade 300 Cast Iron, Gray
Cost	\$4.63E-3 /cm ³	\$49.77E-3 /cm ³	\$3.46E-3 /cm ³
Density	7.85 g/cm ³	7.90 g/cm ³	7.20 g/cm ³
Stable Temperature Range	N/A*	N/A* to 870°C	N/A*
Melting Temperature	1427°C	1375°C	1250°C
Common Manufacturing Methods	Machining, Sheet Metal Fabrication, Drawing	Machining (machine only with tools dedicated to stainless steel materials), Hot Working	Sand Casting, Centrifugal Casting, Machining
Yield Strength	500 MPa	135 MPa	300 MPa
Ultimate Tensile Strength	700 MPa	625 MPa	295 MPa
Brinell Hardness	93 BHN	230 BHN	240 BHN
Coefficient of thermal expansion	1.30E-5 1/°C	1.65E-5 1/°C	1.20E-5 1/°C
Raw Material Source	Chromium, Molybdenum, Carbon, Manganese, Silicon, found in mines. []	Mainly iron but some chromium. Releases large scale of iron ore tailings as result of refinement. Stainless steel is recyclable. []	Product of melting iron ore in a blast furnace. Releases large scale of iron ore tailings as result of refinement. []

APPENDIX D

Random Vibration Data Provided by Stoneridge

The data used for the Random Vibration stress analysis in Ansys. Results are provided in the Pugh Chart for each part.

Test Parameters for Random Vibration			
Random Vibration profile for Class V2, V3	Frequency [Hz]	Power spectral density (PSD) [(m/s ²)/Hz]	Power spectral density (PSD) [G ² /Hz]
	10	20.00	0.2080
	55	6.50	0.0676
	180	0.25	0.0026
	300	0.25	0.0026
	360	0.14	0.0015
	1 000	0.14	0.0015
	RMS acceleration	27.78 m/s ²	2.84 G

Shock Data Provided by Stoneridge

The data used for the Shock simulation analysis in Ansys.

- **Mechanical Shock** → 24hr duration; acceleration = 500 m/s² ; half sine profile for 11ms per shock ; total 60 shocks (10 shocks per direction ±X, ±Y, ±Z)

APPENDIX E

Material Selection Pugh Charts

The exhaustive list of all of the materials and how they perform according to the pugh chart criteria and the weights assigned.

Ring Gear Pugh Charts Cont.

Criteria	Weight	Aluminum, 333.0, permanent mold cast, T6	Aluminum, EN AC-48000, chill cast, T6	Aluminum, A332.0, cast, T6	Aluminum, 336.0, permanent mold cast, T65	Aluminum, 336.0, permanent mold cast, T551	Zinc-aluminum alloy, ZA-27, general casting
Reduce cost from \$1.20	2	\$0.47 (5)	\$0.47 (5)	\$0.51 (5)	\$0.51 (5)	\$0.51 (5)	\$0.98 (3)
Reduce weight from 86.37g	1	36.37 g (5)	35.51 g (5)	35.78 g (5)	35.91 g (5)	35.91 g (5)	66.19 g (3)
Withstands >135N +/- 15N axial load on plunger (% of yield)	Pass / Fail	11.67%	9.63%	8.39%	8.00%	12.27%	7.56%
Withstands specified vibrational load profile (% of yield)	Pass / Fail	1.48%	1.56%	0.47%	0.66%	0.94%	0.45%
Does not seize/fail when operated between -40°C to 105°C (% of yield)	Pass / Fail	1.80% max T 1.79% min T	1.56% max T 1.55% min T	1.49% max T 1.49% min T	2.80% max T 2.79% min T	1.88% max T 1.87% min T	1.47% max T 1.46% min T
Has a Vickers Hardness value between 112 and 178 HV	Pass / Fail	117 HV	113 HV	120 HV	142 HV	117 HV	130 HV
Tolerance \leq +/- 0.001" for ring gear and planetary carrier	Pass / Fail	(+/-) 0.001" for finished part (die casting)	(+/-) 0.001" for finished part (die casting)	(+/-) 0.001" for finished part (die casting)	(+/-) 0.001" for finished part (die casting)	(+/-) 0.001" for finished part (die casting)	(+/-) 0.001" for finished part (die casting)
Is ethically sourced	N/A	Aluminum (bauxite mining) with magnesium and silicon components (found in mines). [4,10]	Aluminum (bauxite mining) with magnesium and silicon components (found in mines). [4,10]	Aluminum (bauxite mining) with magnesium and silicon components (found in mines). [4,10]	Aluminum (bauxite mining) with magnesium and silicon components (found in mines). [4,10]	Aluminum (bauxite mining) with magnesium and silicon components (found in mines). [4,10]	Zinc-Lead mines in China, Southern America. Aluminum (bauxite mining) with magnesium and silicon components (found in mines). [16,4,10]
Does not seize/fail when operated between -40°C to 105°C (% of yield)	N/A						
Has a Young's Modulus \geq 1 GPa	N/A						
Tolerance \leq +/- 0.002" for magnet holder	N/A						
TOTAL		15	15	15	15	15	9

Magnet Holder Pugh Charts

Criteria	Weight	Zamak 5	PTT (30% glass fiber)	PPA (60% glass fiber)	PPA (50% glass fiber, lubricated)	PTT (30% glass fiber, flame retarded)
Reduce cost from \$0.67	2	\$0.67 (0)	\$0.24 (4)	\$0.29 (4)	\$0.30 (4)	\$0.33 (4)
Reduce weight from 36.01g	1	36.01 g (0)	9.08 g (2)	9.63 g (1)	9.14 g (2)	9.25 g (2)
Withstands >135N +/- 15N axial load on plunger (% of yield)	Pass / Fail	12.70%	19.50%	9.80%	14%	24.70%
Withstands specified vibrational load profile (% of yield)	Pass / Fail	0.23%	0.06%	0.04%	0.04%	0.08%
Does not seize/fail when operated between -40°C to 105°C (% of yield)	Pass / Fail	0.24% max T 0.26% min T	0.14% max T 0.15% min T	0.10% max T 0.13% min T	0.14% max T 0.15% min T	0.19% max T 0.20% min T
Has a Young's Modulus ≥ 1 GPa	Pass / Fail	96 GPa	11 GPa	19 GPa	15.9 GPa	11.7 GPa
Tolerance $\leq \pm 0.002''$ for magnet holder	Pass / Fail	(\pm) 0.001'' for finished part (die casting)	(\pm) 0.002'' for finished part (injection molding)	(\pm) 0.002'' for finished part (injection molding)	(\pm) 0.002'' for finished part (injection molding)	(\pm) 0.002'' for finished part (injection molding)
Is ethically sourced	N/A	Zinc-Lead mines in China, Southern America. [16]	Derived from bio-based materials, making them an attractive alternative to traditional petroleum-based polymers. [107]	Recyclable. Its high durability and resistance to degradation ensure that products made from it have a long service life. [108]	Recyclable. Its high durability and resistance to degradation ensure that products made from it have a long service life. [108]	Derived from bio-based materials, making them an attractive alternative to traditional petroleum-based polymers. [107]
Tolerance $\leq \pm 0.001''$ for ring gear and planetary carrier	N/A					
Has a Vickers Hardness value between 112 and 178 HV	N/A					
TOTAL		0	10	9	10	10

Magnet Holder Pugh Charts Cont.

Criteria	Weight	PTT (30% glass fiber, 15% PTFE)	PPA (50% long glass fiber)	LCP (50% glass fiber)	LCP (45% glass fiber)
Reduce cost from \$0.67	2	\$0.35 (4)	\$0.34 (4)	\$0.62 (2)	\$0.66 (2)
Reduce weight from 36.01g	1	8.54 g (4)	8.98 g (3)	9.68 g (1)	9.68 g (1)
Withstands >135N +/- 15N axial load on plunger (% of yield)	Pass / Fail	21.30%	10.70%	16.20%	20.40%
Withstands specified vibrational load profile (% of yield)	Pass / Fail	0.07%	0.03%	0.06%	0.07%
Does not seize/fail when operated between -40°C to 105°C (% of yield)	Pass / Fail	0.13% max T 0.14% min T	0.12% max T 0.12% min T	0.21% max T 0.22% min T	0.22% max T 0.24% min T
Has a Young's Modulus \geq 1 GPa	Pass / Fail	8.96 GPa	17.9 GPa	22 GPa	18.2 GPa
Tolerance \leq +/- 0.002" for magnet holder	Pass / Fail	(+/-) 0.002" for finished part (injection molding)	(+/-) 0.002" for finished part (injection molding)	(+/-) 0.002" for finished part (injection molding)	(+/-) 0.002" for finished part (injection molding)
Is ethically sourced	N/A	Derived from bio-based materials, making them an attractive alternative to traditional petroleum-based polymers. [107]	Recyclable. Its high durability and resistance to degradation ensure that products made from it have a long service life. [108]	Uses dangerous chemicals for production, but then becomes inert. Inhalation of liquid-crystal polymers will irritate the respiratory tract. [113]	Uses dangerous chemicals for production, but then becomes inert. Inhalation of liquid-crystal polymers will irritate the respiratory tract. [113]
Tolerance \leq +/- 0.001" for ring gear and planetary carrier	N/A				
Has a Vickers Hardness value between 112 and 178 HV	N/A				
TOTAL		12	11	5	5

Magnet Holder Pugh Charts Cont.

Criteria	Weight	LCP (40% glass fiber)	LCP (30% glass fiber)	LCP (15% glass fiber)	Epoxy SMC (55% long carbon fiber)
Reduce cost from \$0.67	2	\$0.68 (2)	\$0.73 (2)	\$0.78 (2)	\$1.47 (1)
Reduce weight from 36.01g	1	9.30 g (2)	8.87 g (3)	8.16 g (5)	8.11 g (5)
Withstands >135N +/- 15N axial load on plunger (% of yield)	Pass / Fail	20.20%	17.90%	9.20%	10.90%
Withstands specified vibrational load profile (% of yield)	Pass / Fail	0.07%	0.06%	0.03%	0.22%
Does not seize/fail when operated between -40°C to 105°C (% of yield)	Pass / Fail	0.19% max T 0.20% min T	0.14% max T 0.18% min T	0.07% max T 0.08% min T	0.26% max T 0.27% min T
Has a Young's Modulus \geq 1 GPa	Pass / Fail	15 GPa	13.8 GPa	12.1 GPa	55.1 GPa
Tolerance \leq +/- 0.002" for magnet holder	Pass / Fail	(+/-) 0.002" for finished part (injection molding)	(+/-) 0.002" for finished part (injection molding)	(+/-) 0.002" for finished part (injection molding)	(+/-) 0.002" for finished part (injection molding)
Is ethically sourced	N/A	Uses dangerous chemicals for production, but then becomes inert. Inhalation of liquid-crystal polymers will irritate the respiratory tract. [113]	Uses dangerous chemicals for production, but then becomes inert. Inhalation of liquid-crystal polymers will irritate the respiratory tract. [113]	Uses dangerous chemicals for production, but then becomes inert. Inhalation of liquid-crystal polymers will irritate the respiratory tract. [113]	Has a longer lifetime due to its high durability and the ability to recycle it, the total life cycle impact is lower than for other materials. [110]
Tolerance \leq +/- 0.001" for ring gear and planetary carrier	N/A				
Has a Vickers Hardness value between 112 and 178 HV	N/A				
TOTAL		Fail	Fail	Fail	Fail

Planet Carrier Pugh Charts

Criteria	Weight	Zamak 5	PA66/6 (30% glass fiber)	PA66/6 (35% glass fiber)	PF (high strength glass fiber, molding)	PTT (30% glass fiber)
Reduce cost from \$0.32	2	\$0.32 (0)	\$0.09 (4)	\$0.09 (4)	\$0.11 (4)	\$0.11 (4)
Reduce weight from 16.40g	1	16.40 g (0)	3.41 g (5)	3.53 g (4)	4.97 g (1)	4.15 g (3)
Withstands >135N +/- 15N axial load on plunger (% of yield)	Pass / Fail	7.50%	15.26%	11.91%	20.26%	11.93%
Withstands specified vibrational load profile (% of yield)	Pass / Fail	10.26%	0.74%	0.62%	3.61%	1.07%
Does not seize/fail when operated between -40°C to 105°C (% of yield)	Pass / Fail	0.11% max T 0.12% min T	0.04% max T 0.04% min T	0.03% max T 0.05% min T	0.09% max T 0.14% min T	0.05% max T 0.06% min T
Has a Young's Modulus \geq 1 GPa	Pass / Fail	96 GPa	5.5 GPa	6.5 GPa	13.1 GPa	11 GPa
Tolerance \leq +/- 0.001" for ring gear and planetary carrier	Pass / Fail	(+/-) 0.001" for finished part (die casting)	(+/-) 0.002" for finished part (injection molding)	(+/-) 0.002" for finished part (injection molding)	(+/-) 0.002" for finished part (injection molding)	(+/-) 0.002" for finished part (injection molding)
Is ethically sourced	N/A	Zinc-Lead mines in China, Southern America. [16]	Renowned as sustainable alternatives to synthetic nylon fibers, bio-polyamides offer biodegradability and non-toxicity. [105]	Renowned as sustainable alternatives to synthetic nylon fibers, bio-polyamides offer biodegradability and non-toxicity. [105]	Lab-made, but Phenol is mainly obtained from non-renewable resources. [106]	Derived from bio-based materials, making them an attractive alternative to traditional petroleum-based polymers. [107]
Tolerance \leq +/- 0.002" for magnet holder	N/A					
Has a Vickers Hardness value between 112 and 178 HV	N/A					
TOTAL		0	13	12	8	11

Planet Carrier Pugh Charts Cont.

Criteria	Weight	PA66/6 (33% glass fiber, lubricated)	PPA (60% glass fiber)	PPA (50% glass fiber)	PPA (50% glass fiber, lubricated)	Epoxy bisphenol molding compound (65% long glass fiber)
Reduce cost from \$0.32	2	\$0.13 (4)	\$0.13 (4)	\$0.14 (4)	\$0.14 (4)	\$0.14 (4)
Reduce weight from 16.40g	1	3.46 g (5)	4.40 g (2)	4.13 g (3)	4.18 g (3)	4.63 g (1)
Withstands >135N +/- 15N axial load on plunger (% of yield)	Pass / Fail	13.49%	5.97%	7.35%	6.32%	15.86%
Withstands specified vibrational load profile (% of yield)	Pass / Fail	1.36%	1.28%	1.10%	1.97%	4.62%
Does not seize/fail when operated between -40°C to 105°C (% of yield)	Pass / Fail	0.05% max T 0.05% min T	0.03% max T 0.06% min T	0.05% max T 0.05% min T	0.05% max T 0.06% min T	0.14% max T 0.12% min T
Has a Young's Modulus \geq 1 GPa	Pass / Fail	8 GPa	19 GPa	15.5 GPa	15.9 GPa	72.5 GPa
Tolerance \leq +/- 0.001" for ring gear and planetary carrier	Pass / Fail	(+/-) 0.002" for finished part (injection molding)	(+/-) 0.002" for finished part (injection molding)	(+/-) 0.002" for finished part (injection molding)	(+/-) 0.002" for finished part (injection molding)	(+/-) 0.002" for finished part (injection molding)
Is ethically sourced	N/A	Renowned as sustainable alternatives to synthetic nylon fibers, bio-polyamides offer biodegradability and non-toxicity. [105]	Recyclable. Its high durability and resistance to degradation ensure that products made from it have a long service life. [108]	Recyclable. Its high durability and resistance to degradation ensure that products made from it have a long service life. [108]	Recyclable. Its high durability and resistance to degradation ensure that products made from it have a long service life. [108]	Has a longer lifetime due to its high durability and the ability to recycle it, the total life cycle impact is lower than for other materials. [110]
Tolerance \leq +/- 0.002" for magnet holder	N/A					
Has a Vickers Hardness value between 112 and 178 HV	N/A					
TOTAL		13	10	11	11	9

Planet Carrier Pugh Charts Cont.

Criteria	Weight	PPA (45% glass fiber)	PTT (30% glass fiber, flame retarded)	PPA (50% long glass fiber)	PTT (30% glass fiber, 15% PTFE)	PPA (45% glass fiber, flame retarded)
Reduce cost from \$0.32	2	\$0.14 (4)	\$0.15 (4)	\$0.16 (4)	\$0.16 (4)	\$0.20 (3)
Reduce weight from 16.40g	1	4.13 g (3)	4.23 g (3)	4.10 g (3)	3.90 g (3)	4.56 g (2)
Withstands >135N +/- 15N axial load on plunger (% of yield)	Pass / Fail	7.43%	15.12%	6.50%	13.05%	11.03%
Withstands specified vibrational load profile (% of yield)	Pass / Fail	1.97%	1.81%	2.42%	1.56%	2.37%
Does not seize/fail when operated between -40°C to 105°C (% of yield)	Pass / Fail	0.05% max T 0.05% min T	0.07% max T 0.08% min T	0.05% max T 0.05% min T	0.05% max T 0.06% min T	0.05% max T 0.09% min T
Has a Young's Modulus \geq 1 GPa	Pass / Fail	15.4 GPa	11.7 GPa	17.9 GPa	8.96 GPa	16 GPa
Tolerance \leq +/- 0.001" for ring gear and planetary carrier	Pass / Fail	(+/-) 0.002" for finished part (injection molding)	(+/-) 0.002" for finished part (injection molding)	(+/-) 0.002" for finished part (injection molding)	(+/-) 0.002" for finished part (injection molding)	(+/-) 0.002" for finished part (injection molding)
Is ethically sourced	N/A	Recyclable. Its high durability and resistance to degradation ensure that products made from it have a long service life. [108]	Derived from bio-based materials, making them an attractive alternative to traditional petroleum-based polymers. [107]	Recyclable. Its high durability and resistance to degradation ensure that products made from it have a long service life. [108]	Derived from bio-based materials, making them an attractive alternative to traditional petroleum-based polymers. [107]	Recyclable. Its high durability and resistance to degradation ensure that products made from it have a long service life. [108]
Tolerance \leq +/- 0.002" for magnet holder	N/A					
Has a Vickers Hardness value between 112 and 178 HV	N/A					
TOTAL		11	11	11	11	8

Planet Carrier Pugh Charts Cont.

Criteria	Weight	LCP (50% glass fiber)	LCP (45% glass fiber)	PA66/6 (30% carbon fiber)	LCP (40% glass fiber)	LCP (30% mineral filled)
Reduce cost from \$0.32	2	\$0.28 (2)	\$0.30 (2)	\$0.30 (2)	\$0.31 (2)	\$0.32 (2)
Reduce weight from 16.40g	1	4.43 g (2)	4.43 g (2)	3.16 g (5)	4.25 g (2)	4.08 g (3)
Withstands >135N +/- 15N axial load on plunger (% of yield)	Pass / Fail	10.21%	12.85%	8.47%	11.95%	11.95%
Withstands specified vibrational load profile (% of yield)	Pass / Fail	2.41%	1.58%	1.48%	2.87%	1.13%
Does not seize/fail when operated between -40°C to 105°C (% of yield)	Pass / Fail	0.08% max T 0.08% min T	0.08% max T 0.10% min T	0.05% max T 0.06% min T	0.07% max T 0.08% min T	0.03% max T 0.06% min T
Has a Young's Modulus \geq 1 GPa	Pass / Fail	22 GPa	18.2 GPa	70.6 GPa	15 GPa	72.5 GPa
Tolerance \leq +/- 0.001" for ring gear and planetary carrier	Pass / Fail	(+/-) 0.002" for finished part (injection molding)	(+/-) 0.002" for finished part (injection molding)	(+/-) 0.002" for finished part (injection molding)	(+/-) 0.002" for finished part (injection molding)	(+/-) 0.002" for finished part (injection molding)
Is ethically sourced	N/A	Uses dangerous chemicals for production, but then becomes inert. Inhalation of liquid-crystal polymers will irritate the respiratory tract. [113]	Uses dangerous chemicals for production, but then becomes inert. Inhalation of liquid-crystal polymers will irritate the respiratory tract. [113]	Renowned as sustainable alternatives to synthetic nylon fibers, bio-polyamides offer biodegradability and non-toxicity. [105]	Uses dangerous chemicals for production, but then becomes inert. Inhalation of liquid-crystal polymers will irritate the respiratory tract. [113]	Uses dangerous chemicals for production, but then becomes inert. Inhalation of liquid-crystal polymers will irritate the respiratory tract. [113]
Tolerance \leq +/- 0.002" for magnet holder	N/A					
Has a Vickers Hardness value between 112 and 178 HV	N/A					
TOTAL		6	6	9	6	7

Planet Carrier Pugh Charts Cont.

Criteria	Weight	LCP (30% glass fiber)	LCP (15% glass fiber)	LCP (unfilled)	PPA (50% carbon fiber)	Epoxy SMC (55% long carbon fiber)
Reduce cost from \$0.32	2	\$0.33 (2)	\$0.36 (1)	\$0.36 (1)	\$0.55 (1)	\$0.67 (1)
Reduce weight from 16.40g	1	4.05 g (3)	3.73 g (4)	3.53 g (4)	3.71 g (4)	3.71 g (4)
Withstands >135N +/- 15N axial load on plunger (% of yield)	Pass / Fail	11.48%	9.23%	13.18%	5.43%	6.55%
Withstands specified vibrational load profile (% of yield)	Pass / Fail	1.98%	1.48%	1.25%	2.96%	9.92%
Does not seize/fail when operated between -40°C to 105°C (% of yield)	Pass / Fail	0.06% max T 0.07% min T	0.04% max T 0.05% min T	0.04% max T 0.04% min T	0.06% max T 0.06% min T	0.10% max T 0.11% min T
Has a Young's Modulus \geq 1 GPa	Pass / Fail	13.8 GPa	12.1 GPa	71 GPa	35 GPa	55.1 GPa
Tolerance \leq +/- 0.001" for ring gear and planetary carrier	Pass / Fail	(+/-) 0.002" for finished part (injection molding)	(+/-) 0.002" for finished part (injection molding)	(+/-) 0.002" for finished part (injection molding)	(+/-) 0.002" for finished part (injection molding)	(+/-) 0.002" for finished part (injection molding)
Is ethically sourced	N/A	Uses dangerous chemicals for production, but then becomes inert. Inhalation of liquid-crystal polymers will irritate the respiratory tract. [113]	Uses dangerous chemicals for production, but then becomes inert. Inhalation of liquid-crystal polymers will irritate the respiratory tract. [113]	Uses dangerous chemicals for production, but then becomes inert. Inhalation of liquid-crystal polymers will irritate the respiratory tract. [113]	Recyclable. Its high durability and resistance to degradation ensure that products made from it have a long service life. [108]	Has a longer lifetime due to its high durability and the ability to recycle it, the total life cycle impact is lower than for other materials. [110]
Tolerance \leq +/- 0.002" for magnet holder	N/A					
Has a Vickers Hardness value between 112 and 178 HV	N/A					
TOTAL		Fail	Fail	Fail	Fail	Fail

APPENDIX F

First Principle Analysis - Matlab Code

The code to verify and streamline the first principle analyses in which the applied loads were found. The resultant outputs were inputted into the FEA model.

```
syms F d_m l f T_DS
displayFormula("(T_DS = (F*d_m / 2) * ((l + pi*f*d_m) ./ (pi * d_m - f*l))")
```

$$T_{DS} = \frac{F d_m}{2} \frac{(l + \pi f d_m)}{\pi d_m - f l}$$

```
% Lead screw torque equation parameters
F = 170*2; % Force (N) by the plunger that acts on drive nut - SF OF 2
d_m = 0.00515; % (m) Diameter of drive screw (diametric pitch)
n = 1;%
p = 0.001814068; % (pitch 1/14 in = 0.07142 in = m)
l = n*p; %lead
f = 0.3; %friction coefficient (0.1 - 0.3 for ULTEM 4001 vs Stainless steel)

% Lead screw torque
T_DS = (F*d_m / 2) * ((l + pi*f*d_m) ./ (pi * d_m - f*l)) / 0.37
T_DS_MH = T_DS % torque from drive screw onto the magnet holder

d_DS_MH = 0.0075; % distance from drive screw center hole to one of three magnet carrier nubs
F_flat_MH = (T_DS_MH/d_DS_MH)/3 % N - force on one flat of magnet holder nub

% Force on planetary gear holes of planet carrier (ALL MODELED FOR ONE PLANET GEAR)
d_DS_PC = 0.01212; % distance from drive screw center hole to one of three planet holes
F_flat_PC = F_flat_MH % N - dont calculate force yet! - according to Umbriac
F_axle_PC = (3*F_flat_PC*(d_DS_MH/2))/(3*(d_DS_PC/2)) % force at each axle hole of planet carrier
T_DS_PC = T_DS_MH;

% Torque on the sun gear from torque on planet carrier (using 250 notes)
S = 15; % number of teeth on sun gear
R = 75; % number of teeth on ring gear
T_s = T_DS_PC * (S/(S+R)) / 0.95
```

```
T_DS = 1.0091
T_DS_MH = 1.0091

F_flat_MH = 44.8496

F_flat_PC = 44.8496
F_axle_PC = 27.7535

T_s = 0.1770
```

```
% calculating reaction forces on sun gear to get forces on the planet gear
% rearrange T_s = F_t * d_s/2
d_s = 0.0079375; % (m) pitch diameter of sun gear (0.3125 in)
theta = 20; % pressure angle for sun gear
F_SP1_t = (T_s*2 / d_s)/3
F_SP1_r = F_SP1_t *tand(theta)

% force balance equations on Planet gear 1
F_axle_PC_x = F_axle_PC*cos(pi/3)
F_axle_PC_y = F_axle_PC*sin(pi/3)

F_RP1_r = F_axle_PC_x - F_SP1_r % x
F_RP1_t = F_axle_PC_y - F_SP1_t % y
F_RP = sqrt(F_RP1_t^2 + F_RP1_r^2)
P_RP = 12.48/8.224e-6

d_ring = 1.5625*0.0254;
T_ring_teeth = 3*(F_RP*d_ring)

d_ring_extrusion = 0.036515;
F_ring_extrusion = (T_ring_teeth/d_ring_extrusion)/3
```

```
F_SP1_t = 14.8693
F_SP1_r = 5.4120

F_axle_PC_x = 13.8767
F_axle_PC_y = 24.0352

F_RP1_r = 8.4647
F_RP1_t = 9.1659
F_RP = 12.4766
P_RP = 1.5175e+06

T_ring_teeth = 1.4855

F_ring_extrusion = 13.5606
```

APPENDIX G

Convergence Testing for Mesh Size

The actual values and results confirming the conclusions of the convergence testing. Highlighted in green is the selected mesh size.

RING GEAR		
Mesh Size	Max Max principle stress	% difference
1.00E-02	7.69E+06	n/a
5.00E-03	8.91E+06	14.78%
1.00E-03	1.15E+07	25.33%
7.50E-04	1.24E+07	7.81%
6.00E-04	1.65E+07	28.33%
5.00E-04	1.69E+07	1.98%
4.00E-04	1.90E+07	11.67%
3.00E-04	1.96E+07	3.41%

PLANET CARRIER		
Mesh Size	Max Max principle stress	% difference
1.00E-02	1.30E+07	n/a
5.00E-03	1.40E+07	7.39%

MAGNET HOLDER		
Mesh Size	Max Max principle stress	% difference
1.00E-02	2.77E+07	n/a
5.00E-03	2.96E+07	106.88%
1.00E-03	3.01E+07	1.70%

APPENDIX H

First Principles - Thermal Analysis - Finding CTE Values

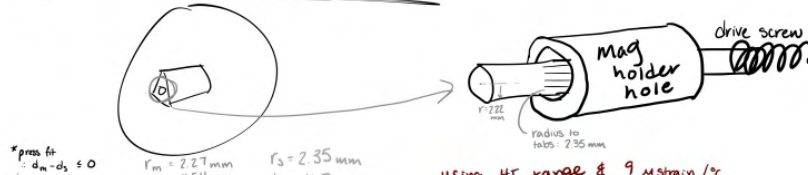
The tolerances allowable for each type of interference, and the hand calculations that verify the resulting CTE range of each part.

Part Interactions	Interference Type	Tolerance (mm)
Drive Screw and Magnet Holder	Pressfit	$\leq - 0.0508$
Drive Screw and Planet Carrier	Slipfit	≥ 0.0254
Axles and Planet Carrier	Pressfit	$\leq - 0.0432$
Planet Gears and Ring Gear	Gear Mesh	0*

*Refer to the body section for explanation for this tolerance value.

All interference values were determined using the Machinery's Handbook [101].

Magnet Holder * FROM -40°C to 105°C



$$\Delta d = d \alpha \Delta T$$

CTE

* press fit: $d_m - d_s \leq 0$
(screw should have a larger diameter)

$\Delta d_m = d_m \alpha_m \Delta T$ (room temp to high) \rightarrow room temp to low

$\Delta d_s = d_s \alpha_s \Delta T$ (room temp to high) \rightarrow room temp to low

and $d_m + \Delta d_m - (d_s + \Delta d_s) \leq 0.0508$
to keep press-fit in tact

FROM ANSI $1.00 \times 2 \approx 0.0508$

Using conservative values,
CTE_{magnet holder} = 9.318 - 11.36 $\mu\text{strain}/^\circ\text{C}$

using HT range & 9 $\mu\text{strain}/^\circ\text{C}$

$$\Delta d_m = 4.54 \text{ mm } \alpha_m (80^\circ\text{C})$$

$$\Delta d_s = 4.7 \text{ mm } (9 \mu\text{strain}/^\circ\text{C})(80^\circ\text{C}) \rightarrow 4.54 + 363.2 \alpha_m - (3388.7) \leq 0.0508$$

$$4.54 \text{ mm} + \Delta d_m - (4.7 \text{ mm} + \Delta d_s) \leq 0.0508$$

$$\alpha_m \leq 9.318 \mu\text{strain}/^\circ\text{C}$$

using LT range & 9 $\mu\text{strain}/^\circ\text{C}$

$$\Delta d_m = 4.54 \text{ mm } \alpha_m (65^\circ\text{C}) \rightarrow 4.54 + 295.1 \alpha_m - (2749.5) \leq 0.0508$$

$$\Delta d_s = 4.7 \text{ mm } (9 \mu\text{strain}/^\circ\text{C})(65^\circ\text{C})$$

$$\alpha_m \leq 9.302 \mu\text{strain}/^\circ\text{C}$$

using HT range & 10.998 $\mu\text{strain}/^\circ\text{C}$

$$\Delta d_s = 4.7 \text{ mm } (10.998 \mu\text{strain}/^\circ\text{C})(80^\circ\text{C}) \rightarrow 4.54 + 363.2 \alpha_m - (4135.248) \leq 0.0508$$

$$\alpha_m \leq 11.373 \mu\text{strain}/^\circ\text{C}$$

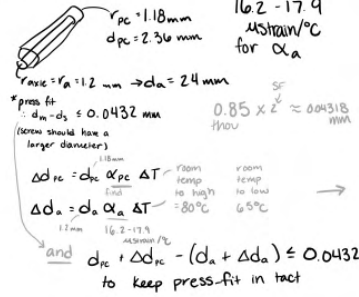
using LT range & 10.998 $\mu\text{strain}/^\circ\text{C}$

$$\Delta d_s = 4.7 \text{ mm } (10.998 \mu\text{strain}/^\circ\text{C})(65^\circ\text{C}) \rightarrow 4.54 + 295.1 \alpha_m - (3356.834) \leq 0.0508$$

$$\alpha_m \leq 11.36 \mu\text{strain}/^\circ\text{C}$$

CTE of drive screw:
5 - 6.11 $\mu\text{strain}/^\circ\text{F}$
9 - 10.998 $\mu\text{strain}/^\circ\text{C}$

Planet Carrier:



Using conservative values,
CTE_{planet carrier} = 16.46 - 18.19 $\mu\text{strain}/^\circ\text{C}$

using HT range & 16.2 $\mu\text{strain}/^\circ\text{C}$

$$\Delta d_{pc} = 2.36 \text{ mm } \alpha_{pc} (80^\circ\text{C})$$

$$\Delta d_s = 2.4 \text{ mm } (16.2 \mu\text{strain}/^\circ\text{C})(80^\circ\text{C}) \rightarrow 2.36 + 188.8 \alpha_{pc} - (3110.4) \leq 0.0432$$

$$2.36 \text{ mm} + \Delta d_{pc} - (2.4 \text{ mm} + \Delta d_s) \leq 0.0432$$

$$\alpha_{pc} \leq 16.46 \mu\text{strain}/^\circ\text{C}$$

using LT range & 16.2 $\mu\text{strain}/^\circ\text{C}$

$$\Delta d_{pc} = 2.36 \text{ mm } \alpha_{pc} (65^\circ\text{C}) \rightarrow 2.36 + 153.4 \alpha_{pc} - (2527.2) \leq 0.0432$$

$$\Delta d_a = 2.4 \text{ mm } (16.2 \mu\text{strain}/^\circ\text{C})(65^\circ\text{C})$$

$$\alpha_{pc} \leq 16.46 \mu\text{strain}/^\circ\text{C}$$

using HT range & 17.9 $\mu\text{strain}/^\circ\text{C}$

$$\Delta d_a = 2.4 \text{ mm } (17.9 \mu\text{strain}/^\circ\text{C})(80^\circ\text{C}) \rightarrow 2.36 + 188.8 \alpha_{pc} - (3436.8) \leq 0.0432$$

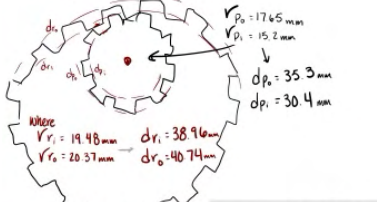
$$\alpha_{pc} \leq 18.19 \mu\text{strain}/^\circ\text{C}$$

using LT range & 17.9 $\mu\text{strain}/^\circ\text{C}$

$$\Delta d_a = 2.4 \text{ mm } (17.9 \mu\text{strain}/^\circ\text{C})(65^\circ\text{C}) \rightarrow 2.36 + 153.4 \alpha_{pc} - (2792.4) \leq 0.0432$$

$$\alpha_{pc} \leq 18.19 \mu\text{strain}/^\circ\text{C}$$

Ring Gear:



$\Delta d_r = d_r \alpha_r \Delta T$

$\Delta d_p = d_p \alpha_p \Delta T$

$\alpha_p = 33 \mu\text{strain}/^\circ\text{C}$

$d_r + \Delta d_r - (d_p + \Delta d_p) \leq 0$
to keep gear tooth interaction

25.74 - 28.58 $\mu\text{strain}/^\circ\text{C}$

outer & 80°C

$$\Delta d_{r_o} = (40.74) \alpha_r (80)$$

$$\Delta d_{p_o} = (35.3)(33)(80) \rightarrow 40.74 + (32592) \alpha_r - (93192) \leq 0$$

$$d_{r_o} + \Delta d_{r_o} - (d_{p_o} + \Delta d_{p_o}) \leq 0$$

$$\alpha_r \leq 28.58 \mu\text{strain}/^\circ\text{C}$$

outer & 65°C

$$\Delta d_{r_o} = (40.74) \alpha_r (65)$$

$$\Delta d_{p_o} = (35.3)(33)(65) \rightarrow 40.74 + (26481) \alpha_r - (75715.5) \leq 0$$

$$\alpha_r \leq 28.58 \mu\text{strain}/^\circ\text{C}$$

inner & 80°C

$$\Delta d_{r_i} = (38.96) \alpha_r (80)$$

$$\Delta d_{p_i} = (30.4)(33)(80) \rightarrow 38.96 + (31168) \alpha_r - (80256) \leq 0$$

$$d_{r_i} + \Delta d_{r_i} - (d_{p_i} + \Delta d_{p_i}) \leq 0$$

$$\alpha_r \leq 25.74 \mu\text{strain}/^\circ\text{C}$$

inner & 65°C

$$\Delta d_{r_i} = (38.96) \alpha_r (65)$$

$$\Delta d_{p_i} = (30.4)(33)(65) \rightarrow 38.96 + (25324) \alpha_r - (65208) \leq 0$$

$$\alpha_r \leq 25.73 \mu\text{strain}/^\circ\text{C}$$

First Principles - Thermal Analysis - CTE Validation

MATLAB code for validation of the CTE calculations. All materials passed the tolerances specified by the Machinery's Handbook.

```
%read CTE data
CTE_data = readtable('FEA Data Results.xlsx', Sheet='E ');
CTE_MH = table2array(CTE_data(2:end, 2)); %CTE Magnet Holder
CTE_PC = table2array(CTE_data(2:end, 6)); %CTE planet carrier
CTE_RG = table2array(CTE_data(2:end, 10)); %CTE ring gear
CTE_DS = 11; %CTE drive screw
CTE_axle = 16.2; %CTE axles

%SET TEMP
T_new = -40; % check 105 or -40
delta_T = (T_new - 25);
```

original column headers
as table variable names.

```
MH_DS_original_tolerance = -1.5000e-04
MH_DS_new_tolerance = 24x1
10^-3 x
-0.1518
-0.1614
-0.1644
-0.1555
-0.1555
-0.1520
-0.1520
-0.1496
-0.1712
-0.1540
:
```

Drivescrew and Magnet Holder hole interaction - PRESS FIT

```
%ORIGINAL TOLERANCE
MH_original_d = 4.55/1000; %m, original center diameter
DSRidges_original_d = 4.7/1000; %m, ridge to ridge diameter
MH_DS_original_tolerance = MH_original_d - DSRidges_original_d %tolerance between the magnet holder and drive screw (press fit)

%NEW TOLERANCE
MH_delta_d = (CTE_MH*delta_T*MH_original_d)*(10^-6); %expansion difference, delta_L/L_original = CTE*deltaT
MH_new_d = MH_delta_d + MH_original_d; %new magnet holder diameter

DSRidges_delta_d = (CTE_DS*delta_T*DSRidges_original_d)*10^-6; %drive screw expansion
DSRidges_new_d = DSRidges_delta_d + DSRidges_original_d; %new drive screw diameter from ridges

MH_DS_new_tolerance = MH_new_d - DSRidges_new_d %new diameter tolerance

MH_DS_PressFitCheck = MH_DS_new_tolerance <= 2 * 0.0254/1000 %PASS if less than or equal to
```

```
MH_DS_PressFitCheck = 24x1 logical array
1
1
1
1
1
1
1
1
1
1
1
1
1
1
1
1
1
1
1
1
```

Drive Screw and Planet Carrier hole interaction - SLIP FIT

```
%ORIGINAL TOLERANCE
PC_original_d = 4.55 /1000;
DS_original_d = 4.45/1000;
PC_DS_original_tolerance = PC_original_d - DS_original_d

%NEW TOLERANCE
PC_delta_d = (CTE_PC*delta_T*PC_original_d)*(10^-6); %expansion difference, delta_L/L_original = CTE*deltaT
PC_new_d = PC_delta_d + PC_original_d; %new planet carrier diameter

DS_delta_d = (CTE_DS*delta_T*DS_original_d)*(10^-6); %drive screw expansion (NOT RIDGE SURFACE)
DS_new_d = DS_delta_d + DS_original_d; %new drive screw diameter from smooth surface (NOT RIDGE SURFACE)

PC_DS_new_tolerance = PC_new_d - DS_new_d

PC_DS_SlipFitCheck = PC_DS_new_tolerance >= 2 * 0.0127/1000 % PASS if new tolerance is greater than specified
```

```
PC_DS_original_tolerance = 1.0000e-04
PC_DS_new_tolerance = 24x1
10^-3 x
0.1016
0.0980
0.0884
0.0961
0.0854
0.0943
0.0943
0.0973
0.1002
0.0943
:
```

```
PC_DS_SlipFitCheck = 24x1 logical array
1
1
1
1
1
1
1
1
1
1
1
1
1
1
1
1
1
1
1
1
```

Axle and Planet Carrier hole interaction - PRESS FIT

```
%ORIGINAL TOLERANCE
PC_axle_original_d = 2.36/1000;
Axle_original_d = 2.39/1000;
PC_axle_original_tolerance = PC_axle_original_d - Axle_original_d

%NEW TOLERANCE
PC_axle_delta_d = (CTE_PC*delta_T*PC_axle_original_d)*(10^-6); %expansion difference, delta_L/L_original = CTE*deltaT
PC_axle_new_d = PC_axle_delta_d + PC_axle_original_d; %new planet carrier axle hole diameter

Axle_delta_d = (CTE_axle*delta_T*Axle_original_d)*(10^-6); %new axle hole diameter
Axle_new_d = Axle_delta_d + Axle_original_d; %new axle diameter

PC_axle_new_tolerance = PC_axle_new_d - Axle_new_d % new axle hole / Planet carrier tolerance

PC_axle_PressFitCheck = PC_axle_new_tolerance <= 2* 0.0216/1000 %PASS if new tolerance is less than specified
```

```
PC_axle_original_toleranc e = -3.0000e-05
PC_axle_new_tolerance = 24x1
10^-4 x
-0.2831
-0.3017
-0.3515
-0.3115
-0.3669
-0.3209
-0.3209
-0.3055
-0.2902
-0.3209
:
```

```
PC_axle_PressFitCheck = 24x1 logical array
1
1
1
1
1
1
1
1
1
1
1
1
1
1
1
1
1
1
1
1
```

First Principles - Thermal Analysis for Stress

MATLAB code for thermal stress for the magnet holder and drive screw interactions and for the axle and planet carrier interactions.

Thermal Analysis - Stress Analysis

```
syms delta d Eo do Ei vi vo di

%read Youngs Modulus data

|
data = readtable('FEA Data Results.xlsx', Sheet='E '); % units in GPA = N/mm^2
E_MH = table2array(data(1:24, 3)); %E Magnet Holder
E_PC = table2array(data(1:24, 7)); %E planet carrier
E_RG = table2array(data(1:24, 11)); %E ring gear
E_DS = 29; %E drive screw
E_axle = 27.9; % E axle

data = readtable('FEA Data Results.xlsx', Sheet='E ');
CTE_MH = table2array(data(1:24, 2)); %CTE Magnet Holder
CTE_PC = table2array(data(1:24, 6)); %CTE planet carrier
CTE_RG = table2array(data(1:24, 10)); %CTE ring gear
CTE_DS = 11; %CTE drive screw
CTE_axle = 16.2; %CTE axles

data = readtable('FEA Data Results.xlsx', Sheet='Delta Data');
delta105_MH = table2array(data(:, 4)); %new tolerance between drive screw and Magnet Holder at 105
delta40_MH = table2array(data(:, 3)); %new tolerance between drive screw and planet carrier at -40
delta105_PC = table2array(data(:, 8)); %new tolerance between axle and planet carrier at 105
delta40_PC = table2array(data(:, 7)); %new tolerance between axle and planet carrier at -40

v_MH = table2array(data(:, 2)); %poissions ratio of magnet holder
v_PC = table2array(data(:, 6)); %poissions ratio of planet carrier
v_DS = 0.3; %poissions ratio of drive screw
v_axle = 0.25; %poissions ratio of axle

%All necessary dimensions
MH_original_d = 4.55; %mm, original center diameter
DSRidges_original_d = 4.7; %mm, ridge to ridge diameter

PC_axle_original_d = 2.36;
Axle_original_d = 2.39;

% % DS + MH
% delta = delta40_MH *1000;
% d = MH_original_d; %nominal diameter
% do = 12.7; %outer hub diameter
% di = 0; %shaft internal diameter
% vi = v_DS;
% vo = v_MH;
% Ei = E_DS;
% Eo = E_MH;

% Axle + PC
delta = delta105_PC *1000;
d = PC_axle_original_d; %nominal diameter
do = 7.112; %outer hub diameter
di = 0; %shaft internal diameter
vi = v_axle;
vo = v_PC;
Ei = E_axle;
Eo = E_PC;

P = delta./(((d./Eo).*((do.^2+d.^2)/(do.^2-d.^2)) + vo) + ((d./Ei).*((d.^2+di^2)/(d^2-di^2)) - vi))
```

Ring Gear - Thermal Stress Analysis

MATLAB code for the bending stress on the ring gear teeth.

```
syms F d_m l f T_DS

displayFormula("T_DS = (F*d_m / 2) * ((l + pi*f*d_m) ./ (pi * d_m - f*l))")

CTE_data = readtable('FEA Data Results.xlsx', Sheet='E ');

% Lead screw torque equation parameters
F = 170*2; % Force (N) by the plunger that acts on drive nut - SF OF 2

CTE_DS = 11; %CTE drive screw
T_new = -40; % check 105 or -40
delta_T = (T_new - 25) ;
d_m_original = 0.00515;
d_m_delta = (CTE_DS.*delta_T.*d_m_original)*10^-6; %drive screw expansion
d_m = d_m_original +d_m_delta ; % (m) Diameter of drive screw (diametric pitch)
n = 1;%
p = 0.001814068; % (pitch 1/14 in = 0.07142 in = m)
l = n*p; %lead
f = 0.3; %friction coefficient (0.1 - 0.3 for ULTEM 4001 vs Stainless steel)

% Lead screw torque
T_DS = (F*d_m / 2) * ((l + pi*f*d_m) ./ (pi * d_m - f*l)) / 0.37
T_DS_MH = T_DS % torque from drive screw onto the magnet holder

d_DS_MH = 0.0075; % distance from drive screw center hole to one of three magnet
F_flat_MH = (T_DS_MH/d_DS_MH)/3 % N - force on one flat of magnet holder nub

% Force on planetary gear holes of planet carrier (ALL MODELED FOR ONE PLANET GEAR)
d_DS_PC = 0.01212; % distance from drive screw center hole to one of three planet
F_flat_PC = F_flat_MH % N - dont calculate force yet! - according to Umbricac
F_axle_PC = (3*F_flat_PC*(d_DS_MH/2))/(3*(d_DS_PC/2)) % force at each axle hole c
T_DS_PC = T_DS_MH;

% Torque on the sun gear from torque on planet carrier (using 250 notes)
S = 15; % number of teeth on sun gear
R = 75; % number of teeth on ring gear
T_s = T_DS_PC * (S/(S+R)) / 0.95

% calculating reaction forces on sun gear to get forces on the planet gear
% rearrange T_s = F_t * d_s/2
```

```

% force balance equations on Planet gear 1
F_axle_PC_x = F_axle_PC*cos(pi/3)
F_axle_PC_y = F_axle_PC*sin(pi/3)

F_RP1_r = F_axle_PC_x - F_SP1_r % x
F_RP1_t = F_axle_PC_y - F_SP1_t % y
F_RP = sqrt(F_RP1_t^2 + F_RP1_r^2)

CTE_RG = table2array(CTE_data(1:end, 10)); %CTE ring gear
d_rg_original = 0.0396875; % in m (1.5625 in) (pitch diameter)
d_rg_delta = (CTE_RG.*delta_T.*d_rg_original)*10^-6; %ring gear expansion
d_rg = d_rg_original +d_rg_delta ; % (m) Diameter of ring gear (pitch diameter)
m = d_rg*1000./(75); % mm (module d/N)
F = 8.636; %face width in mm
Y = 0.435;

STRESS_RING = F_RP1_t./(F.*m.*Y) % in Mpa

P_RP = 12.48/8.224e-6

d_ring = 1.5625*0.0254;
T_ring_teeth = 3*(F_RP*d_ring)

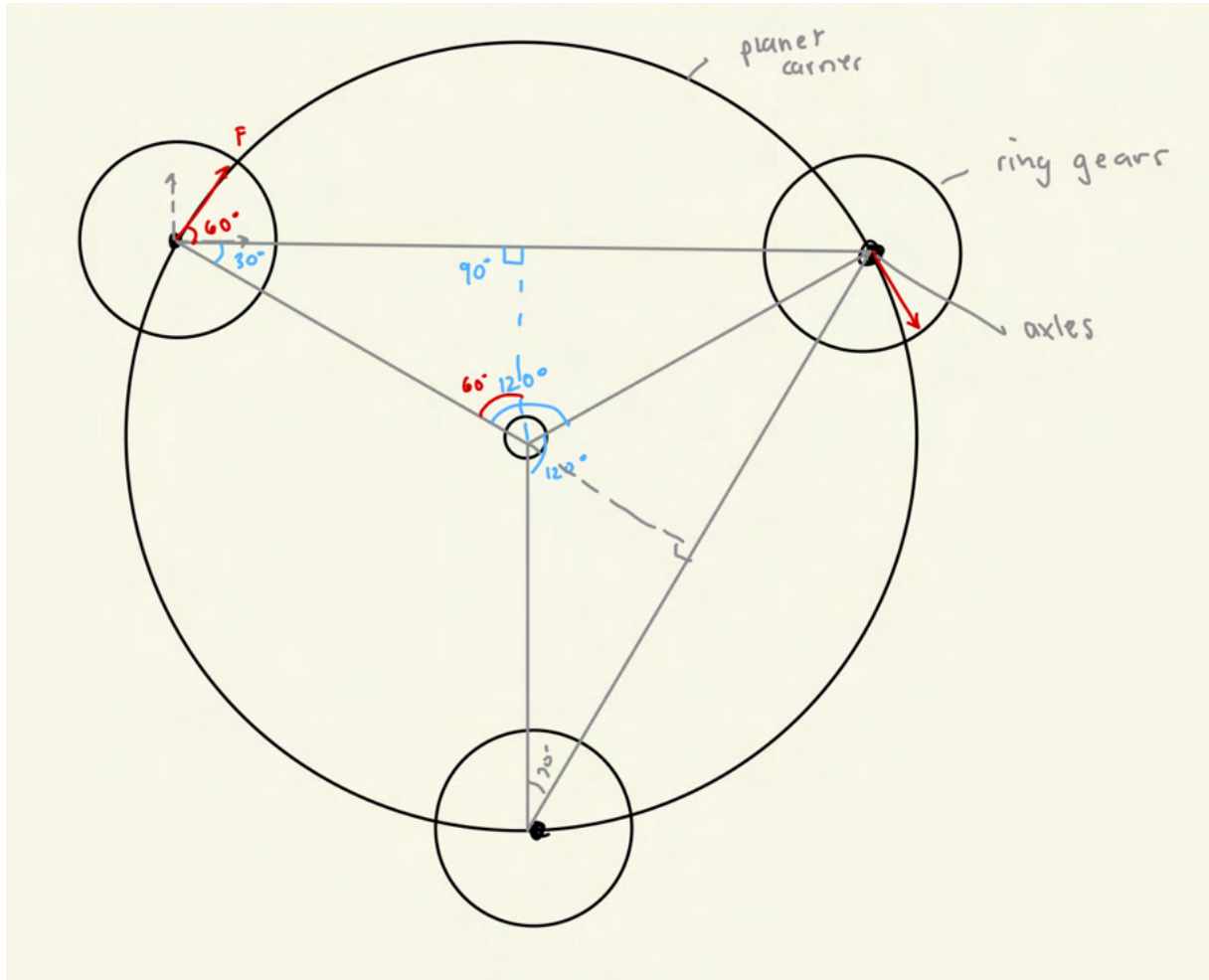
d_ring_extrusion = 0.036515;
F_ring_extrusion = (T_ring_teeth/d_ring_extrusion)/3

```


APPENDIX I

Ring Gear Force Angle Derivation

This diagram shows the angles of the forces that the planet gear axles enact on the planet carrier. This was done using the fact that the gears were evenly dispersed along the diameter. Simple trigonometric relationships were defined below.



APPENDIX J

Cost Analysis Spreadsheets

This cost analysis was an extrapolated cost from Stoneridge and from the Granta EduPack. Stoneridge provided a unit cost for each of the three parts, and this was compared to the pricing of Zinc-Zamak 5 in the Granta EduPack. Based on this, the team was able to find the percentage of the unit cost that was based on the raw materials and extrapolate this through each of the materials to find the unit cost and tooling, labor, and overhead (TLO) cost.

Polymers (injection molding)		in order to find this we were given the information from stoneridge of their plunger and used the material database against the unit price to find the % influence of the raw material cost vs the tooling cost (qty of output would be the same)					
Material	Max price of range from edupack (USD/m ³)	Volume of each part (m ³)	Price per volume(\$)	Unit price with TLO (zinc is from stoneridge) (\$)	% cost of price of material	% cost of TLO of component	actual TLO cost (\$/part)
PA66 (30-33% glass	7.81E+03	4.83E-06	0.0378	0.22	17.16%	82.84%	0.182

Ring Gear Metals (Die Cast)										
Material	% cost reduction from unit price (price difference /original price)	Max price of range from edupack (USD/m ³)	Volume of each part (m ³)	Price per volume(\$)	Unit price with TLO (\$)	Density	weight	% cost of price of material	% cost of TLO on component	
Aluminum, 359.0, cast, T6	64.47%	1.08E+04	1.31E-05	0.14	0.427	2.70E+03	0.0353862	33.12%	66.88%	
Aluminum, C355.0, permanent	63.16%	1.12E+04	1.31E-05	0.15	0.443	2.74E+03	0.03591044	33.12%		
Aluminum, 354.0, cast, T6	62.17%	1.15E+04	1.31E-05	0.15	0.455	2.81E+03	0.03682786	33.12%		
Aluminum, 332.0, permanent	61.51%	1.17E+04	1.31E-05	0.15	0.463	2.80E+03	0.0366968	33.12%		
Aluminum, 333.0, permanent	61.19%	1.18E+04	1.31E-05	0.15	0.467	2.80E+03	0.0366968	33.12%		
Aluminum, 390.0, die cast, F	61.19%	1.18E+04	1.31E-05	0.15	0.467	2.76E+03	0.03617256	33.12%		
Aluminum, A390.0, permanent	61.19%	1.18E+04	1.31E-05	0.15	0.467	2.76E+03	0.03617256	33.12%		
Aluminum, A390.0, permanent	61.19%	1.18E+04	1.31E-05	0.15	0.467	2.76E+03	0.03617256	33.12%		
Aluminum, EN AC-48000, ch	61.19%	1.18E+04	1.31E-05	0.15	0.467	2.71E+03	0.03551726	33.12%		
Aluminum, 319.0, permanent	60.86%	1.19E+04	1.31E-05	0.16	0.471	2.82E+03	0.03695892	33.12%		
Aluminum, 336.0, permanent	57.24%	1.30E+04	1.31E-05	0.17	0.514	2.74E+03	0.03591044	33.12%		
Aluminum, 336.0, permanent	57.24%	1.30E+04	1.31E-05	0.17	0.514	2.74E+03	0.03591044	33.12%		
Aluminum, A332.0, cast, T6	57.24%	1.30E+04	1.31E-05	0.17	0.514	2.73E+03	0.03577938	33.12%		
Zinc-aluminum alloy, ZA-27, c	25.99%	2.25E+04	1.31E-05	0.29	0.890	5.05E+03	0.0661853	33.12%		
Zinc Zamak 5	0.00%	3.04E+04	1.31E-05	0.40	1.203	6.75E+03	0.0884655	33.12%		

Magnet Holder Polymers (injection molding)										
Material	% cost reduction from unit price (price difference /original price)	Max price of range from edupack (USD/m ³)	Volume of each part (m ³)	Price per volume(\$)	Unit price with TLO (\$)	Density	weight	% cost of price of material	% cost of TLO on component	actual TLO cost
PTT (30% glass fiber)	0.641345719	7.58E+03	5.44E-06	0.04	0.240	1.67E+03	0.0090848	17.16%	82.84%	0.199
PPA (60% glass fiber)	0.5651671111	9.19E+03	5.44E-06	0.05	0.291	1.77E+03	0.0096288	17.16%	82.84%	0.241
PPA (50% glass fiber, lubrica	0.5467139825	9.58E+03	5.44E-06	0.05	0.304	1.68E+03	0.0091392	17.16%	82.84%	0.252
PTT (30% glass fiber, flame r	0.5031833838	1.05E+04	5.44E-06	0.06	0.333	1.70E+03	0.009248	17.16%	82.84%	0.276
PPA (50% long glass fiber)	0.4889886233	1.08E+04	5.44E-06	0.06	0.342	1.65E+03	0.008976	17.16%	82.84%	0.284
PTT (30% glass fiber, 15% P	0.4842570365	1.09E+04	5.44E-06	0.06	0.346	1.57E+03	0.0085408	17.16%	82.84%	0.286
LCP (50% glass fiber)	0.07260898306	1.96E+04	5.44E-06	0.11	0.621	1.78E+03	0.0096832	17.16%	82.84%	0.515
LCP (45% glass fiber)	0.0158299412	2.08E+04	5.44E-06	0.11	0.659	1.78E+03	0.0096832	17.16%	82.84%	0.546
Zinc Zamak 5	0	3.04E+04	5.44E-06	0.17	0.670	6.75E+03	0.03672	25.37%	74.63%	0.505
LCP (40% glass fiber)	-0.007827992903	2.13E+04	5.44E-06	0.12	0.675	1.71E+03	0.0093024	17.16%	82.84%	0.559
LCP (30% glass fiber)	-0.08353338204	2.29E+04	5.44E-06	0.12	0.726	1.63E+03	0.0088672	17.16%	82.84%	0.601
LCP (15% glass fiber)	-0.163970358	2.46E+04	5.44E-06	0.13	0.780	1.50E+03	0.00816	17.16%	82.84%	0.646
Epoxy SMC (55% long carbon	-1.185993111	4.62E+04	5.44E-06	0.25	1.465	1.49E+03	0.0081056	17.16%	82.84%	1.213

Planet Carrier											
Polymers (injection molding)											
Material	% cost reduction from unit price (price difference / original price)	Max price of range from edupack (USD/m ³)	Volume of each part (m ³)	Price per volume(\$)	Unit price with TLO (\$)	Density	weight	% cost of price of material	% cost of TLO on component	actual TLO cost	
PA66/6 (30% glass fiber)	0.7088279793	6.43E+03	2.49E-06	0.016	0.093	1.37E+03	0.003406642	17.16%	82.84%	0.077	
PA66/6 (35% glass fiber)	0.7056581439	6.50E+03	2.49E-06	0.016	0.094	1.42E+03	0.003530972	17.16%	82.84%	0.078	
PF (high strength glass fiber,	0.662186116	7.46E+03	2.49E-06	0.019	0.108	2.00E+03	0.0049732	17.16%	82.84%	0.090	
PTT (30% glass fiber)	0.6567521125	7.58E+03	2.49E-06	0.019	0.110	1.67E+03	0.004152622	17.16%	82.84%	0.091	
PA66/6 (33% glass fiber, lubri	0.6105630828	8.60E+03	2.49E-06	0.021	0.125	1.39E+03	0.003456374	17.16%	82.84%	0.103	
PPA (60% glass fiber)	0.5838458989	9.19E+03	2.49E-06	0.023	0.133	1.77E+03	0.004401282	17.16%	82.84%	0.110	
Epoxy bisphenol molding com	0.5743363928	9.40E+03	2.49E-06	0.023	0.136	1.86E+03	0.004625076	17.16%	82.84%	0.113	
PPA (50% glass fiber)	0.571619391	9.46E+03	2.49E-06	0.024	0.137	1.66E+03	0.004127756	17.16%	82.84%	0.114	
PPA (50% glass fiber, lubricat	0.5661853875	9.58E+03	2.49E-06	0.024	0.139	1.68E+03	0.004177488	17.16%	82.84%	0.115	
PPA (45% glass fiber)	0.5521475452	9.89E+03	2.49E-06	0.025	0.143	1.66E+03	0.004127756	17.16%	82.84%	0.119	
PTT (30% glass fiber, flame r	0.5245246941	1.05E+04	2.49E-06	0.026	0.152	1.70E+03	0.00422722	17.16%	82.84%	0.126	
PPA (50% long glass fiber)	0.5109396853	1.08E+04	2.49E-06	0.027	0.156	1.65E+03	0.00410289	17.16%	82.84%	0.130	
PTT (30% glass fiber, 15% P	0.5064113491	1.09E+04	2.49E-06	0.027	0.158	1.57E+03	0.003903962	17.16%	82.84%	0.131	
PPA (45% glass fiber, flame r	0.3886746066	1.35E+04	2.49E-06	0.034	0.196	1.83E+03	0.004550478	17.16%	82.84%	0.162	
LCP (50% glass fiber)	0.1124460956	1.96E+04	2.49E-06	0.049	0.284	1.78E+03	0.004426148	17.16%	82.84%	0.235	
LCP (45% glass fiber)	0.05810606061	2.08E+04	2.49E-06	0.052	0.301	1.78E+03	0.004426148	17.16%	82.84%	0.250	
PA66/6 (30% carbon fiber)	0.04904938811	2.10E+04	2.49E-06	0.052	0.304	1.27E+03	0.003157982	17.16%	82.84%	0.252	
LCP (40% glass fiber)	0.03546437937	2.13E+04	2.49E-06	0.053	0.309	1.71E+03	0.004252086	17.16%	82.84%	0.256	
LCP (30% mineral filled)	0.003766025641	2.20E+04	2.49E-06	0.055	0.319	1.64E+03	0.004078024	17.16%	82.84%	0.264	
Zinc Zamak 5	0	3.04E+04	2.49E-06	0.076	0.320	6.75E+03	0.01678455	25.37%	74.63%	0.244	
LCP (30% glass fiber)	-0.03698900058	2.29E+04	2.49E-06	0.057	0.332	1.63E+03	0.004053158	17.16%	82.84%	0.275	
LCP (15% glass fiber)	-0.1139707168	2.46E+04	2.49E-06	0.061	0.356	1.50E+03	0.0037299	17.16%	82.84%	0.295	
LCP (unfilled)	-0.118499053	2.47E+04	2.49E-06	0.061	0.358	1.42E+03	0.003530972	17.16%	82.84%	0.297	
PPA (50% carbon fiber)	-0.7117111014	3.78E+04	2.49E-06	0.094	0.548	1.49E+03	0.003705034	17.16%	82.84%	0.454	
Epoxy SMC (55% long carbo	-1.092091346	4.62E+04	2.49E-06	0.115	0.669	1.49E+03	0.003705034	17.16%	82.84%	0.555	

APPENDIX K

FMEAs for the Three Components and Two Manufacturing Methods

Tables for the associated failure modes of each of the three components as well as both pressure die casting and injection molding.

Magnet Holder FMEA

Magnet Holder										
Function	Potential Failure Mode	Potential Effect(s) of Failure	Severity	Potential Cause(s) of failure / Mechanism(s) of Failure	Occurance	Process Controls	Detectability	Risk Priority Number (RPN)	Recommended Actions	Responsibility
Securely Carry Magnet	- Magnet Detachment	- Loss of actuator functionality - Loss of hall sensor functionality - Inaccurate plunger extensions and retractions - Collars fail to engage/disengage	10	- Poor tolerancing on Magnet Holder component - Poor assembly of Magnet on Magnet holder	2	- End of line (EOL) part quality inspections - Proper assessment of Cp & Cpk tests from supplier for component	2	40	- Ensure manufacturer/supplier are capable of ensuring quality parts	Stoneridge
Die cast manufacturing - Form Desired Geometry	- Cold Shut	- Weak structural integrity of components	8	- Premature solidification	2	- Flow simulation, process optimization	2	32	- Improve mold design, increase molten metal temperature	Stoneridge
Transmit Torque to the Drive Screw	- Fracture/ Cracking - Component Deformation - Press fit becomes a loose/slip fit	- Loss of actuator functionality - XX	9	- Material coefficient of thermal expansion (CTE) mismatch between magnet holder and drivescrew - Stress experienced on component exceeds the selected material's yield strength	2	- Material testing - Design review for load capabilities	1	18	- Thorough review of material selection process and reassessment of capability analysis	Stoneridge
Die cast manufacturing - Fill mold with material	- Misruns	- Incomplete parts that are unusable	8	- Low temperature, slow pouring	2	- Temperature control, pour rate adjustment	1	16	- Optimize temperature and pour rate, preheat the die	Stoneridge
Turn the Clock Spring	- Inaccurately winds the clockspring (above or below nominal winding and its tolerance) - Clock Spring fractures / wears	- Actuator becomes unreliable - Inaccurate plunger extensions and retractions	7	- Material coefficient of thermal expansion (CTE) mismatch between magnet holder and drivescrew - Excessive load translated to the clock spring reduces its lifetime	2	- Material testing / Material selection reassessment - Design review for load capabilities	1	14	- Cyclic life testing at varying temperatures for nominal loads	Stoneridge
Die cast manufacturing - Eject Cast Part	- Ejector Marks	- Surface defects, part rejection	4	- Improper ejection settings	1	- Ejection mechanism adjustment, lubrication	1	4	- Calibrate ejection pins, apply appropriate lubrication	Stoneridge

Planet Carrier FMEA

Planet Carrier										
Function	Potential Failure Mode	Potential Effect(s) of Failure	Severity	Potential Cause(s) of failure / Mechanism(s) of Failure	Occurance	Process Controls	Detectability	Risk Priority Number (RPN)	Recommended Actions	Responsibility
Transmit Torque to the Magnet Holder	- Fracture/ Cracking - Component Deformation - Slip/Loose fit between drive screw and planet carrier becomes a press fit	- Loss of actuator functionality - Inncurate plunger extensions and retractions - Collars fail to engage/ disengage	10	- Poor tolerancing on Planet Carrier - Poor assembly of Planet Carrier, Planet Gear Axles, Planet Gears, and Drive Screw - Material coefficient of thermal expansion (CTE) mismatch between planet carrier and drivescrew - Stress experienced on compnent exceeds the selected material's yield strength	2	- End of line (EOL) part quality inspections - Proper assessment of Cp & Cpk tests from supplier for component - Material testing / Material selection reassessment - Design review for load capabilites	2	40	- Ensure manufacturer/ supplier are capable of ensuring quality parts - Cyclic life testing at varying temperatures for nominal loads	Stoneridge
Die cast manufacturing - Form Desired Geometry	- Cold Shut	- Weak structural integrity of components	8	- Premature solidification	2	- Flow simulation, process optimization	2	32	- Improve mold design, increase molten metal temperature	Stoneridge
Die cast manufacturing - Fill mold with material	- Misruns	- Incomplete parts that are unusable	8	- Low temperature, slow pouring	2	- Temperature control, pour rate adjustment	1	16	- Optimize temperature and pour rate, preheat the die	Stoneridge
Hold planet gears	- Press fit between Planetary Gear axles and Planet Carrier become loose/slip fit - Misalignment	- Increased wear on gears / reduced lifetime - Transmits torque ineffeciently	7	- Material coefficient of thermal expansion (CTE) mismatch between magent holder and drivescrew - Excessive load translated between the magnet holder and planet carrier	2	- Material testing / material selection reassessment - Design review for load capabilites	1	14	- Cyclic life testing at varying temperatures for nominal loads	Stoneridge
Die cast manufacturing - Eject Cast Part	- Ejector Marks	- Surface defects, part rejection	4	- Improper ejection settings	1	- Ejection mechanism adjustment, lubrication	1	4	- Calibrate ejection pins, apply appropriate lubrication	Stoneridge

Pressure Die Casting FMEA

Manufacturing Method - Pressure Die Casting										
Function	Potential Failure Mode	Potential Effect(s) of Failure	Severity	Potential Cause(s) of failure / Mechanism(s) of Failure	Occurance	Process Controls	Detectability	Risk Priority Number (RPN)	Recommended Actions	Responsibility
Die cast manufacturing - Form Desired Geometry	- Cold Shut	- Weak structural integrity of components	8	- Premature solidification	2	- Flow simulation, process optimization	2	32	- Improve mold design, increase molten metal temperature	Stoneridge
Die cast manufacturing - Fill mold with material	- Misruns	- Incomplete parts that are unusable	8	- Low temperature, slow pouring	2	- Temperature control, pour rate adjustment	1	16	- Optimize temperature and pour rate, preheat the die	Stoneridge
Die cast manufacturing - Eject Cast Part	- Ejector Marks	- Surface defects, part rejection	4	- Improper ejection settings	1	- Ejection mechanism adjustment, lubrication	1	4	- Calibrate ejection pins, apply appropriate lubrication	Stoneridge

Injection Molding FMEA

Manufacturing Method - Injection Molding										
Function	Potential Failure Mode	Potential Effect(s) of Failure	Severity	Potential Cause(s) of failure / Mechanism(s) of Failure	Occurance	Process Controls	Detectability	Risk Priority Number (RPN)	Recommended Actions	Responsibility
Fill Mold with Material	- Short Shots	- Incomplete parts, material waste	8	- Insufficient material, premature cooling	2	- Process monitoring, material flow analysis	2	32	- Optimize material temperature and flow, ensure proper mold operation	Stoneridge
Cool and Eject Part	- Warping	- Dimensional non-conformance, part rejection	8	- Uneven cooling, improper ejection timing	2	- Cooling system design, ejection mechanism adjustment	2	32	- Ensure uniform cooling, adjust ejection timing	Stoneridge
Ensure Surface Finish Quality	- Sink Marks	- Aesthetic defects, structural weaknesses	6	- Insufficient cooling, high shrinkage materials	2	- Material selection, process optimization	2	24	- Use materials with low shrinkage, optimize cooling time	Stoneridge
Maintain Mold Integrity	- Mold Wear or Damage	- Increased downtime, repair costs	8	- Repeated cycles, abrasive materials	1	- Regular maintenance checks, material suitability assessment	2	16	- Improve mold design, operate within specified conditions (i.e. temperature)	Stoneridge
Achieve Desired Part Shape	- Flash	- Excess material, poor fit in assembly	6	- Excessive material, high injection pressure	1	- Mold design review, pressure adjustments	2	12	- Improve mold precision, regulate injection parameters	Stoneridge

REFERENCES

- [1] 1/2" 110V AC Electric Brass Solenoid Valve 110-Volts. (n.d.). Retrieved September 28, 2023, from <https://www.electricsolenoidvalves.com/1-2-110v-ac-electric-brass-solenoid-valve/>
- [2] 14:00-17:00. (n.d.-a). ISO 1328-1:2013. ISO. Retrieved September 28, 2023, from <https://www.iso.org/standard/45309.html>
- [4] 6063 Aluminum: Get to Know its Properties and Uses—Gabrian. (n.d.). Retrieved September 28, 2023, from <https://www.gabrian.com/6063-aluminum-properties/>
- [5] A Basic Guide About Machining in Delrin—WayKen. (2021, September 28). Rapid Prototype Manufacturing in China - WayKen. <https://waykenrm.com/blogs/a-basic-guide-about-machining-in-delrin/>
- [6] A Complete Guide to PEEK Material & Properties—WayKen. (2022, February 17). Rapid Prototype Manufacturing in China - WayKen. <https://waykenrm.com/blogs/peek-material-and-properties/>
- [7] Active Stabilizer Bar Systems – BWI Group. (n.d.). Retrieved September 28, 2023, from <https://www.bwigroup.com/active-stabilizer-bar-systems/>
- [8] All About Mild Steel: Definition, Composition, and Properties. (n.d.). Retrieved September 28, 2023, from <https://www.xometry.com/resources/materials/mild-steel/>
- [9] Aluminium: Specifications, Properties, Classifications and Classes. (2005, May 17). AZoM.Com. <https://www.azom.com/article.aspx?ArticleID=2863>
- [10] Aluminum Production & Manufacturing Process Explained. (n.d.). HARBOR Aluminum. Retrieved September 28, 2023, from <https://www.harboraluminum.com/en/aluminum-process>
- [11] American Iron and Steel Institute 1018 | TSA Manufacturing. (2015, July 27). <https://www.tsamfg.com/1018/>
- [12] ANSI/AGMA 2000-A88. (n.d.). Retrieved September 28, 2023, from https://members.agma.org/MyAGMA/MyAGMA/Store/Item_Detail.aspx?iProductCode=2000_A88&Category=STANDARDS
- [13] Anti-sway bars—The plus of dryving dynamics | ST suspensions. (n.d.). Retrieved September 28, 2023, from https://www.stsuspensions.com/products/anti-sway_bars
- [14] Athipatla, H. C., & Brankovich, M. (2023, September 20). Stoneridge Sponsor Meetings [Personal communication].
- [15] autoLYNX SWAY BAR DISCONNECT – Apex Performance Products. (n.d.). Retrieved September 28, 2023, from <https://www.apexdesignsusa.com/products/autolynx-sway-bar-disconnect>
- [16] Buratovic, E., Cocalic, D., Danestig, M., Eliasson, K., & Everlid, L. (2017). Controversial Materials: Ethical issues in the production of mineral based raw materials. Uppsala Universitet. <chrome-extension://efaidnbmnnnibpcajpcglclefindmkaj/https://www.diva-portal.org/smash/get/diva2:1130590/FULLTEXT01.pdf>
- [17] Cast Bronze Alloys -Operating Temperatures and Hardness Ratings. (2019, November 11). National Bronze Manufacturing. <https://www.nationalbronze.com/News/cast-bronze-alloys-operating-temperatures-and-hardness-ratings/>
- [18] Cooper, H. (2020). ME Capstone Design Process Framework.
- [19] Current Scrap Metal Prices In The US [2023 Updated] | Scrap Metal Pricer. (n.d.). Retrieved September 28, 2023, from <https://www.scrapmetalspricer.com/>
- [20] CUSN6 / CUSN8. (n.d.). Bronze Bearing Company. Retrieved September 28, 2023, from <http://www.bronzebearingcompany.com/en/product/fosfortennbrons-cusn6cusn8/>

- [21] Daily Metal Price: Tin Price (USD / Pound) Chart for the Last 2 Years. (n.d.). Retrieved September 28, 2023, from <https://www.dailymetalprice.com/metalpricecharts.php?c=sn&u=lb&d=480>
- [22] Dengel, B. (2021, January 15). Finding the ideal materials for gears | Gear Solutions Magazine Your Resource to the Gear Industry. <https://gearsolutions.com/features/finding-the-ideal-materials-for-gears/>
- [23] DuPont Transportation & Industrial Delrin® Family Page. (n.d.). Retrieved September 28, 2023, from <https://www.dupont.com/content/dupont/amer/us/en/products/mobility/delrin-archived.html>
- [24] Dutta, P. (2018, November 13). Phosphor Bronze Facts, Composition, Properties, Uses. Chemistry Learner. <https://www.chemistrylearner.com/phosphor-bronze.html>
- [25] Fairtrade Standard for Gold and Associated Precious Metals for Artisanal and Small-Scale Mining. (2023). Fairtrade International. chrome-extension://efaidnbmninnibpcapjpcglclefindmkaj/https://files.fairtrade.net/standards/2015-04-15_EN_Gold-and-Precious_Metals.pdf
- [26] J1950_201604: Proving Ground Vehicle Corrosion Testing—SAE International. (n.d.). Retrieved September 28, 2023, from https://www.sae.org/standards/content/j1950_201604/
- [27] Jindal, K. (2023, April 7). What is PEEK Material? | The Definitive Guide. PlasticRanger. <https://plasticranger.com/what-is-peek-material/>
- [28] Kolstad, C. (n.d.). Pneumatic Cylinders—A Technical Guide. Tameson.Com. Retrieved September 28, 2023, from <https://tameson.com/pages/pneumatic-cylinders>
- [29] Li, H.-Y. (2012). Time–temperature–property curves for quench sensitivity of 6063 aluminum alloy. *Trans. Nonferrous Met. Soc. China*, 23, 38–45.
- [30] Material Guide: How Sustainable is Nylon? (2020, August 30). Good On You. <https://goodonyou.eco/material-guide-nylon/>
- [31] Material Properties of Thermoplastic PEEK - Polyetheretherketone. (2019, February 27). Dielectric Manufacturing. <https://dielectricmfg.com/knowledge-base/peek/>
- [32] Material, W. (2022, June 15). Aluminum 6063-T6 T5; AA 6063 Aluminum Alloy Properties. World Material. <https://www.theworldmaterial.com/6063-aluminum-alloy/>
- [33] Mike. (2020, July 27). PA6 (Nylon 6) price index. Businessanalytiq. <https://businessanalytiq.com/procurementanalytics/index/pa6-price-index/>
- [34] Mild Steel | Density, Strength, Hardness, Melting Point. (2021, May 12). Material Properties. <https://material-properties.org/mild-steel-density-strength-hardness-melting-point/>
- [35] Minerals | Free Full-Text | Titanium: An Overview of Resources and Production Methods. (n.d.). Retrieved September 28, 2023, from <https://www.mdpi.com/2075-163X/11/12/1425>
- [36] Mopar 68044411AC Front Disconnect Stabilizer Bar Actuator Kit for 07-18 Jeep Wrangler JK. (n.d.). Retrieved September 19, 2023, from <https://www.quadratec.com/p/mopar/front-disconnect-stabilizer-bar-actuator-kit-wrangler-jk-68044411AC>
- [37] New 10.5" Diaphragm Clutch Kit for Mopar Dodge Plymouth Chrysler A-833 4-speed | eBay. (n.d.). Retrieved September 28, 2023, from <https://www.ebay.com/itm/293966675249>
- [38] Nylon 6 (Cast, Polyamide)—Poly-Tech Industrial. (2011, March 28). Poly-Tech Industrial - We Make Things Possible through the Power of Innovation. <https://www.polytechindustrial.com/products/plastic-stock-shapes/nylon-6>
- [39] Nylon 6: Definition, properties and common uses. (n.d.). Retrieved September 19, 2023, from <https://europlas.com.vn/en-US/nylon-6-definition-properties-and-common-uses>

- [40] Nylon (Cast NYLON) Rod, Sheet & Tube—Order Online. (n.d.). Professional Plastics. Retrieved September 19, 2023, from <https://www.professionalplastics.com/NYLON6CASTRODSHEETTUBE>
- [41] Nylon Cast Type 6 Unfilled | Emco Industrial Plastics. (n.d.). Retrieved September 28, 2023, from <https://www.emcoplastics.com/nylon-cast-type-6-unfilled/>
- [42] Nylon vs. Delrin: Durable Materials Ideal for High-Wear Parts. (n.d.). Retrieved September 28, 2023, from <https://www.protolabs.com/resources/blog/nylon-vs-delrin/>
- [43] OEM E-Disco (SmartBar) Study. (n.d.). JK-Forum.Com - The Top Destination for Jeep JK and JL Wrangler News, Rumors, and Discussion. Retrieved September 19, 2023, from <https://www.jk-forum.com/forums/stock-jk-tech-12/oem-e-disco-smartbar-study-153545/>
- [44] Overview of materials for Nylon 6, Cast. (n.d.). Retrieved September 28, 2023, from <https://www.matweb.com/search/DataSheet.aspx?MatGUID=8d78f3cfcb6f49d595896ce6ce6a2ef1&cck=1>
- [45] PET | Properties, Price & Application. (2021, March 9). Material Properties. <https://material-properties.org/pet-properties-application-price/>
- [46] Phosphor Bronze – Copper Alloy UNS C51000. (2012, August 14). AZoM.Com. <https://www.azom.com/article.aspx?ArticleID=6415>
- [47] Phosphor bronze 5% Sn, UNS C51000, H02 Temper flat products. (n.d.). Retrieved September 28, 2023, from <https://www.matweb.com/search/datasheet.aspx?matguid=97d71ced64534f4ba13b763e5f35e0c8&n=1&cck=1>
- [48] Plastic Gears: Design, Materials, Types, Advantages, and Disadvantages. (n.d.). Retrieved September 19, 2023, from <https://www.iqsdirectory.com/articles/gear/plastic-gears.html>
- [49] Polyamide—Nylon | Properties, Price & Application. (2021, March 16). Material Properties. <https://material-properties.org/polyamide-nylon-properties-application-price/>
- [48] Polycarbonate | Properties, Price & Application. (2021, March 9). Material Properties. <https://material-properties.org/polycarbonate-properties-application-price/>
- [49] Polycarbonate (PC)—Properties, Uses, & Structure—Guide. (n.d.). Retrieved September 28, 2023, from <https://omnexus.specialchem.com/selection-guide/polycarbonate-pc-plastic>
- [50] Polycarbonate Plastic | View Polycarbonate Strength, Impact Resistance. (n.d.). Curbell Plastics. Retrieved September 28, 2023, from <https://www.curbellplastics.com/materials/plastics/polycarbonate/>
- [51] Polycarbonate vs. PETG: Material Differences and Comparisons. (n.d.). Retrieved September 28, 2023, from <https://www.xometry.com/resources/materials/polycarbonate-vs-petg/>
- [52] Polycarbonate—An overview | ScienceDirect Topics. (n.d.). Retrieved September 28, 2023, from <https://www.sciencedirect.com/topics/materials-science/polycarbonate>
- [53] Polyether ether ketone (PEEK): Characteristics, Features, and Process. (n.d.). Retrieved September 28, 2023, from <https://www.xometry.com/resources/materials/polyether-ether-ketone/>
- [54] Polyethylene Terephthalate (PET) Production Process | Vaisala. (n.d.). Retrieved September 28, 2023, from <https://www.vaisala.com/en/chemical-industry-solutions/chemicals-allied-products/polyethylene-terephthalate-pet-production-process>
- [55] Polyethylene Terephthalate: Uses, Advantages, and Disadvantages. (n.d.). Retrieved September 28, 2023, from <https://www.xometry.com/resources/materials/polyethylene-terephthalate/>
- [56] Rapid, T. (2021, June 16). Die Casting Tolerance Standards. TEAM Rapid Manufacturing Co., Ltd. <https://www.teamrapidtooling.com/blog/die-casting-tolerance-standards/>

- [57] Rockwell to Brinell Hardness Conversion Chart. (2022, July 21). Hardness Tester. <https://www.hardnessgauge.com/rockwell-to-brinell/>
- [58] SAE-AISI 1018 (G10180) Carbon Steel: MakeItFrom.com. (n.d.). Retrieved September 28, 2023, from <https://www.makeitfrom.com/material-properties/SAE-AISI-1018-G10180-Carbon-Steel>
- says, V. (2020, December 30). Sway Bars Explained: What They Do & How They Work? Low Offset. <https://low-offset.com/workshop/sway-bars-explained/>
- [59] SD741 – SPEC Clutch, Inc. (n.d.). Retrieved September 28, 2023, from <https://specclutch.com/product/sd741/>
- solenoid valve magnetic—Google Search. (n.d.). Retrieved September 28, 2023, from https://www.google.com/search?q=solenoid+valve+magnetic&tbm=isch&ved=2ahUKEwiE7P3-6M6BAxUcEt4AHSIoCsQQ2-cCegQIABAA&oq=solenoid+valve+magnetic&gs_lcp=CgNpbWcQAzIGCAAQCBAAeMgYIABAIEB4yBggAEAgQHjIHCAAQGBCABDIHCAAQGBCABDoKCAAQigUQsQMQQzoHCAAQigUQQzoFCAAQgARQyQJY7BRg2BVoAXAAeACAawCIAZoFkgECMTGYAQCgAQQgAQtdnd3Mtdt2l6LWltZ8ABAQ&scient=img&ei=fTwWZcS9Opyk-LYPotCooAw&bih=708&biw=1340&rlz=1C5CHFA_enUS966US966#imgrc=1mK8ItbleVrE_M
- [60] SPEC Clutch SD741 SPEC Stage 1 Clutch Kits | Summit Racing. (n.d.). Retrieved September 28, 2023, from https://www.summitracing.com/parts/sxc-sd741?srltid=AfmBOorg1eIXTcMNraH8djGbzPLE__S7zIKqgpbGrror0WomH_pUemFkf4
- [61] SPEEDAIRE, 1 1/2 in Air Cylinder Bore Dia., 1/2 in Stroke, Air Cylinder—5TDX9|5TDX9—Grainger. (n.d.). Retrieved September 28, 2023, from <https://www.grainger.com/product/SPEEDAIRE-Air-Cylinder-1-1-2-in-Air-5TDX9>
- [62] Steel vs. Titanium—Strength, Properties, and Uses. (n.d.). Retrieved September 28, 2023, from <https://www.thomasnet.com/articles/metals-metal-products/steel-vs-titanium-strength-properties-and-uses>
- [63] Technologies, S. (2021, June 7). Know Your Materials: Polyethylene Terephthalate (PET). SyBridge Technologies. <https://sybridge.com/know-your-materials-pet/>
- [64] Titanium. (n.d.). Retrieved September 28, 2023, from <https://www.scrapmetalbuyers.com/titanium>
- [65] Titanium | Geoscience Australia. (n.d.). Retrieved September 28, 2023, from <https://www.ga.gov.au/education/classroom-resources/minerals-energy/australian-mineral-facts/titanium>
- [66] Titanium vs Steel, What's the Difference | Titanium and Steel Comparison | CNCLATHING. (n.d.). Retrieved September 28, 2023, from <https://www.cnclathing.com/guide/titanium-vs-steel-whats-the-difference-titanium-and-steel-comparison-cnclathing>
- [67] Waqar, E. (2022, April 1). How does Sway Bar work? | What is an Anti-roll Bar? Mechanical Boost. <https://mechanicalboost.com/sway-bar/>
- [68] What Are Sway Bars? How They Work, Common Issues, and More. (2023, July 27). In The Garage with CarParts.Com. <https://www.carparts.com/blog/what-are-sway-bars-how-they-work-common-issues-and-more/>
- [69] What is Delrin (POM-H) and what are its material properties? (n.d.). Hubs. Retrieved September 19, 2023, from <https://www.hubs.com/knowledge-base/what-is-delrin/>
- [70] What is Zamak 5—Zamak 5 Zinc Alloy Composition, Properties & Zamak 5 vs A380.0 | Diecasting-mould. (n.d.). Retrieved September 28, 2023, from <https://www.diecasting-mould.com/news/what-is-zamak-5-zamak-5-zinc-alloy-composition-properties-zamak-5-vs-a380-0-diecasting-mould>

- [71] Why Zinc Die Casting is Used for Automotive Components. (2019, April 30). Pacific Die Casting Corp.
<https://pacdiecast.com/aluminum-die-casting/why-zinc-die-casting-is-used-for-automotive-components/>
- [72] Woo, S. (2018). Estimating the Lifetime of the Pneumatic Cylinder in Machine Tool Subjected to Repetitive Pressure Loading. *Journal of US-China Public Administration*, 15.
<https://doi.org/10.17265/1548-6591/2018.05.004>
- [73] Wynn, D., & Clarkson, J. (2005). Models of designing. In J. Clarkson & C. Eckert (Eds.), *Design process improvement: A review of current practice* (pp. 34–59). Springer.
https://doi.org/10.1007/978-1-84628-061-0_2
- [74] Zamak 5 Properties | Zinc Alloy 5. (n.d.). Dynacast. Retrieved September 19, 2023, from <https://www.dynacast.com/en/knowledge-center/material-information/die-cast-metals/zinc-casting-metals/zamak-5>
- [75] ZAMAK 5—ZnC Group. (n.d.). <https://www.zamak.us/>. Retrieved September 19, 2023, from https://www.zamak.us/portfolio_item/zamak-5/
- [76] Zinc die-casting alloy Zamak 5 Price \$US/MT in EXW China. (n.d.). ScrapMonster. Retrieved September 19, 2023, from <https://www.scrapmonster.com//metal-prices/zinc-die-casting-alloy-zamak-5-price/916>
- [77] Daly, S.R., J.L. Christian, C.M. Seifert, and R. Gonzalez (2012). Design heuristic methods in engineering concept generation. *Journal of Engineering Education*. 101(4): 601-629.
- [78] “M Series Magnetic Proximity Sensors.” Automation Direct. Accessed October 19, 2023.
<chrome-extension://efaidnbmnnnibpcajpcglclefindmkaj/https://cdn.automationdirect.com/static/specs/ip69kproxmag1218maf.pdf>.
- [79] “Rotary Encoder, Ø50mm, Ø8mm Shaft, 600PPR, Totem P.” Accessed October 19, 2023.
<https://www.wolfautomation.com/rotary-encoder-o50mm-o8mm-shaft-600ppr-1/>.
- [80] HTMSensors. “FCM1-1202N-ARS4.” Accessed October 19, 2023.
<https://www.htmsensors.com/fcm1-1202n-ars4/>.
- [81] “Limit Switch: Lever Hinge (PN# 176110-1) | AutomationDirect.” Accessed October 19, 2023.
https://www.automationdirect.com/adc/shopping/catalog/sensors_-z-_encoders/limit_switches/lever_actuator/176110-1?utm_source=msn%20cpc&utm_medium=cpc&utm_term=&utm_campaign=Shopping%20-%20Discrete%20Sensors&utm_adgroup=Discrete%20Sensors&msclkid=23bb893548531a0b8486ec15c913dd46&utm_content=Discrete%20Sensors.
- [82] “Home » Shop » Data Logging/Dash Systems » Autosport Labs » 500mm String Potentiometer Sensor.” Accessed October 19, 2023.
http://www.bmotorsports.com/shop/product_info.php/products_id/5791.
- [83] “Manufactured by - OMEGA ENGINEERING.” Accessed October 19, 2023.
<https://www.radwell.com/en-US/Buy/OMEGA%20ENGINEERING/OMEGA%20ENGINEERING/PX309-100AI/>.
- [84] “Topology Optimization - an Overview | ScienceDirect Topics.” Accessed October 19, 2023.
<https://www.sciencedirect.com/topics/computer-science/topology-optimization>.
- [85] Shah, Chinmay, S. Thigale, and Rathin Shah. “Optimizing Weight of a Gear Using Topology Optimization,” 2018. <https://www.semanticscholar.org/paper/Optimizing-weight-of-a-Gear-using-Topology-Shah-Thigale/4ac8cdcc875277cdf0cb7ffcf4c7e5131e356349/figure/7>.
- [86] BUDYNAS, R., & Nisbett, J. K. (2018). *Shigley's mechanical engineering design*. McGraw-Hill US Higher Ed USE.

- [87] “Friction - Friction Coefficients and Calculator.” Accessed October 19, 2023. https://www.engineeringtoolbox.com/friction-coefficients-d_778.html.
- [88] Rezaei, Fatemeh, Mohammad H. Yarmohammadian, Abbas Haghshenas, Ali Fallah, and Masoud Ferdosi. “Revised Risk Priority Number in Failure Mode and Effects Analysis Model from the Perspective of Healthcare System.” *International Journal of Preventive Medicine* 9 (January 29, 2018): 7. <https://doi.org/10.4103/2008-7802.224046>.
- [89] MasterSeries. “Is Your Finite Element Mesh Size Appropriate?,” October 12, 2022. <https://www.masterseries.com/blog/fe-mesh-size>.
- [90] Ullman, D. G. (1992). *The mechanical design process* (Vol. 2). New York: McGraw-Hill.
- [91] Atlas Scientific. “7 Types Of Pressure Sensors,” December 19, 2022. <https://atlas-scientific.com/blog/types-of-pressure-sensors/>.
- [92] “Hall-Effect Sensor - US1881 (Latching) - COM-09312 - SparkFun Electronics.” Accessed October 19, 2023. <https://www.sparkfun.com/products/9312>.
- [93] Dynapar. “Motor Encoder Speed & Position Overview | Dynapar.” Accessed October 19, 2023. https://www.dynapar.com/technology/encoder_basics/motor_encoders/.
- [94] “Limit Switch: Lever Hinge (PN# 176110-1) | AutomationDirect.” Accessed October 19, 2023. https://www.automationdirect.com/adc/shopping/catalog/sensors_-z-_encoders/limit_switches/lever_actuator/176110-1?utm_source=msn%20cpc&utm_medium=cpc&utm_term=&utm_campaign=Shopping%20-%20Discrete%20Sensors&utm_adgroup=Discrete%20Sensors&msclkid=23bb893548531a0b8486ec15c913dd46&utm_content=Discrete%20Sensors.
- [95] “Overview of Proximity Sensors | OMRON Industrial Automation.” Accessed October 19, 2023. <https://www.ia.omron.com/support/guide/41/introduction.html>.
- [96] “How to Perform a Random Vibration Analysis” [Video] Ansys Innovation Courses <https://courses.ansys.com/index.php/courses/random-vibration-analysis/>
- [97] American plastics corp: Delrin. (n.d.). Retrieved November 21, 2023, from <https://americanplasticscorp.com/products/delrin/>
- [98] Brazel, Christopher, and Stephen Rosen. *Fundamental Principles of Polymeric Materials*. 3rd ed. John Wiley & Sons, Inc., 1970. <http://ebookcentral.proquest.com/lib/umichigan/detail.action?docID=7103479>.
- [99] Oberg, Erik, Franklin D. Jones, Holbrook L. Horton, and Henry H. Ryffel. *Machinery's Handbook*. 29th ed. Industrial Press, 2012.
- [100] “Von Mises Stress: Definition, Derivation, Equation, Calculation, Example [Pdf],” February 16, 2022. <https://mechcontent.com/von-mises-stress/>.
- [101] Oberg E. Jones F. D. Horton H. L. & Ryffel H. H. (2004). *Machinery's handbook : a reference book for the mechanical engineer designer manufacturing engineer draftsman toolmaker and machinist* (2th ed. rev.). Industrial Press. <https://library.uc.edu.kh/userfiles/pdf/19.Machinery%27s%20handbook.pdf>
- [102] *Thermodynamics: An engineering approach*. (2018). <https://www.mheducation.com/highered/product/thermodynamics-engineering-approach-boles-cengel/M9781259822674.html>
- [103] “EngineeringPaper.Xyz: Lead Screw Torque and Efficiency Calculations.” Accessed November 21, 2023. <https://engineeringpaper.xyz/dRttcDo7GXeCD2iHLc5R7x>.
- [104] “What Is FMEA? Failure Mode & Effects Analysis | ASQ.” Accessed November 21, 2023. <https://asq.org/quality-resources/fmea>.

- [105] “(25) Introducing PPA (Polyphthalamide): A High-Performance Engineering Plastic for Diverse Applications | LinkedIn.” Accessed December 11, 2023. <https://www.linkedin.com/pulse/introducing-ppa-polyphthalamide-high-performance-engineering-linda-wu/>.
- [106] “(25) Polytrimethylene Terephthalate (PTT) Polymers Market Size, Growth and Forecast from 2023 - 2030 | LinkedIn.” Accessed December 11, 2023. <https://www.linkedin.com/pulse/polytrimethylene-terephthalate-ptt-polymers-market-size-growth/>.
- [107] “Fiberglass Sustainability | AAMA Fiberglass Material Council.” Accessed December 11, 2023. <https://fgiaonline.org/pages/fiberglass-green-and-sustainability>.
- [108] Markets, Research and. “Global Bio-Polyamide (PA-6, PA-66, Specialty Polyamides) Market Size, Share & Trends Analysis Report 2023-2030.” GlobeNewswire News Room, September 28, 2023. <https://www.globenewswire.com/en/news-release/2023/09/28/2751233/28124/en/Global-Bio-polyamide-PA-6-PA-66-Specialty-Polyamides-Market-Size-Share-Trends-Analysis-Report-2023-2030.html>.
- [109] “Substituting Phenol in Phenol–Formaldehyde Resins for Wood Modification by Phenolic Cleavage Products from Vacuum Low-Temperature Microwave-Assisted Pyrolysis of Softwood Kraft Lignin | Cellulose.” Accessed December 11, 2023. <https://link.springer.com/article/10.1007/s10570-023-05295-5>.
- [110] “All About Liquid-Crystal Polymer.” Accessed December 11, 2023. <https://www.xometry.com/resources/materials/liquid-crystal-polymer/>.
- [111] Machine Design. “Mineral Fillers Improve Plastics,” October 1, 2015. <https://www.machinedesign.com/materials/article/21834429/mineral-fillers-improve-plastics>.
- [112] Minerals Education Coalition. “Mica.” Accessed December 11, 2023. <https://mineralseducationcoalition.org/minerals-database/mica/>.
- [113] RecycleNation. “Is Carbon Fiber Better for the Environment than Steel? – RecycleNation.” Accessed December 11, 2023. <https://recyclenation.com/2015/10/is-carbon-fiber-better-for-environment-than-steel/>.
- [114] “Sheet Moulding Compound - an Overview | ScienceDirect Topics.” Accessed December 11, 2023. <https://www.sciencedirect.com/topics/engineering/sheet-moulding-compound>.
- [115] “Sheet Moulding Compound - an Overview | ScienceDirect Topics.” Accessed December 11, 2023. <https://www.sciencedirect.com/topics/engineering/sheet-moulding-compound>.
- [116] “Sustainability Aspects of SMC/BMC Based Products.” SMC/BMC, June 2011. <chrome-extension://efaidnbmnnnibpcajpcglclefindmkaj/https://www.allbro.com.au/download-catalogue/position-paper-european-alliance-smc-bmc.pdf>.
- [117] “What Is Calcium Carbonate Filler and Its Characteristics.” Accessed December 11, 2023. <https://europas.com.vn/en-US/what-is-calcium-carbonate-filler-what-characteristics-do-they-have>.
- [118] BUDYNAS, Richard ; Nisbett, J. Keith. (n.d.). Shigley’s Mechanical Engineering Design. NY: McGraw-Hill US Higher Ed USE. Accessed December 11, 2023.

TEAM MEMBER BIOS

Lillian Adams



I am Lily Adams and I am a senior studying Mechanical Engineering from Troy, Michigan. Within this area of study, I am particularly interested in CAD design and performance testing. I have recently explored roles in systems engineering which have allowed me to apply software and firmware knowledge to the hardware foundation I have learned through my major here. I have worked for the past two summers in internships within the additive manufacturing industry which has taught me many new prototyping and design skills. I will be graduating in May of 2024 and after graduation I will be working at Markforged in Boston full-time as a Systems Print Engineer.

Marisa Bladecki



I am Marisa Bladecki, and I am a senior student originally from Troy, Michigan. I'm majoring in Mechanical Engineering with a minor in Material Science & Engineering. My interest in engineering stems from my desire to create medical technologies that will improve patient outcomes. I have a specific interest in surgical robotics, as I recently interned at Intuitive Surgical. I will be graduating in May of 2024 and I plan on returning to the University of Michigan the next school year in order to pursue a master's degree in mechanical engineering. I enjoy hiking and anything related to the outdoors!

Andres Garcia



I am Andres Garcia and I am a senior originally from the south side of Chicago, majoring in Mechanical Engineering. I will be graduating in May 2024 and am hoping to explore more design oriented opportunities in a variety of work cultures in the near future, with an emphasis on Computer Aided Engineering. This past summer I interned at Tesla's Fremont Factory as a Quality Engineer, sparking my passion for the automotive industry.

Avani Yerva



I am Avani Yerva and I am a senior majoring in Mechanical Engineering. I am from Troy, MI. I am pursuing a concentration in Robotics and will be doing my Master's in the Fall. I will be graduating in May 2024. My interests are in the automotive and medical device industries. I have worked in the Locomotor Control Systems Laboratory at the University of Michigan where I spent time testing lower-limb exoskeletons. I also worked at Medtronic this past summer as a Design Assurance and Test Method Engineer.